GOODYEAR AEROSPACE

GOODYEAR AEROSPACE CORPORATION

CODE IDENT NO. 25500

GOODYEAR AEROSPACE
CORPORATION

AKRON, OHIO 44315

SYSTEM DEFINITION STUDY

OF

DEPLOYABLE, NON-METALLIC SPACE STRUCTURES

FREDERICK J. STIMLER

FOR

NASA MARSHALL SPACE FLIGHT CENTER

HUNTSVILLE, ALABAMA 35812

CONTRACT NO. NAS 8-35498

GAC 19-1615 JUNE 1984

FOREWORD

Goodyear Aerospace Corporation (GAC), Akron, Ohio, conducted an eight month study of deployable, non-metallic space structures for NASA-MSFC under Contract No. NAS 8-35498. GAC's experience in flexible/inflatable/deployable and rigidized structures for space over the last 20 years was used to address the problems of today and applications of the future. Advanced materials and fabrication techniques have provided new ways of conquering the hostile space environment for these unique structures.

In addition to reviewing typical inflatable/deployable subsystems and systems of interest to the space community, many important performance parameters unique to space applications were discussed. Potential experiments within the shuttle cargo bay, either as a free flyer satellite or when tethered from the shuttle, are presented for consideration. Basic technical data has been included in appendices as a point of departure for future similar applications.

R. L. Middleton was the Contracting Officer's Representative (COR) for NASA-MSFC, while F. J. Stimler served as Project Engineer for the Engineered Fabrics Division.

TABLE OF CONTENTS

LIST OF FIGURES

LIST OF FIGURES, continued

LIST OF TABLES

SECTION I -- INTRODUCTION AND SUMMARY

Goodyear Aerospace Corporation (GAC) summarizes the state-of-the-art for non-metallic materials and fabrication techniques considered suitable for future space structures. This report will serve as a handbook of data, offer innovative ideas, and guide designers of structures for the future. This report, along with reference 1, should offer a good point of departure for future detailed design studies. Reference 1 shows representative photographs and cites the best references available.

Recent success with the Spacelab/Shuttle flight experiment has proven that a flexible element in the transfer tunnel is a viable solution for a manned space structure. These same materials have been proposed for deployable components or subsystems for rigid space station structures.

With the discovery of new flexible materials such as [1]Nicalon [R] a silicon carbide fiber and [2]Nextel [R] a ceramic fiber, which are suitable for high temperature applications of 2500 to 3000°F, many deceleration, reentry, recovery and thermal insulation problems can now be solved for tough non-metallic space applications.

Typical subsystems and systems for space applications using inflatable and deployable materials are described. To develop these subsystem and system concepts the requirements for space stations or platforms were discussed with knowledgeable government and industry personnel. Typical performance parameters of these structures are analyzed to answer questions often asked when flexible structures are considered for space applications.

The data reported herein is compatible with typical space station configurations as shown in Figure I-1. This concept is representative of the many space station proposals considered by NASA and industry during the last few years.

Nicalon [R] [1]Trademark of Nippon Carbon Co., Ltd., Japan

Nextel [R] [2]Trademark of 3M Co., St. Paul, MN

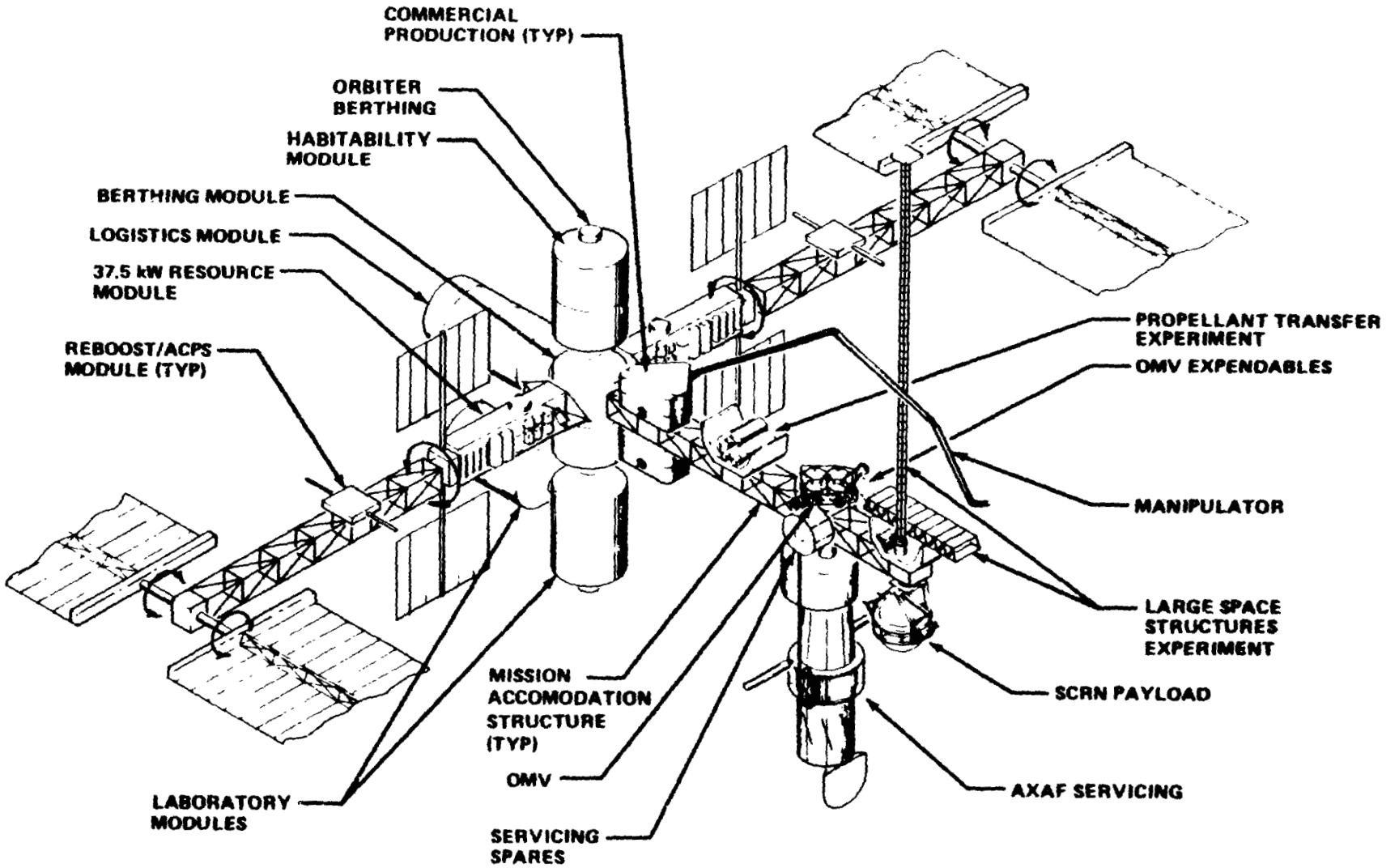

FIGURE I-1 -- A POTENTIAL SPACE STATION CONFIGURATION

There are many applications for non-metallic expandable structures in space, especially now that new and approved materials are available. The data presented in this report should be of assistance in solving the unique problems of extremely large packageable structures to be deployed in space or in the use of flexible materials where rigid materials cannot perform the requirements of a particular application.

SECTION II -- TYPICAL INFLATABLE/DEPLOYABLE SUBSYSTEMS AND SYSTEMS

A. INFLATABLE/RIGIDIZED SPACE HANGAR (UNPRESSURIZED)

Studies (References 2 and 3) have shown that deployable, unpressurized hangars attached to a space station platform have a viable and practical use in space.

Reference 2 summarizes desired features for space service hangars as follows:

1. Sized to accept OMV, OTV, and large spacecraft (compatible with orbiter dimensions) offering berthing and docking provisions and ingress/egress for the suited astronauts.
2. Orbiter - compatible mounting system and a rail system to enable movement of vehicles.
3. Totally enclosed with door designed to allow maximum access sibly provide ingress/egress at both ends.
4. Movable track-mounted work stations required to enable optimum access of astronaut to serviced items.
5. Tool stations located at strategic positions in the hangar.
6. Track-mounted space station RMS attached to Service Hangar/Space Station to allow transfer of OMV,OTV, Servicers, Spacecraft to and from the Service Hangar to the orbiter or deployment for launch.
7. Closed circuit TV, track-mounted and pivotable to present procedures/ drawings.
8. Micrometeoroid/debris, and radiation protection, along with thermal control on Service Hangar.

9. No required orientation of Service Hangar or space station due to servicing.
10. Lighting aids, electric power.
11. Foot restraints/handholds/work platforms 1 to 2 meters wide.
12. Communications.
13. Payload Cradle/Carriage - Carousel Mechanism.
14. OTV replacement items and refueling capability.
15. Minimum life support system (emergency).
16. Storage capability - service equipment, spare parts.
17. Restraint of loose parts and tools during servicing.

Goodyear recommends an unpressurized hangar having nonmetallic walls which can be deployed from the packaged condition and rigidized for the operational phase. Several concepts have been studied in the past, however, tne one shown in Figure IIA-1 is representative for OTV maintenance (Reference 3). It is understood that NASA's first interests are hangars for the OMV(TMS), then for satellite servicing and, finally, for the OTV servicing. The concept shown in Figure IIA-1 is compatible with shuttle delivery and contemplated OTV sizes. The OMV is 14 feet in diameter and 3 feet wide, thus indicating the use of a smaller hangar than shown in the figure. Goodyear offers a concept herein and delays the detail design until all operational requirements can be defined.

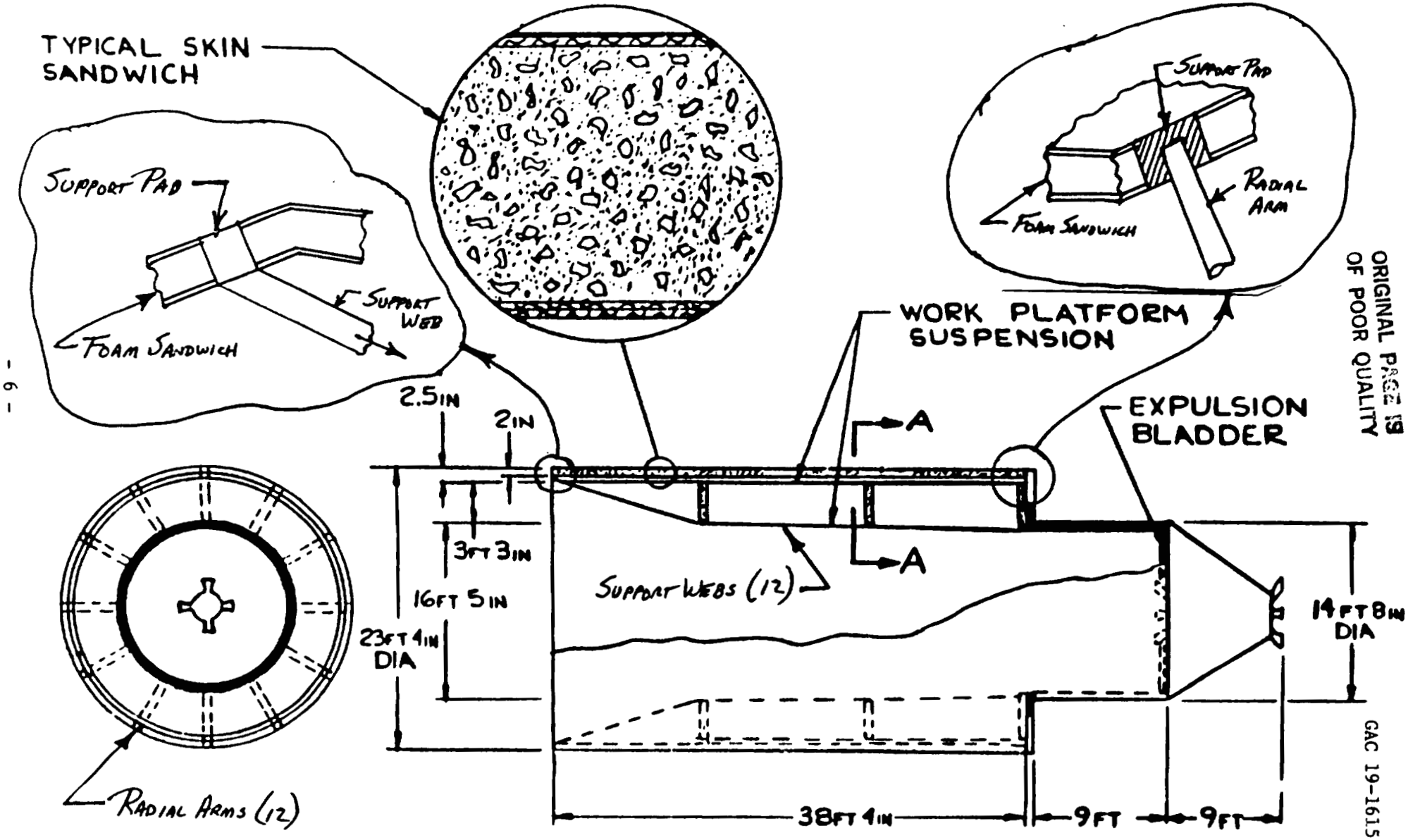

FIGURE IIA-1-- INFLATABLE HANGAR FOR ORBIT TRANSFER VEHICLE (OTV) MAINTENANCE

The flexible material considered for the OTV hangar is the elastic recovery type which was investigated for the airlock experiment and the lunar STEM* system. The airlock experiment is defined in Appendix A, while the lunar system material is defined in Appendix B. The proposed elastic recovery material will be modified to include a positive deployment mechanism and also a rigidization technique. The positive deployment is considered necessary because of the large hangar size and to ensure an orderly deployment from its storage volume. The airlock material has been qualified to the space requirements of the Skylab era. The STEM material was geared for the lunar environment. Additional material studies by Goodyear and others resulted in a rigidized foam system suitable for protection from micrometeoroids in space. This experience is used to choose a preliminary material concept for the hangar to guide discussion of the other technical disciplines within the report.

Figure IIA-1 is a sketch of the inflatable hangar concept GAC recommends at this time. The basic structure is 2-1/2 inch foam with fiberglass skins. Inflation is used for controlled deployment and a gelatin system is proposed for rigidization. The work platforms are one meter wide and held in place axially by straps, webbing, and mechanical attachments. Location and number of platforms can be determined later, although two are indicated in the sketch. Open areas are provided in the platform areas to permit suited astronauts to move axially in the hangar. Velcro, snaps, hooks, net bags, straps, etc., will be added as required to enhance maintenance operations. Rigid subsystems can be added once the hangar is deployed and rigidized again to improve function. The total inflatable hangar system weighs approximately 4,100 lbs.

* STEM - Stay Time Extension Module

Concentrated loads are usually transmitted to flexible surfaces by use of fan patches, pads, catenaries, cables or similar mechanisms to prevent tears or other failures. The 12 radial arms at the closed end of the hangar provide the interface between the hangar structure and the storage can. These radial arms facilitate the folding of the hangar structure and eventual storage in the packaged condition. The 12 support webs are attached to the radial arms at the closed end of the hangar for a structural interface. These webs are attached to pads at the open end of the hangar. The webs provide structural attachment for the work platforms and also facilitate the packaging process.

The materials and construction of the cylindrical shell and the working platforms must exhibit sufficient structural integrity to withstand astronaut working loads and forces generated during placement of equipment. Although these forces are considered as minimal in magnitude, they can be rather locally concentrated. Therefore, one of the critical loadings will be applied bending-moment, necessitating a flexurally rigid construction such as a sandwich structure. The core of the sandwich must be rigid to withstand combined compressive and flexural stresses.

The chemical process of rigidization of the foam core must be one that can be performed and controlled under a space environment in an acceptable time. Certain mechanical and physical properties are desirable. The final rigidized composite core material must be free of harmful voids and cracks, be of uniform composition, have sufficient bond strength between resin matrix and reinforcing fabric to transfer stresses, and must be sufficiently rigid to allow the fabric faces and resin core to act as a sandwich structure.

A structural analysis was made adapting the chemically rigidized foam-fabric sandwich as reported in Reference 4. Here, the rigidized construction shown in Figure IIA-2 is used.

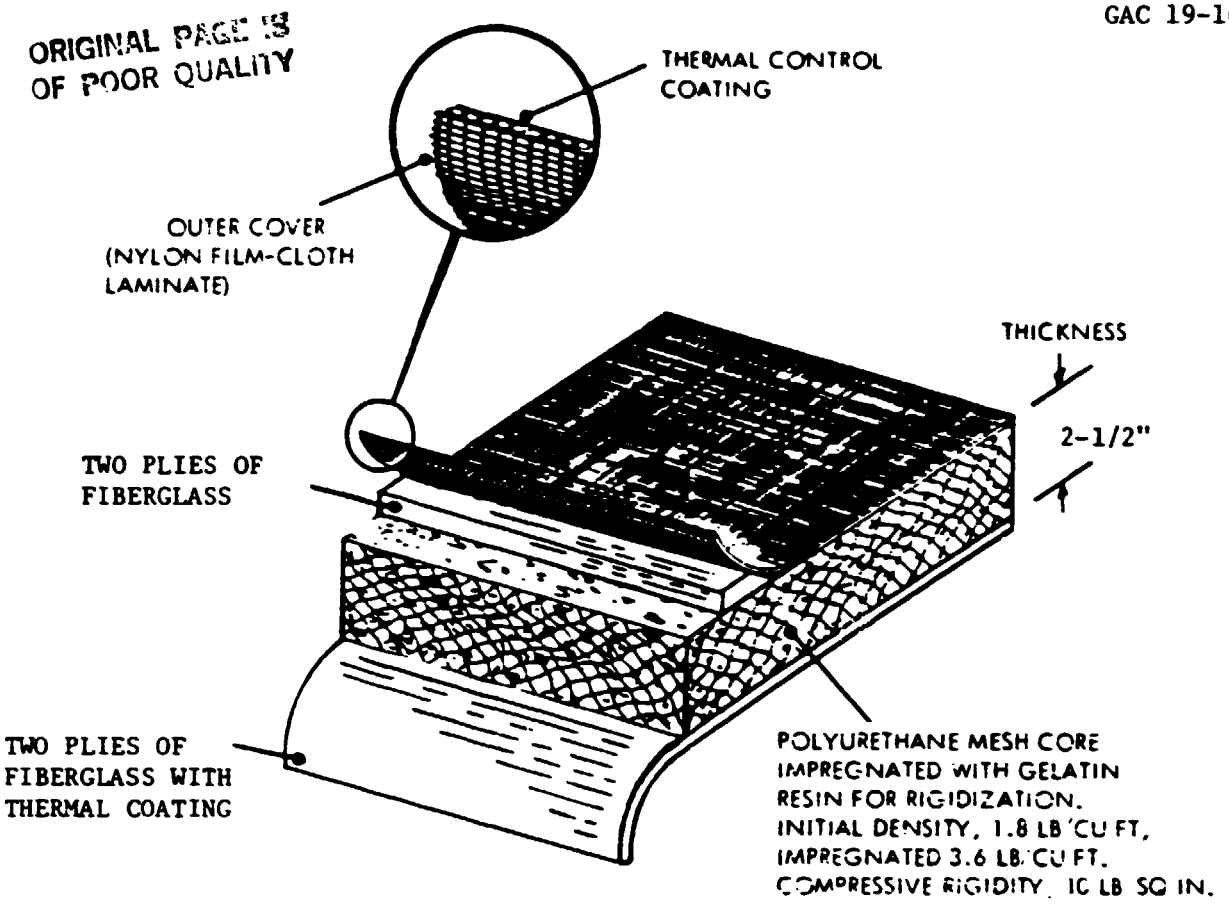

ITEM	MATERIAL WEIGHT GM/CM^2	#/FT^2
*Outer Cover (With Thermal Coating)	0.034	0.068
Interlayer Adhesive	0.005	0.010
Two Plies of Fiberglass	0.036	0.071
Interlayer Adhesive	0.005	0.010
Gelatin - Impregnated Scott Foam (2-1/2")	0.375	0.750
Interlayer Adhesive	0.005	0.010
Two Plies of Fiberglass	0.036	0.071
Inner Coating	0.020	0.040
TOTAL	0.516	1.030

*The outer cover is a film-cloth laminate with the following properties:

(1) Base cloth - Stern and Stern A4787 nylon at 0.84 oz/sq yd.
Warp - 20 denier, 127.5 ends/in., 42 lb/in. grab strength.
Fill - 30 denier, 114 ends/in., 57.5 lb/in. grab strength.

(2) Film - Capron Type 77C, 1/2 mil, 0.43 oz/sq yd.

FIGURE IIA-2 RIGIDIZED SANDWICH CONSTRUCTION

The fiberglass layers are the structural faces of the sandwich. Each is composed of 2 plies of straight 116 fiberglass cloth impregnated with gelatin.

The Scott foam (Ref. 4) is impregnated with ~ 48.5 percent gelatin whose net density is 3.6 lbs/ft^3 and whose compression modulus is 200 psi.

Goodyear made a preliminary stress analysis of this hangar concept in Reference 5, considering critical bending, shear, compression and concentrated loads. Preliminary calculations indicate that the rigidized foam sandwich cylindrical shell is a feasible approach to the design of the hangar. An analysis of the stress and deflection characteristics encountered with an astronaut working on the ring platforms indicates that these platforms and their interface structures are adequate to withstand these working loads.

Mounting provisions are required for lights, electrical circuitry, fuel hose, etc., to have controlled routing and fixed positions.

It is assumed the above mentioned items are stowed in the existing structure and deployed by EVA after the hangar has been deployed and rigidized. The attached provisions will be in place on the hangar/platform assemblies if the provisions are software such as velcro or ties.

Required location/position for the mounting provisions will be determined through analysis and mockup study.

No unusual problems are apparent at this time. Hooks, webbing, snaps, and similar items attached to the hangar surface will not necessarily cause any problems during packaging, deployment or rigidization.

Figure IIA-3 schematically depicts a method of packaging the inflatable OTV hangar. This is a very preliminary study of a complex problem and should be considered in that light. Further clarification is not possible until more design details are formulated.

Sketch Set 1 shows the hangar in deployed condition. Sketch Set 2 shows the location of the toroidal expulsion bladder. The straps and work platforms have been disconnected from the hangar wall for storage ahead of the collapsed expulsion bladder. The platform straps at the closed end of the hangar are left connected and retrieved into the rigid can for storage. This ensures that the platforms will remain with the hangar during the expulsion process.

Sketch Set 3 shows the work platforms and expulsion bladders in stored position. A vacuum bag is positioned over the sandwich structure of the hangar shell in Sketch Set 4. The rigidization mechanism is applied to the foam and fiberglass skins and then the vacuum bag is used to compress the foam sandwich. This may be the least understood part of the process. Sketch Set 5 shows the rigid radial support arms stretched along the hangar axis while the hangar skin is pleat-folded into a diameter compatible with the storage container. An inflatable tube (Chinese whistle or blowout) is added to the pleated skin (Sketch Set 6). The collapsed hangar skin is now rolled up like a window shade in the direction of the storage container (Sketch Set 7). The rolled material is placed into the container and the rigid radial support arms are folded into position to hold the stored hangar in the rigid can (Sketch Set 8 and 9).

The material volume of the 2-1/2 inch foam sandwich is 714 ft^3. Compression to one inch thickness gives a material volume of 143 ft^3. The volume of the storage container (14 ft. dia. x 9 ft. lg.) is 1,385 ft^3. Therefore, the ratio of storage volume to compressed material volume is nearly 10, which is adequate for reasonable packaging.

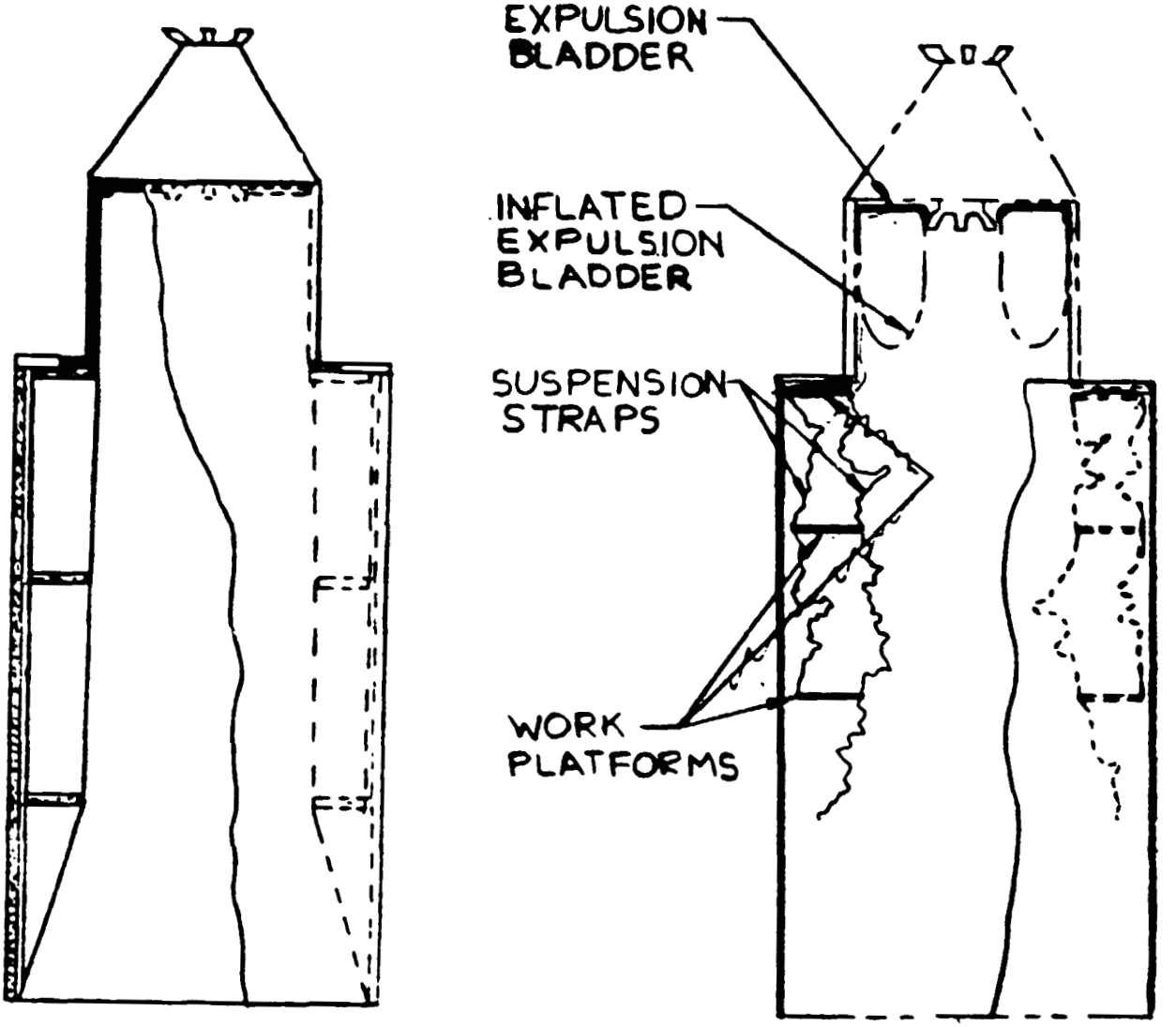

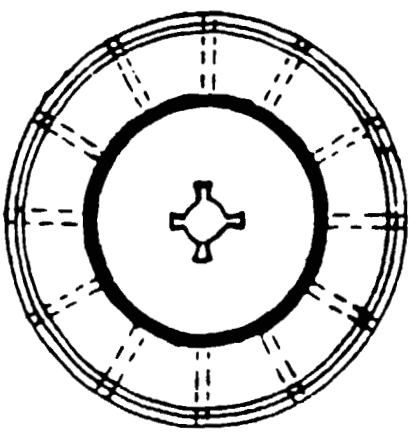

SKETCH SET 1

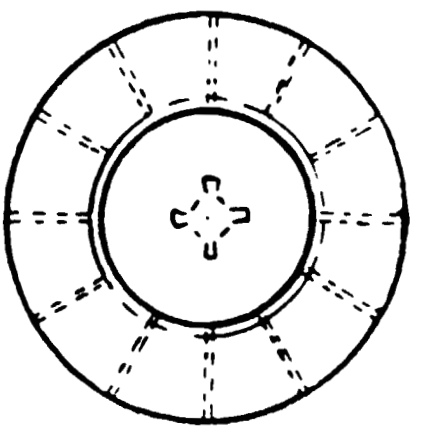

SKETCH SET 2

FIGURE IIA-3A PRELIMINARY PROPOSED PACKAGING TECHNIQUES FOR OTV INFLATABLE HANGAR

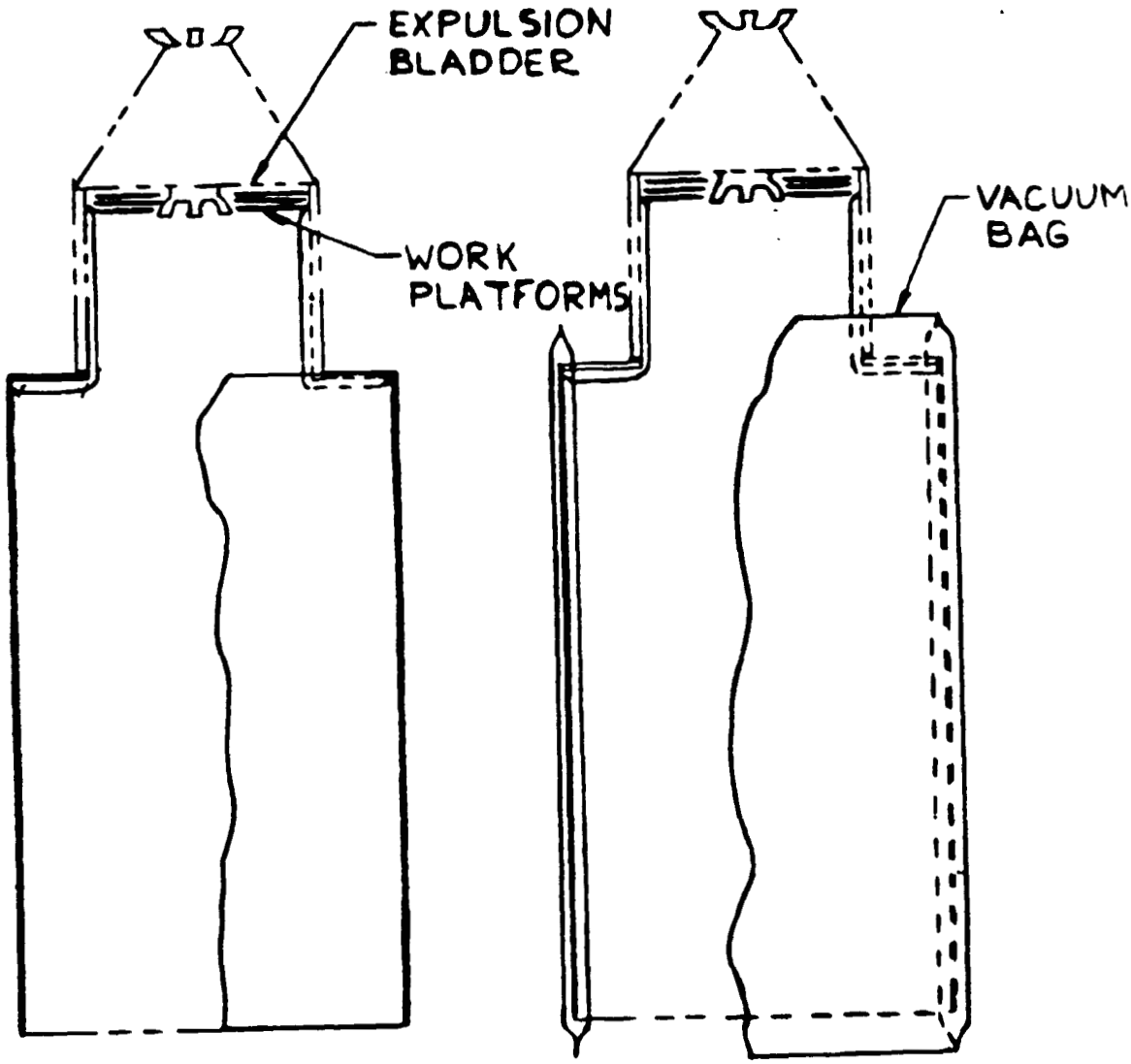

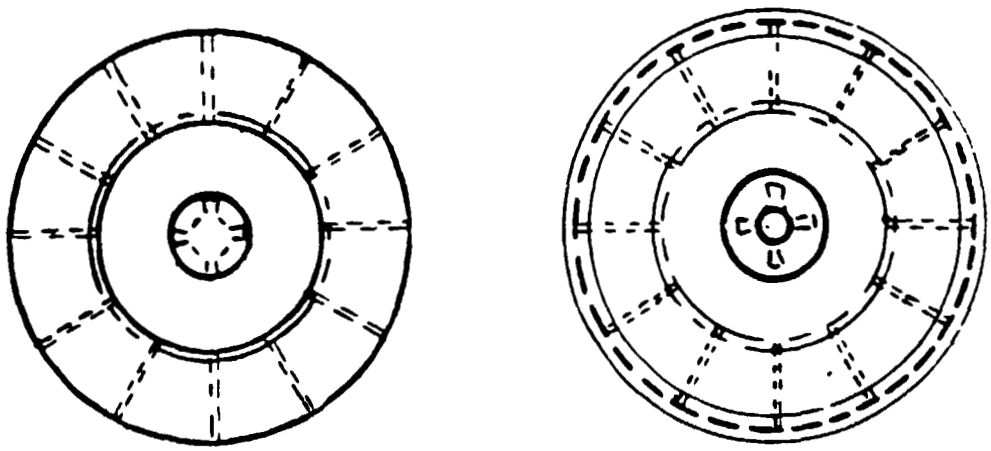

SKETCH SET 3

SKETCH SET 4

FIGURE IIA-3B CONTINUED

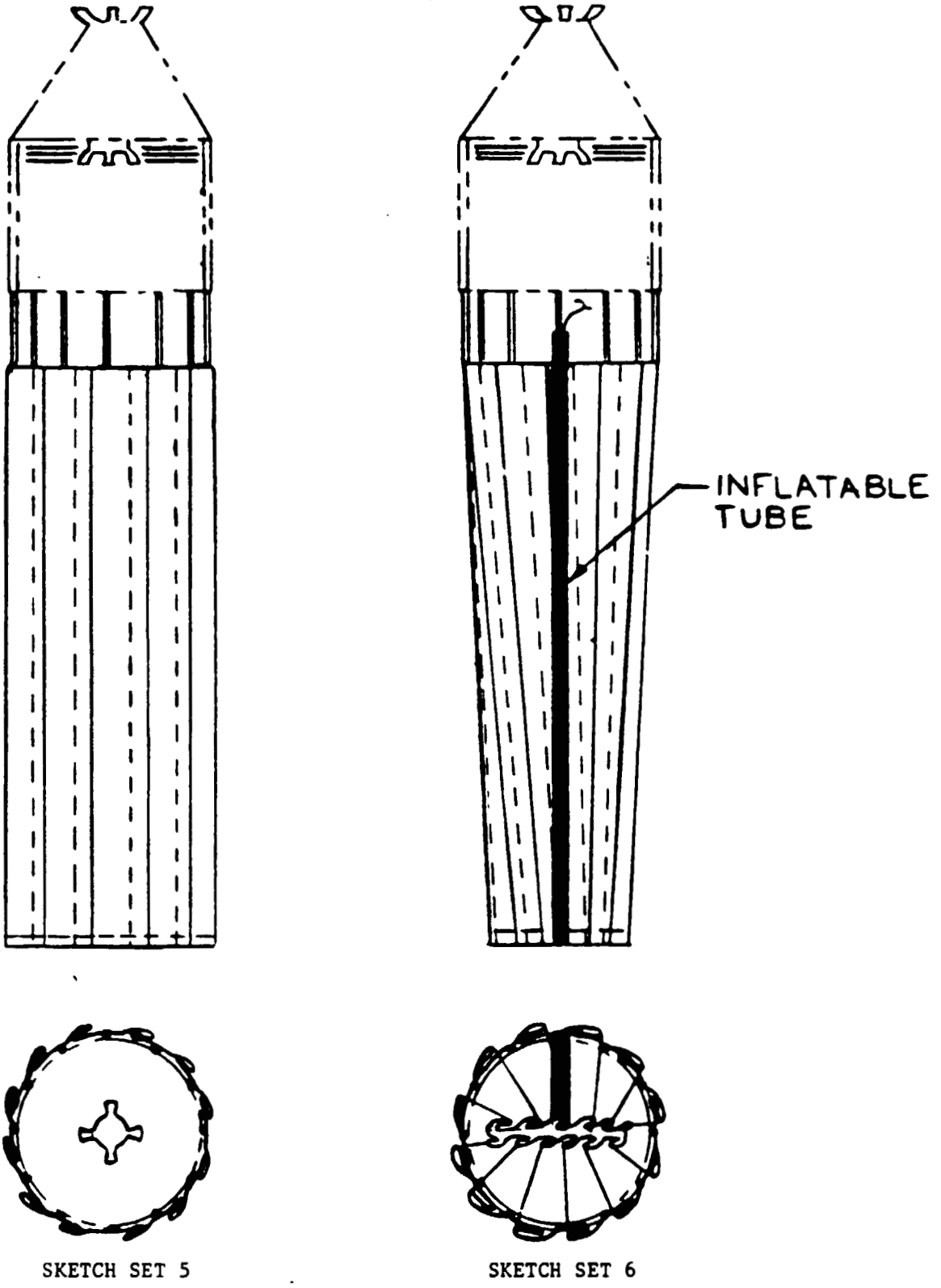

SKETCH SET 5

SKETCH SET 6

FIGURE IIA-3C CONTINUED

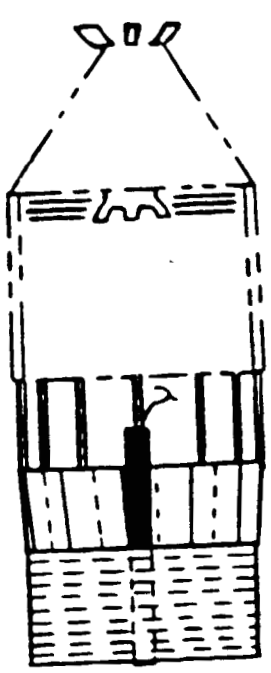

SKETCH SET 7

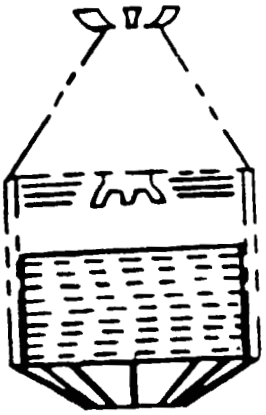

SKETCH SET 8

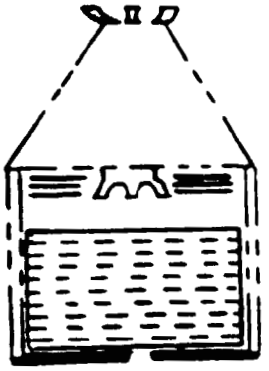

SKETCH SET 9

FIGURE IIA-3D CONTINUED

Some problems do remain unsolved such as -- how do we get rid of the vacuum bag after hangar deployment; what is the best way to initiate the rigidization process; how much EVA activity should be considered during this total process of deployment and erection, etc. These can best be resolved with additional studies to review simpler methods or recent improved ideas.

Goodyear has experience in packing such large structures as nonrigid airship envelopes, the Moby Dick Experiment (Reference 1), crew tunnels, large balloons, large parachutes, and similar structures. Also, GAC's experience in rigidization of space vehicles and payloads should allow ready evaluation of available data and recommendation of a viable solution.

GAC does not have sufficient test data to predict lifetime of the proposed hangar materials in the LEO environment. Past projects have indicated a 5 to 10 year storage and service life for these flexible structures; however, until actual test data is evaluated, it is rather difficult to predict a 20 year lifetime.

Compatibility with flammability, toxicity, and off gassing requirements for manned habitats is not considered viable for the hangar application.

Deployment of the packaged hangar will be initiated by use of a toroidal expulsion bladder at the rigid interface panel (see Figure IIA-3A). The bladder is toroidal to permit clearance with the boom-docking mechanism stowed on the hangar centerline. Once the hangar body is free of the storage container, an inflatable tube system will be activiated to unroll the packaged hangar much like a Chinese whistle. This positive force acting on the rolled hangar will extend the hangar to its longitudinal limit. The expulsion bladder and deployment tube will be held captive rather than allowed to float freely in space.

A low gas pressure will be inserted into the open cell foam to shape the cylindrical hangar. This gas pressure may be considered for removing the vacuum bag to initiate the rigidization process as soon as the shaping process is complete.

The proposed hangar concept utilizes a boom-docking mechanism on the hangar centerline for positioning the payloads with respect to the hangar. A guide rail can also be installed on the inner surface of the hangar for movement of the payload to be compatible with the shuttle RMS or a similar mechanical arm. Movement of the hangar shell along its centerline or opening the cylinder sides like garage doors to effect payload placement may unduly complicate the hangar system.

Ground tests of this hangar concept are possible and desirable to check such features as packaging, deployment, shape control, subsystem assembly, clearances, and similar items. Whether the hangar is deployed from a hanging position under ambient conditions or in the zero-g simulator depends on which would give the most realistic results for the time and money involved.

Adequate factors of safety and packaging capability are difficult to maintain with large, deployable, nonmetallic manned space structures, with internal pressures near 14.7 psig. The circumferential stress for a hangar of 23 foot diameter becomes

$$\sigma_c = pR = 14.7 \left(\frac{23}{2}\right)\left(12\right) = 2029 \text{ lbs/inch}$$

Using a typical factor of safety for manned structures of 5.64 (see page 41), the ultimate strength requirements become 11,441 lbs/inch. Using the characteristics of a qualified space material (see page 35) the structure would require at least 11 plys of material, resulting in a thickness of 0.44 inches. Thus the material becomes too heavy, the seam strengths critical and the structure is no longer packageable.

B. FLEXIBLE/STORABLE ACOUSTIC BARRIER

Goodyear produces several types of flexible sheeting material suitable for sound attenuation over a wide frequency range. The decibel reduction over the frequency range of 100 to 5000 Hertz is shown in Figure IIB-1. In addition, physical properties for Acousta Sheet 200 and 300 are also presented therein.

Goodyear's Acousta Sheet Style 200 was sent to McDonnell Douglas Technical Services Company (MDTSCO) for testing at the NASA White Sands Test Facility for Flammability, Toxicity, and VCM properties in accordance with NASA document NHB 8060.1B. The flammability test was passed since the longest burn was 2.9 inches where 6 inches before burnout is acceptable. The toxicity test was also passed. Acousta 200 is considered acceptable for use in a pressurized habitat area but not under vacuum conditions because of out gassing. In other words, the material is acceptable for space station applications but not for use in the shuttle cargo bay area.

Subjecting the material to 125°C temperature for 24 hours at 10^{-6}torr pressure resulted in a total mass loss of 7.4% (1% is considered acceptable) where the condensible portion was 2.82 % (0.1% is considered acceptable) Vacuum bakeout may alleviate this out gassing problem similar to the technique used successfully with the Spacelab tunnel flexible element.

This test data is reported in WSTF #83-15810 (JSC #4065) as part of NASA JSC materials test results.

During a study of space station crew safety alternatives, (Reference 6) Rockwell International has defined a potential need of a flexible acoustic curtain to provide a quiet enclosure around a crew member living in a noisy environment. The curtain is normally stored in a packaged condition and deployed as required by the crew member to enclose his work station.

Sound Reduction Values

ACOUSTA SHEET 200 AND 300

This chart illustrates the sound transmission loss values expressed in decibel reduction over the hertz frequency range for Acousta sheet 200 (Black) and 300 (Blue). For example, at the 1000 hertz reading, the sound transmission loss was 28 dBA.

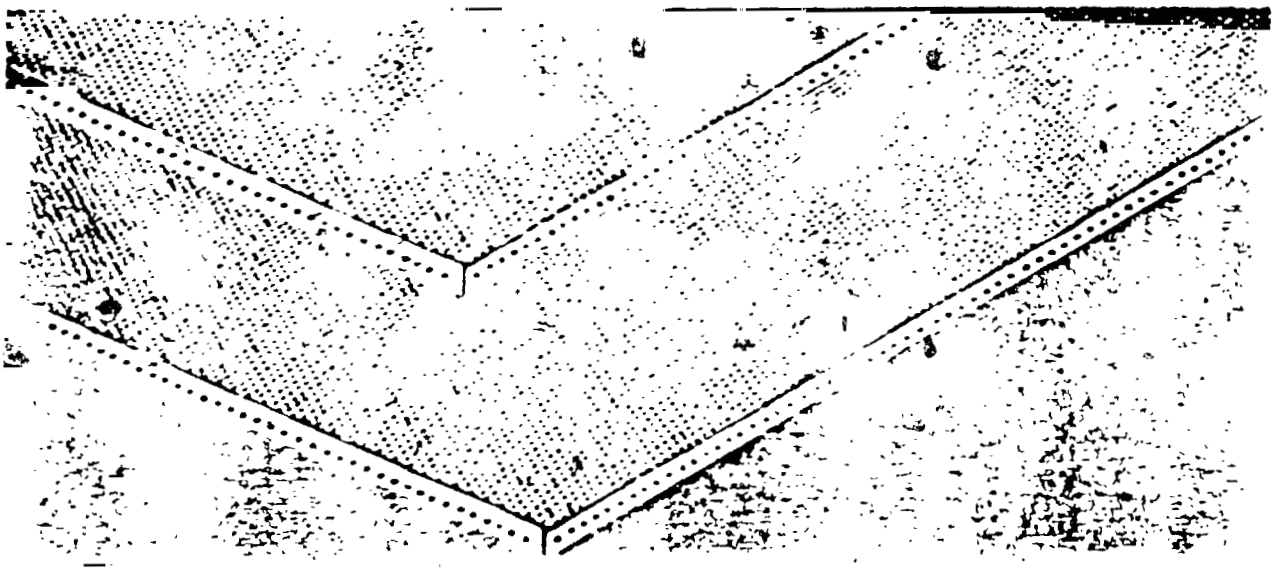

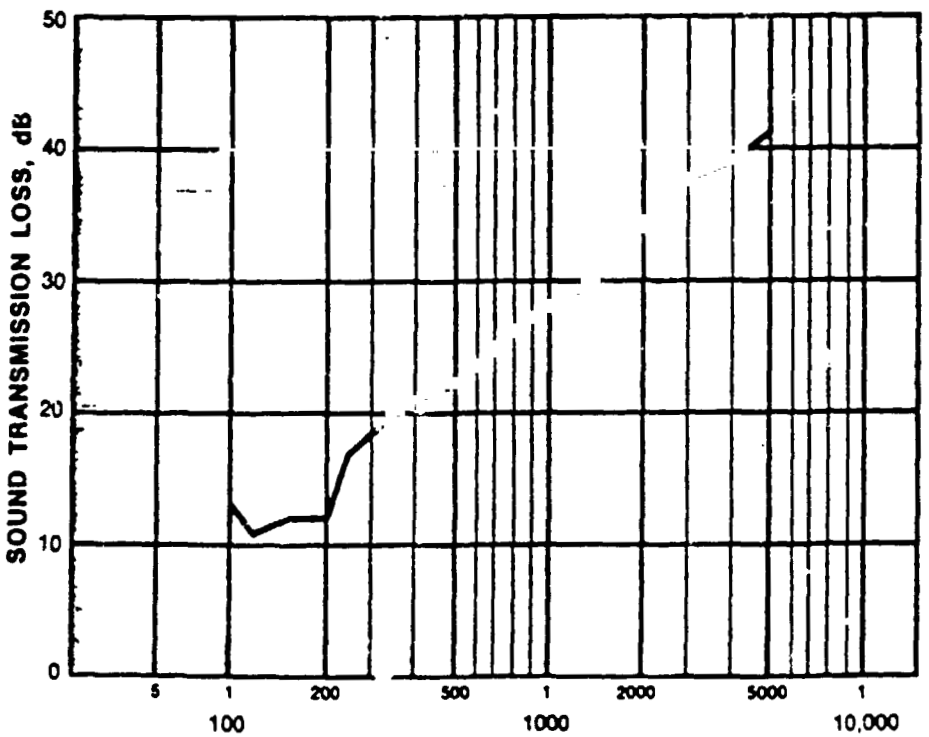

PHYSICAL PROPERTIES*

	Style 200 and Style 300
Noise reduction	See chart
Weight per square foot	1.1 lbs approx
Gauge	0.108" approx
Width	48" ± 2"
Length of Standard roll	45' ± 5'
Maximum pieces per roll	2
Minimum length per roll	15'
Temperature range	0° to 275°F.
Color	Style 200 — Black Style 300 — Blue
Resistance to	
Water	Good
Petroleum	Good
Alkalies	Good
Flame	(1) Self-extinguishing per federal test method 191, method 5903 (2) Index 15 on flame spread for ASTM E-162, Radiant Panel Test (3) Meets M S H A flame resistant requirements

CONSTRUCTION — Style 200 and 300 — 0.108" ga. x 48" x 45'

Hertz —	100	125	160	200	250	315	400	500	800	1000	1250	1600	2000	2500	3150	4000	5000
dBA Loss —	13	11	12	12	17	19	21	22	26	28	29	31	34	36	38	39	41

FREQUENCY, HERTZ (CYCLES PER SECOND)

Chart shows sound transmission loss properties expressed in decibels. Values are tabulated at the eighteen standard frequencies. Sound Transmission Class is 26 and is computed in accordance with ASTM E 90 - 70 and E 413-70 T

*Based on tests conducted under controlled conditions by Riverbank Acoustical Laboratories, Sound Transmission Loss Test TL-75-118 dated August 19, 1975

FIGURE IIB-1 SOUND REDUCTION VALUES FOR ACOUSTA SHEET 200 AND 300

This acoustic curtain can also be used in the space station environment to attenuate the noise by proper placement near the noise source. Reference 7 summarizes comments of the Skylab and Shuttle crews indicating the problem areas and suggesting potential solutions. Isolating the sleep area and quieting the operational area were considered most important. The noise problem appeared to increase with the duration of the mission, thus showing its importance for space station consideration.

C. DEPLOYABLE FABRIC BULKHEAD IN A SPACE HABITAT

Use of an automatically deployable fabric bulkhead in a space habitat in the event of fire, natural out gassing, spills/leakage, or a similar threat may be advisable to isolate the crew members until repair or safe rescue can be effected (see Reference 6). If the bulkhead is deployed from a central station in the space habitat, deployment can be achieved at a faster rate in a controlled manner and pressure loads on the bulkhead minimized because of the lower radii.

Goodyear has developed several materials suitable for this type of application. The acousta sheet material properties are summarized in Figure IIB-1. The material qualified for the flex section spacelab transfer tunnel is defined in Appendix C. These materials are considered acceptable for space habitats meeting the out gassing and flexibility requirements. Modifications to these materials may be necessary for structural considerations in specific applications. The data is presented here for guidance when designing future nonmetallic structures for use in space.

D. EXTENDIBLE TUNNEL FOR SOFT DOCKING

Space station studies have indicated a potential need for a soft docking concept similar in thought to the loading ramps used with airliners at airports. The final interface connection can be made by moving a flexible tunnel between large vehicles or bases which are difficult to maneuver for small distances. Figure IID-1 taken from Reference 8 depicts this concept schematically.

Goodyear Aerospace designed and built a flexible tunnel of this type under NASA contract NAS8-30594 with Marshall Space Flight Center. The tunnel, about four feet in diameter and up to 18 feet long, was designed for use between the Shuttle's crew compartment and the Spacelab. Figures IID-2 and IID-3 depict the flexible tunnel in extended and retracted conditions, respectively. Following interface connections at the free end of the tunnel, pressurization in the tunnel will permit personnel to move from the Shuttle to the space station in a shirtsleeve environment.

The tunnel's interior pressure bladder consists of eight plies of material, including aluminum foil, nylon cloth, and capran film. This has an outer structural liner of Kevlar cloth which has a strength of 1,500 by 1,500 pounds per inch. A polyurethane foam serves as the micrometeroid barrier. A typical multilayer insulation system of aluminized mylar sheets separated by fabric netting is used at the outer surface for passive thermal control in the space environment.

EXTENDABLE TUNNEL
(SOFT)

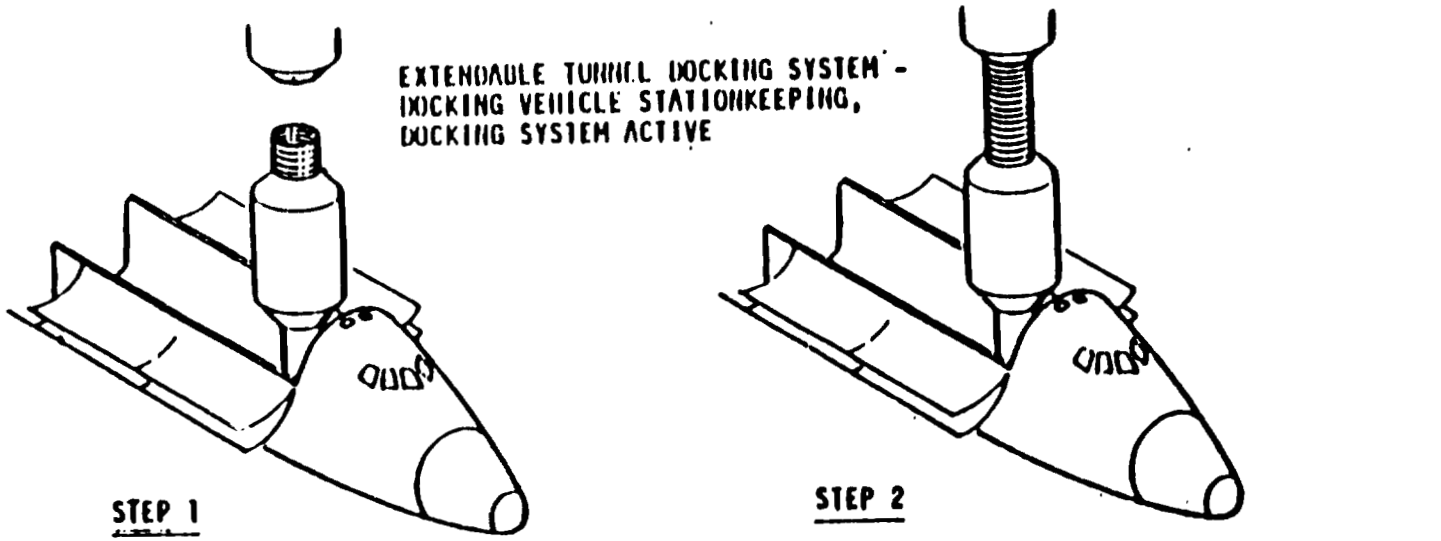

- EXTENDABLE TUNNEL DOCKING SYSTEM CONCEPT

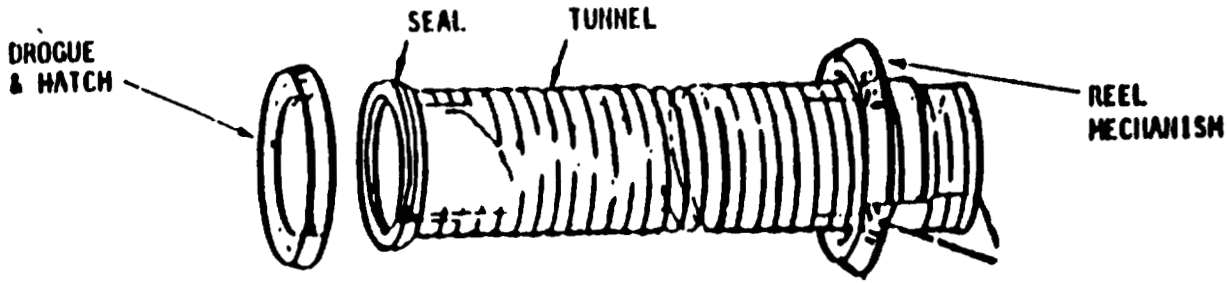

- ONE EXTENDABLE TUNNEL DOCKING SYSTEM CONCEPT ADAPTED FROM A CONCEPT CONSIDERED FOR THE APOLLO IS SHOWN. IT EMPLOYS A DOCKING PORT ATTACHED TO ONE END OF AN ACCORDIAN-LIKE BELLOWS TUBE, EXTENDABLE TO APPROXIMATELY 3m (10 FT) IN LENGTH. TESTS IN TWO-DIMENSIONAL SIMULATED DOCKING OF THE APOLLO USING THIS SYSTEM SHOWED THAT IT WAS FEASIBLE & HAD NO MAJOR PROBLEMS

Rockwell International

SSSV136645

FIGURE IID-1 SCHEMATIC OF EXTENDIBLE TUNNEL (SOFT) DOCKING SYSTEM

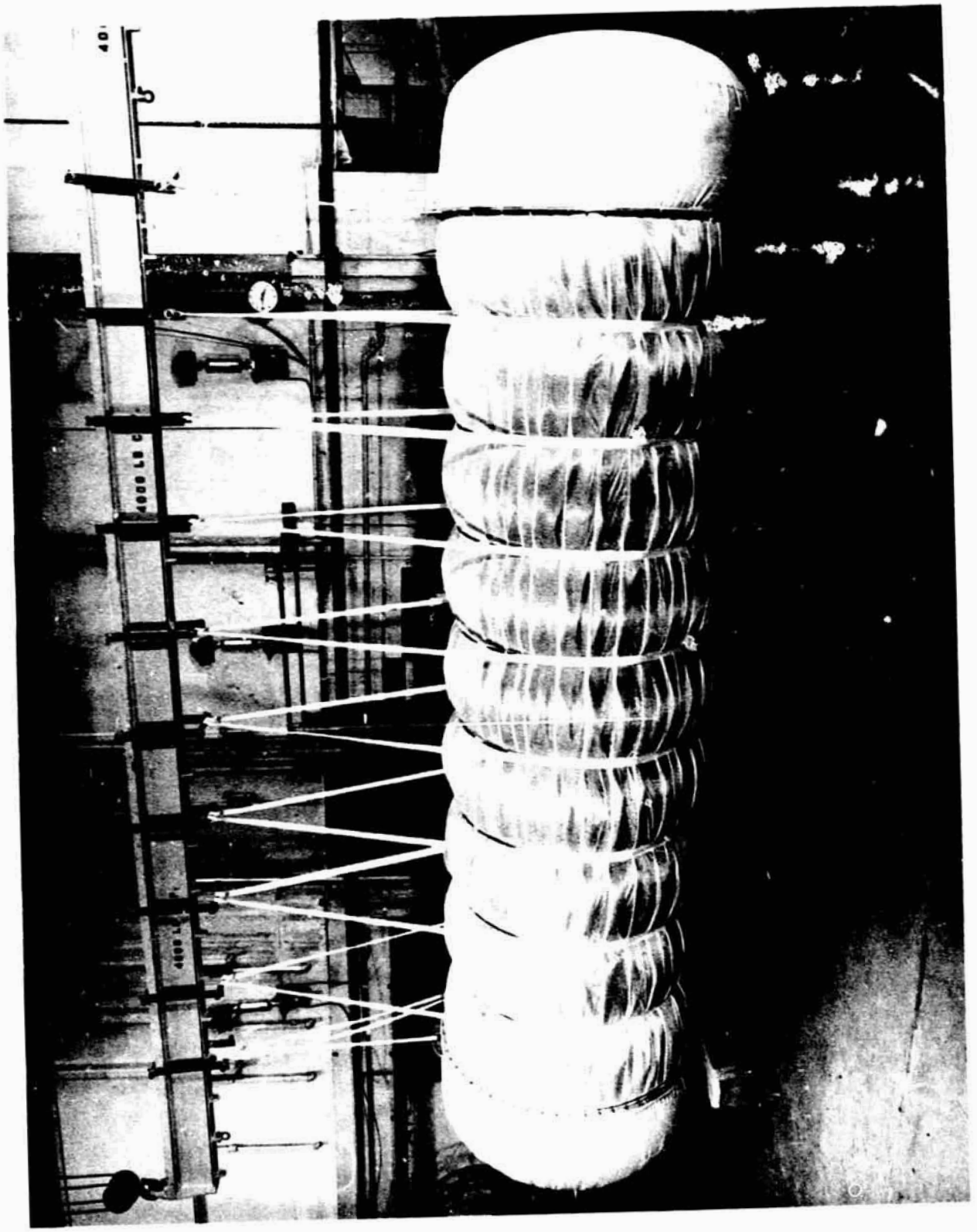

FIGURE II D-2 EXTERNAL VIEW OF FLEXIBLE TUNNEL IN EXTENDED CONDITION

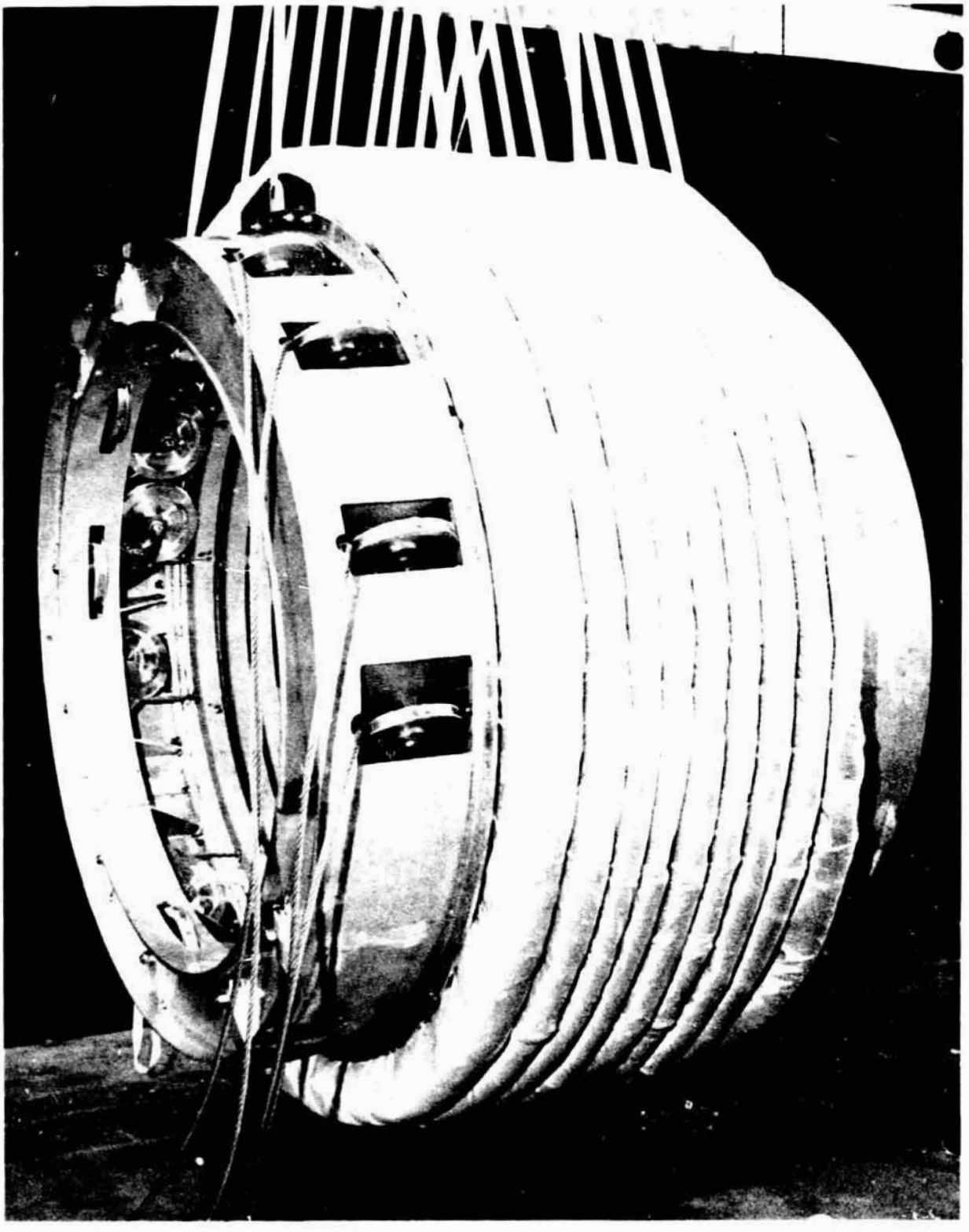

FIGURE IID-3 EXTERNAL VIEW OF FLEXIBLE TUNNEL IN RETRACTED CONDITION

During the study of a large flexible tunnel for Shuttle/Payload Interface (Reference 9) several concepts were investigated. GAC designed, fabricated and functionally tested a 1/4-scale model and a preliminary design and analysis of a full-scale model was completed. This cable-supported tunnel in 1/4-scale model is shown in Figures IID-4, IID-5, and IID-6 for straight deployment, curved deployment, and internal views, respectively. This model work culminated in the design and fabrication of the full-scale ground test model of the cable-supported tunnel previously shown in Figures IID-2 and IID-3 (Reference 10).

This data is presented to summarize the effort GAC has conducted in the soft tunnel concept. It is hoped that this information will lead to new and related ideas to solve the soft-docking phenomenon. New space-compatible materials have since been developed, therefore, it is unlikely that the material construction presented herein will be duplicated in the future.

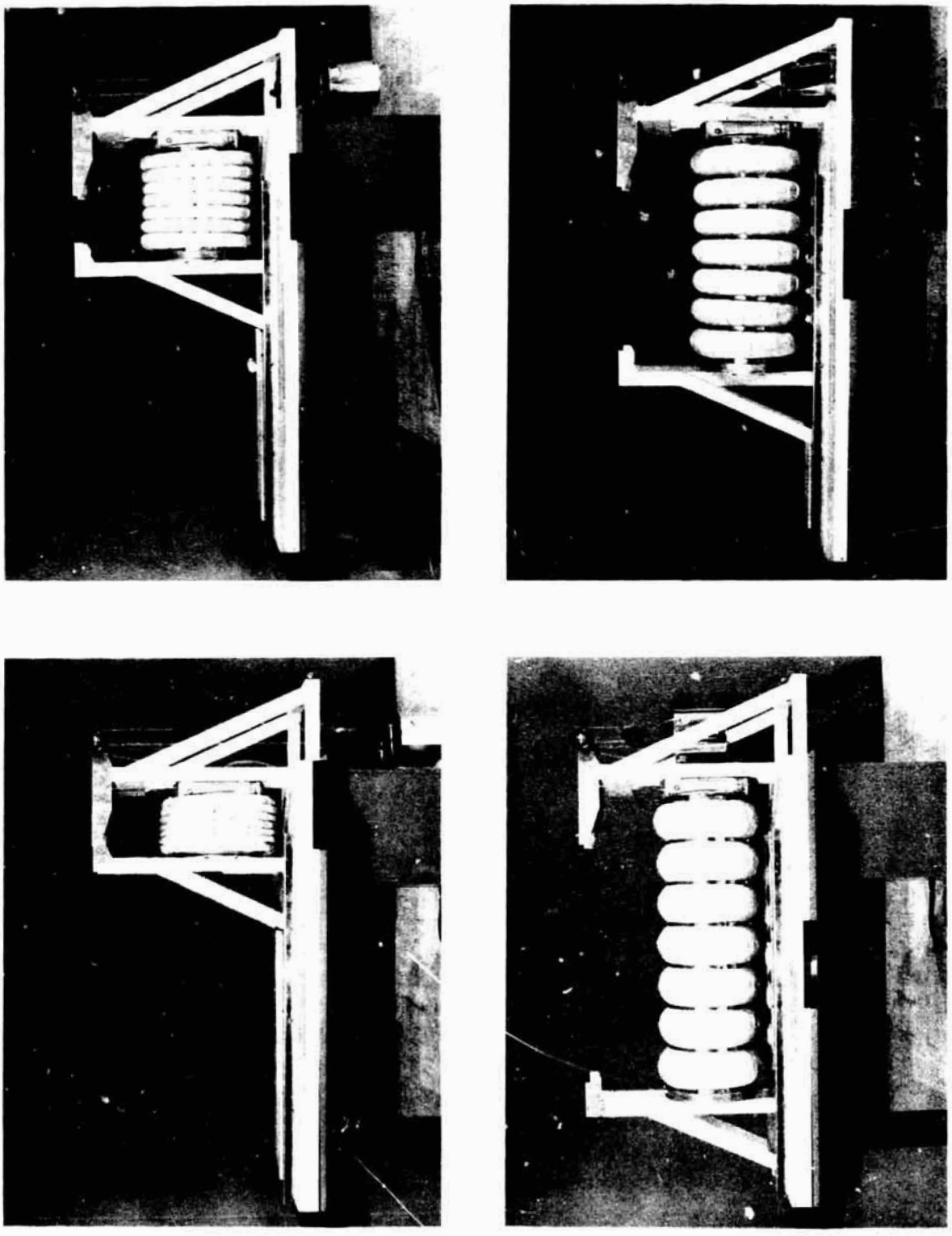

FIGURE IID-4 SHUTTLE/PAYLOAD INTERFACE TUNNEL MODEL - STRAIGHT DEPLOYMENT

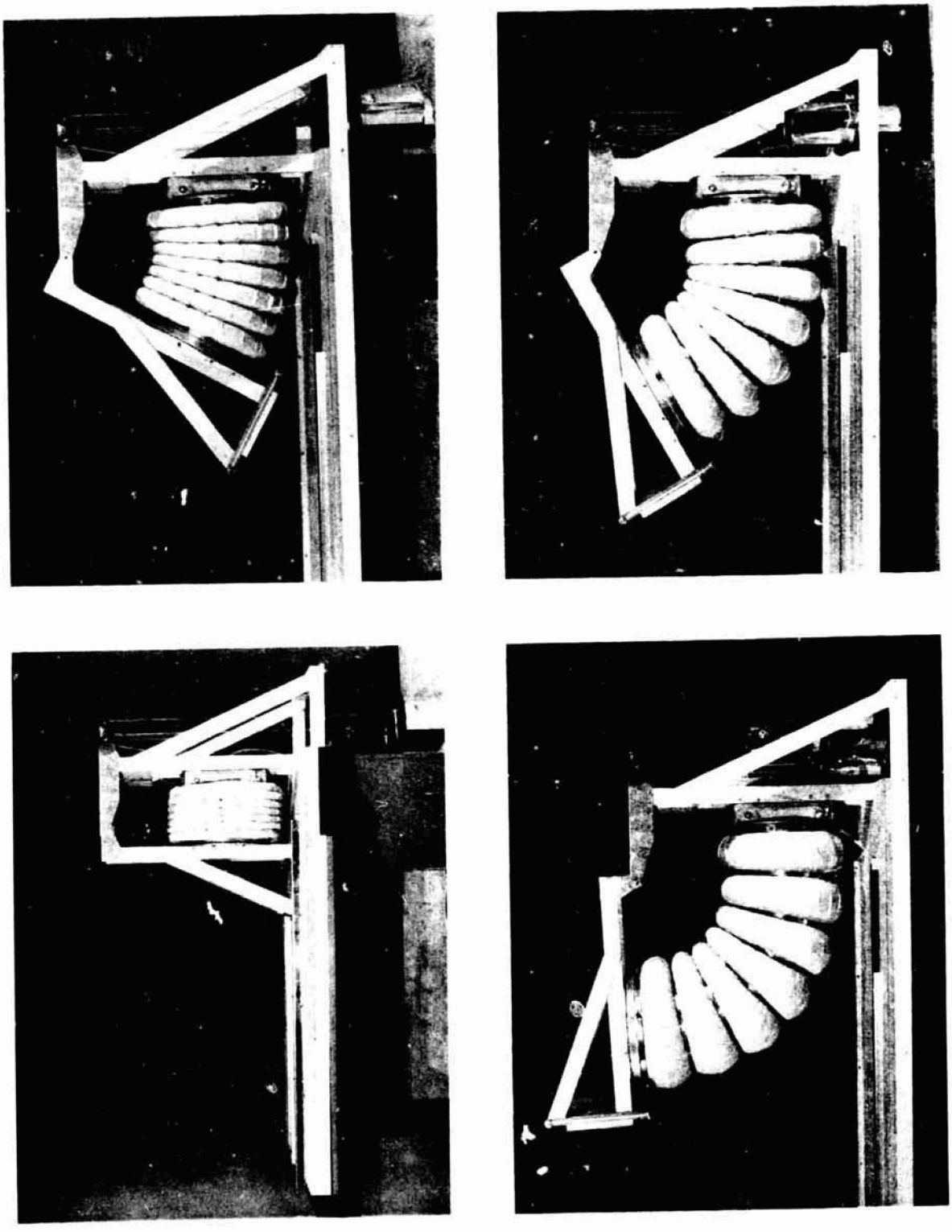

FIGURE IID-5 SHUTTLE/PAYLOAD INTERFACE TUNNEL MODEL - CURVED DEPLOYMENT

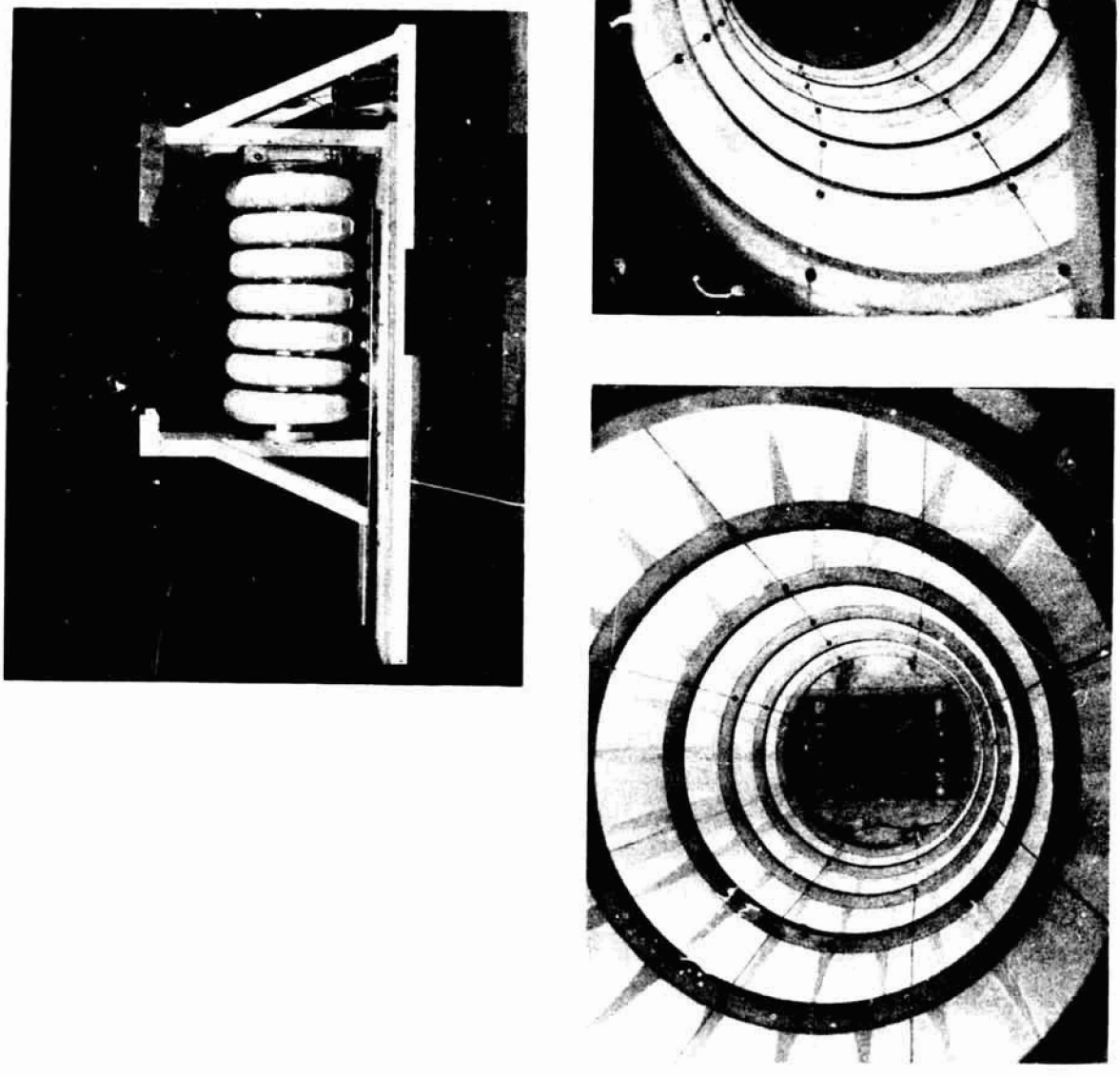

FIGURE IID-6 SHUTTLE/PAYLOAD INTERFACE TUNNEL MODEL - INTERNAL VIEWS

E. DEPLOYABLE SPACE RECOVERY/RE-ENTRY SYSTEMS - PERSONNEL OR MATERIALS

GAC has been active in recovery or escape from space using deployable structures early in the space program. This effort included study of techniques for deployment, inflation, orbital injection and re-entry thermal control.

The early studies on the Dynasoar manned re-entry vehicle and missile recovery systems utilized a deployable structure of Rene 41 wire mesh substructure with CS105 elastomeric coating. The upper temperature limits for the material were considered in the 1,500 to 1,800°F range. Re-entry bodies were designed with radii of sufficient size to ensure that maximum temperatures never exceeded 1,800°F. After passing through the re-entry phase, the CS105 elastomer turned into a ceramic-like material as a result of the heat. Many studies were made of different applications and some models were constructed; however, no prototype hardware was constructed.

Rockwell International (Reference 6) summarized the deployable manned escape systems considered by Government and Industry during the past twenty years. These are shown in Figure IIE-1 for convenience. GAC was involved in the AIRMAT and ENCAP escape systems using experience gained with escape capsule development for government high-speed aircraft. GAC also worked on a saver escape balloon concept similar to Rockwell's which eventually led to the discovery of the Ballute for deceleration and stabilization of bodies traveling at high speed. Ballutes have been very effective as drogues or stabilizers for high speed recovery systems and missiles. GAC presently has production contracts for stabilization and deceleration of 500 and 2,000 pound bomb systems delivered by high-speed aircraft for the Air Force. Many similar deployable Ballute systems have been studied, built, tested and manufactured in quantity. Ballute performance is predictable by GAC structural and dynamic specialists based on test results and extensive experience in the design of "Rag" structures.

PARACONE ESCAPE CONCEPT (MDAC)

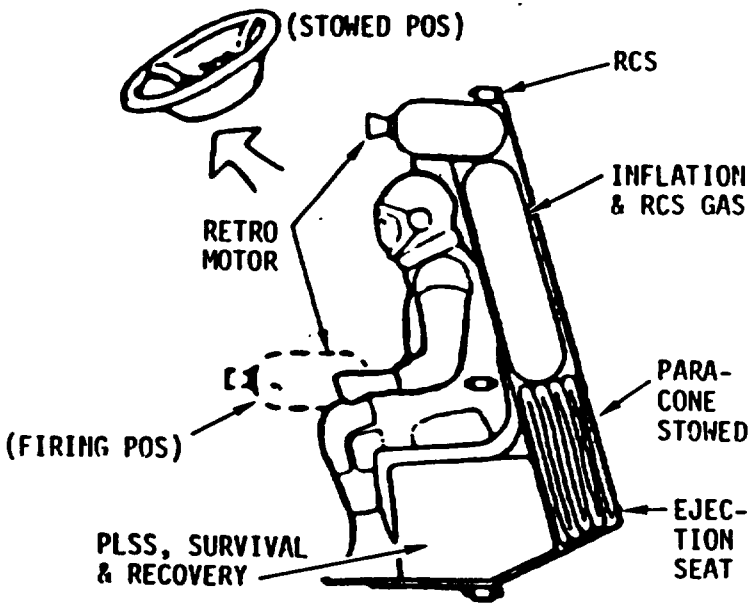

- 1 MAN
- SUIT
- INFLATABLE
- 192 KG (425 LB)
- NEW TECHNOLOGY REQUIREMENTS
  - LARGE INFLATABLE & DEPLOYABLE STRUCTURE
  - MATERIAL

MOOSE ESCAPE CONCEPT MANNED ORBITAL OPERATIONS SAFETY EQUIPMENT (GE)

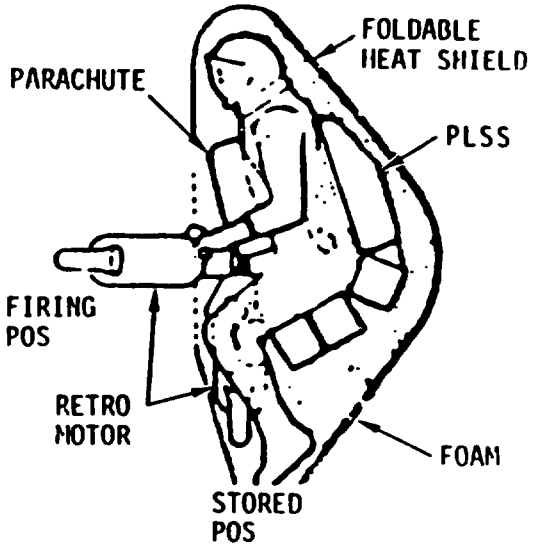

- 1 MAN
- SUIT
- HAND-HELD RETRO
- ALL EQUIPMENT CARRIED EVA
- FOAM-IN-PLACE
- 215 KG (475 LB)
- NEW TECHNOLOGY REQUIREMENTS
  - FOAM IN SPACE
  - FOLDABLE HEAT SHIELD

FIGURE IIE-1 DEPLOYABLE MANNED ESCAPE SYSTEMS

DEPLOYABLE

AIRMAT ESCAPE CONCEPT (GOODYEAR)

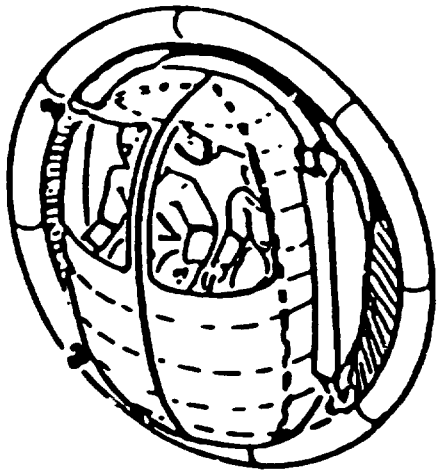

- 2-MAN
- SUITS REQUIRED
- INFLATABLE
- EJECTION SEAT
- 518 KG (1140 LB)
- NEW TECHNOLOGY REQUIREMENTS
  - FLEXIBLE HEAT SHIELD
  - MATERIAL

RIB-STIFFENED EXPANDABLE ESCAPE CONCEPT (ROCKWELL)

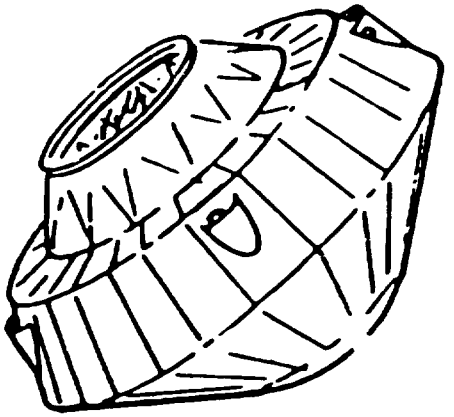

- 3-MAN
- SHIRTSLEEVE ENVIRONMENT
- MECH RIGID
- CANISTER STOPED
- 660 KG (1452 LB)
- NEW TECHNOLOGY REQUIREMENTS
  - ARTICULATING RIB-TRUSS STRUCTURE
  - MATERIAL

FIGURE IIE-1 DEPLOYABLE MANNED ESCAPE SYSTEMS (CONT.)

ENCAP ESCAPE CONCEPT

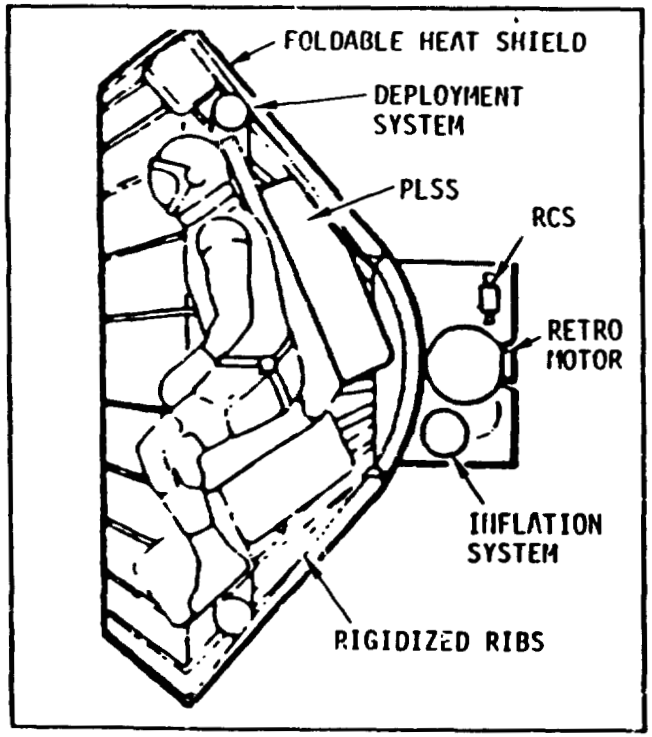

- 1 MAN
- SUIT
- EVA
- MECH RIGID
- 24 KG (588 LB)
- *NEW TECHNOLOGY REQUIREMENTS*
  - MECHANICAL DEPLOYMENT MECHANISM
  - FOLDABLE HEAT SHIELD

SAVER ESCAPE CONCEPT (ROCKWELL)

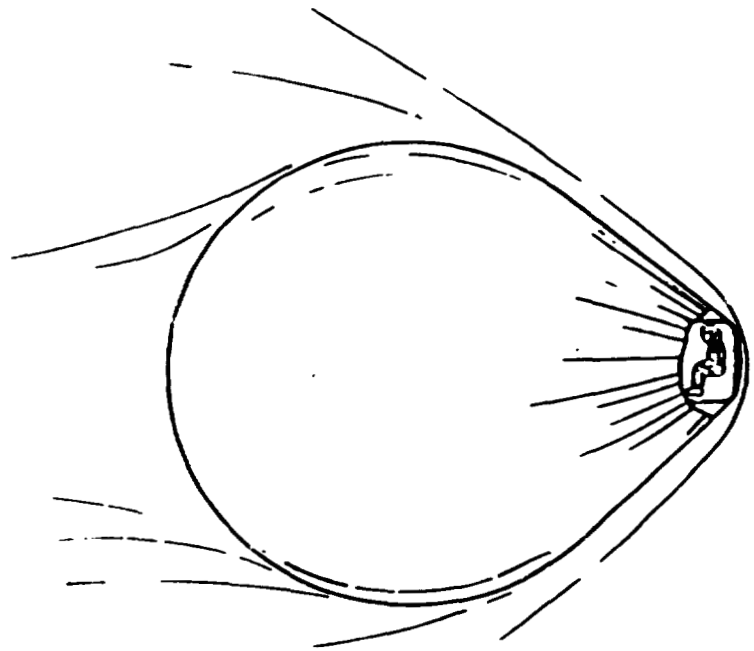

- 1 MAN
- LARGE INFLATABLE LIGHTWEIGHT BALLOON
- SUITS & LIFE SUPPORT REQUIRED
- MODULATED DRAG & DECELERATION g LOADS
- NEW TECHNOLOGY

FIGURE IIE-1 DEPLOYABLE MANNED ESCAPE SYSTEMS (CONCLUDED)

The Ballute is successfully being considered as a decelerating/stabilizing body for an Orbital Transfer Vehicle (OTV) for orbital changes from GEO to LEO. Reference 11 gives a good review of performance parameters for the Ballutes.

New materials have been developed which should open new areas for deployable systems in the recovery/re-entry discipline. Nextel ^{R} and Nicalon ^{R} have recently been developed and tested to temperatures in the 2,500 to 3,000^{o}F range. These materials are available in thread, woven cloth, and non-woven felt pad. Nextel ^{R} is a ceramic fiber product of 3M which becomes rigid at the high temperature condition. Nicalon ^{R} is a silicone carbide fiber which remains flexible to the 3,000^{o}F range. GAC uses these two materials in a limited or multilayer blanket form for OTV Ballute insulation. Thermal tests of representative assemblies have shown the material to be suitable for OTV consideration. Indeed, these new and improved materials could provide realism and viability to the deployable recovery/re-entry systems proposed in the past. Typical Nextel ^{R} and Nicalon ^{R} material samples were provided to NASA-MSFC for testing of flammability and out-gassing characteristics and compatibility with the space environment.

F. MANNED HABITAT FOR A SPACE STATION

A flexible material considered acceptable for space applications is a fabric consisting of Nomex unidirectional cloth coated with Viton B-50 elastomer. Goodyear has qualified this material to strict requirements of the NASA Space Shuttle Orbiter Crew Cabin and Spacelab module. Since much input in the present study relies on work conducted with the flex section, the following paragraphs have been added to summarize the goals and achievements attained while qualifying this unique material.

Each Nomex/Viton B-50 material ply had the following properties:

	Average Values
Strip Tensile Strength	1,074 lb/inch
Weight, after cure	4 .13 oz/yd^2
Thickness, after cure	0.040 inch
Peel Adhesion, after cure	29.7 lb/inch
after post cure	29.7 lb/inch

Tests verified that material XA30A553 met the required values and could be used in constructing the flexible element development test models. (See Appendix C for more details)

Figure IIF-1 shows the inflatable shell GAC proposes as interfaced with the RI strongback defined in RI Habitat Module, Concept 3. (See Reference 3) A planar interface is projected to simplify fabrication and eliminate potential leakage areas. An even number of multiple layers of the Nomex/Viton B-50 qualified material will be laminated together until adequate strength is obtained. The type of interface connection envisioned is shown in Figure IIF-2. A flexible cable will serve as the bead to assure structural integrity during deployment and fully inflated operational conditions. This system has also been used effectively to eliminate pressure leaks at mechanical interfaces.

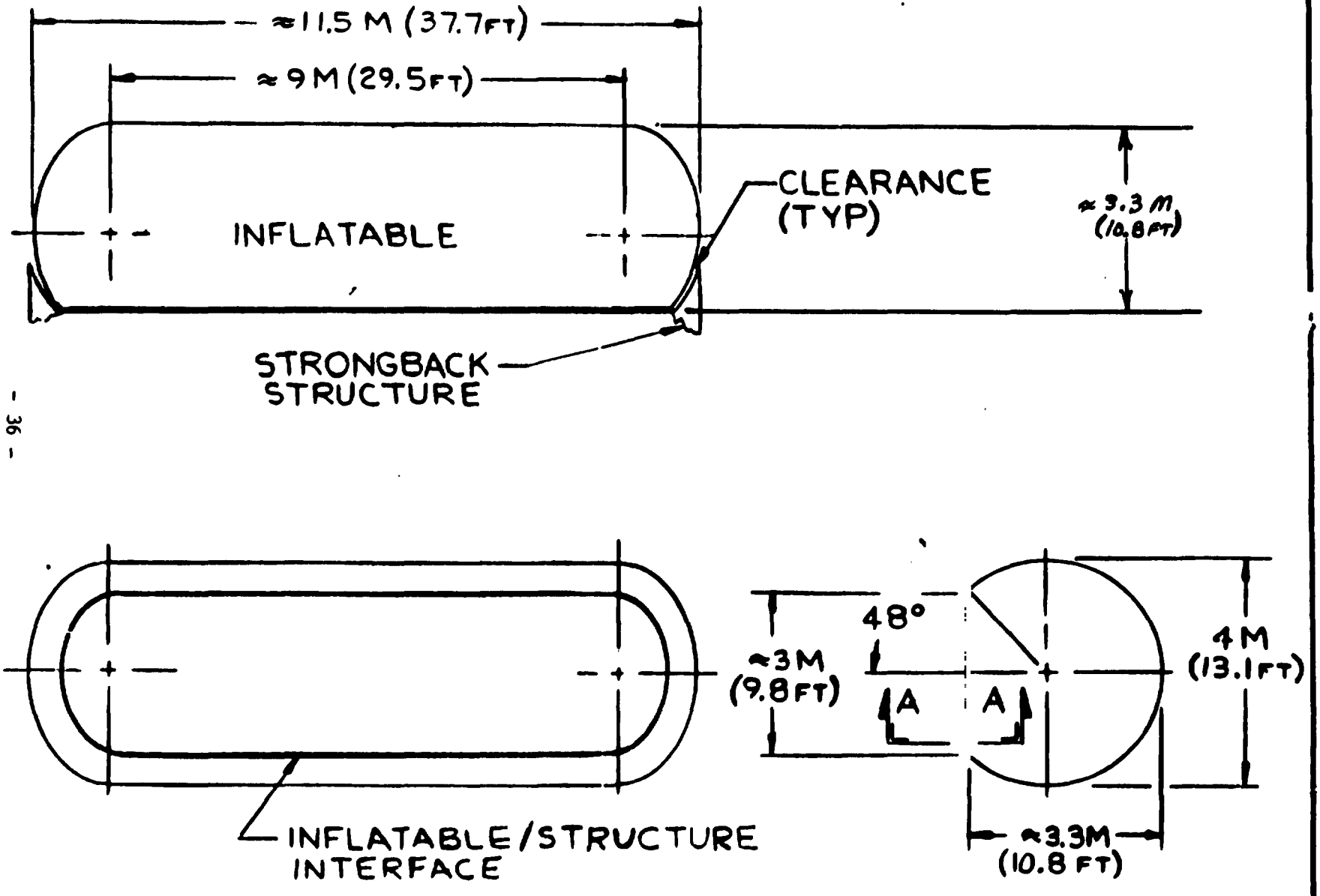

FIGURE IIF-1 INFLATABLE SHELL OF HABITAT MODULE (RI CONCEPT 3)

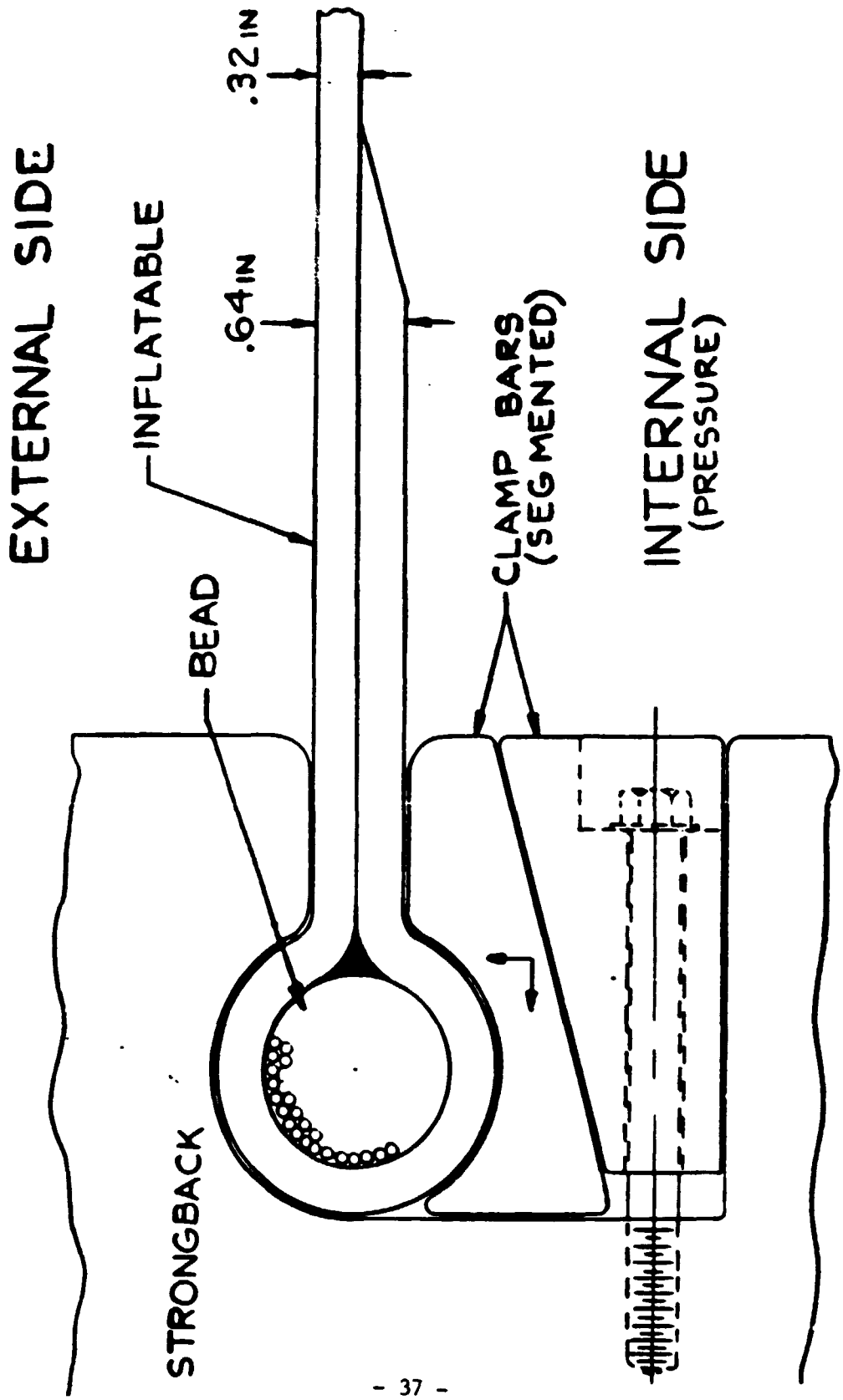

FIGURE IIF-2 INFLATABLE SHELL/STRONGBACK INTERFACE CONNECTION

By attaching film to the rigid surface inboard of bead section, the potential leakage path of the bead is eliminated. Pressure inside the habitat will help film in its sealing action also. Excess material should be provided in bead-crotch area to prevent film from taking any stretching loads resulting from the Habitat internal pressure.

Figures IIF-3 and IIF-4 define the characteristics of the habitat inflatable shell material proposed by GAC for both no-foam and with-foam conditions. Whether or not foam is required for micrometeoroid protection is not known at this time. Future tests will confirm this design feature. The aluminum foil layer was defined as a flame barrier in earlier GAC studies. The foil may not be necessary with the Nomex/Viton B-50 material; however, it is believed that some cosmetic layer would be required on the pressure side so the weight was left in at this time. Present estimates are that each shell weighs approximately 3,700 lbs.

Each of the inflatable shells of the habitat is a 4 meter (13.123 ft.) diameter cylinder. For a design operating pressure of 14.7 psig, the limit circumferential and longitudinal membrane stresses are simply,

$$\sigma_c = pR = 14.7\left(\frac{13.123}{2}\right)\left(12\right) = 1157.5 \text{ lbs/inch} \qquad (1)$$

$$\sigma_\ell = \frac{1}{2}\sigma_c = 578.75 \text{ lbs/inch} \qquad (2)$$

These stresses are carried by the required number of plies of cord-type fabric that is laid-up in a fashion similar to filament winding. The circumferential plies are actually placed at $\pm$ 75 degrees with respect to the longitudinal axis of the cylinder and terminate near the tangency of the cylinder to the end domes. The longitudinal plies are wrapped at $\pm$ 15 degrees with respect to the longitudinal axis of the cylinder and continue on to form the end domes. Woven fabric or rigid metal domes may be used.

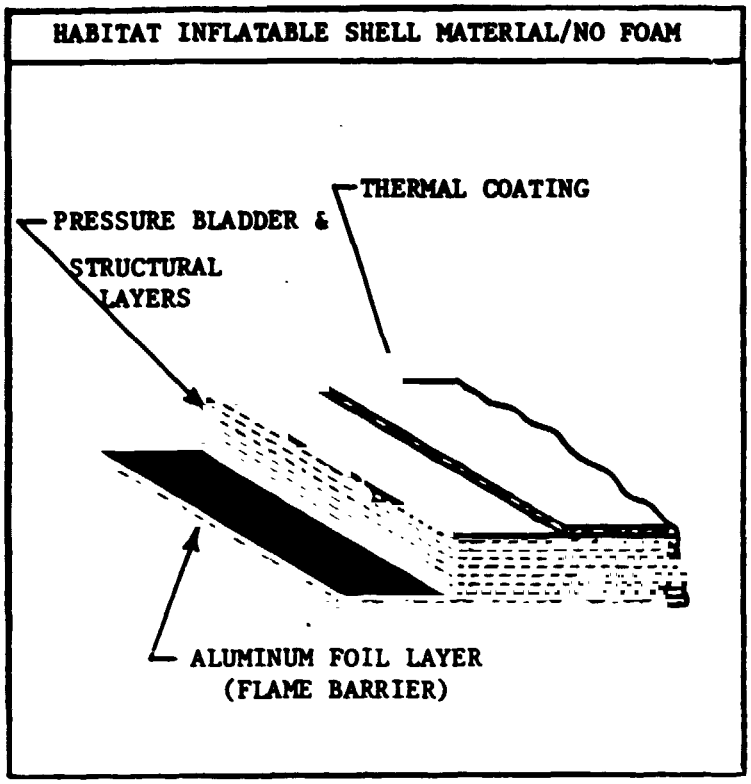

DETAIL WEIGHTS
OF INFLATABLE MATERIALS

CONSTRUCTION	GM/CM^2	OZ/YARD^2
ALUMINUM FOIL LAYER	0.002	0.590
ADHESIVE	0.005	1.474
STRUCTURAL LAYERS	1.370	405
ADHESIVE	0.005	1.474
THERMAL COATING	0.031	9.139
TOTAL	1.42	418

FIGURE IIF-3 CHARACTERISTICS OF HABITAT INFLATABLE SHELL MATERIAL/NO FOAM

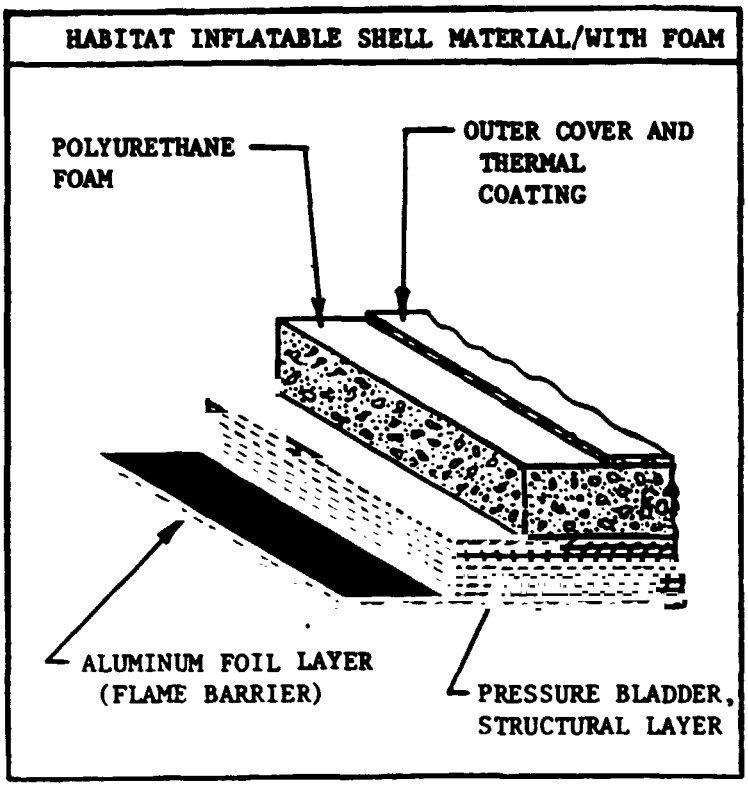

DETAIL WEIGHT
OF INFLATABLE MATERIALS

CONSTRUCTION	GM/CM^2	OZ/YARDS^2
ALUMINUM FOIL LAYER	0.002	0.590
ADHESIVE	0.005	1.474
STRUCTURAL LAYER	1.370	405
TASLAN INTERLOCKING LAYER & ADHESIVE	0.024	7.075
ONE INCH POLYURETHANE FOAM	0.080	23.584
ADHESIVE	0.005	1.474
OUTER COVER AND THERMAL COATING	0.031	9.139
TOTAL	1.52	448

E-1D-1517-711
REF: EOI 380

FIGURE IIF-4 CHARACTERISTICS OF HABITAT INFLATABLE SHELL MATERIAL/WITH FOAM

Design factors as used in the Spacelab Transfer Flex Section are applied. Assuming that the inflatable shell is capable of withstanding a slit one-half inch long, these factors are:

Basic factor of safety = 1.50

Temperature degradation factor at 120°F = 1.03

Concentration factor due to 1/2 inch slit (16 cords cut per each ply) is 3.65

Therefore, the combined factor is, D. F. = 5.64 (6)

Solving the applicable equations gives circumferential plies = 5 and longitudinal plies = 2.55

In order to obtain these required number of plies and also have symmetry, a total of 9 plies are required. With respect to the axis of the cylinder, one ply at 90 degrees, four plies at $\pm$ 75 degrees and four plies at $\pm$ 15 degrees extend past the cylinder to form the end domes. Hence, the total thickness and unit weights become 0.32 inches and 405 oz/yd^2 (1.37 gm/cm^2) over the cylinder and 0.14 inches and 180 oz/yd^2 (0.61 gm/cm^2) over the dome ends.

The above unit weights of the structural layers are combined with those for nonstructural layers in Figure IIF-3. Here, the total unit weights are then 418 oz/yd^2 (1.42 gm/cm^2) over the cylinder and 193 oz/yd^2 (0.65 gm/cm^2) over the dome ends. The following weight estimate uses these unit weights along with the geometry of Figures IIF-1 and IIF-2.

The following weights are for one of the inflatable shells:

Cylinder weight	=	2,750 lbs.
Two Domes	=	600 lbs.
Bead Cable	=	350 lbs.
		3,700 lbs., total

Since the inflatable shell material for the habitat is projected to weigh about 1.4 gm/cm^2, its weight is considerably above the 0.50 gm/cm^2 usually considered adequate for radiation protection of the crew.

Figure IIF-5 depicts schematically the inflatable habitat from packaged to deployed condition within the envelope established by RI. No unusual problems are anticipated at this time. The shell material is thicker than originally anticipated but should offer no functional difficulties. This is no longer an "elastic recovery" material approach because of the structural material requirements.

This RI concept (Reference 3) consists essentially of an inflatable shell mounted on each side of a strongback. The strongback serves as a launch cradle, a mounting platform for equipment, and as a structural support for the airlocks and docking systems. The covers for the stowed inflatables are used as radiators once the inflatable shells are deployed. The deployed module forms two separate sections for safety and redundancy, with the strongback providing a long central floor. The two docking systems and one airlock in the strongback conform to standard habitat module practice for design and placement.

A package volume of 186 ft^3 is available for storing each shell. The shell material volume is around 35 ft^3. This gives a packing factor of over 5 which seems more than adequate.

Mounting of equipment to the inflatable can be accomplished best through use of Velcro, straps with hooks or rings attached or metal (no snag) hardware attached directly to the inflatable inner surface. This hardware can be readily attached using circular or finger patches to distribute the resultant load into the inflatable surface. Rigid equipment can be attached to the inflatable shell once the habitat is in operation.

Rather than add other inflatable frames to the shell, it is recommended that rigid foldable or telescoping frames be attached to the inflatable surface once deployed and used as a building-block concept to add more equipment.

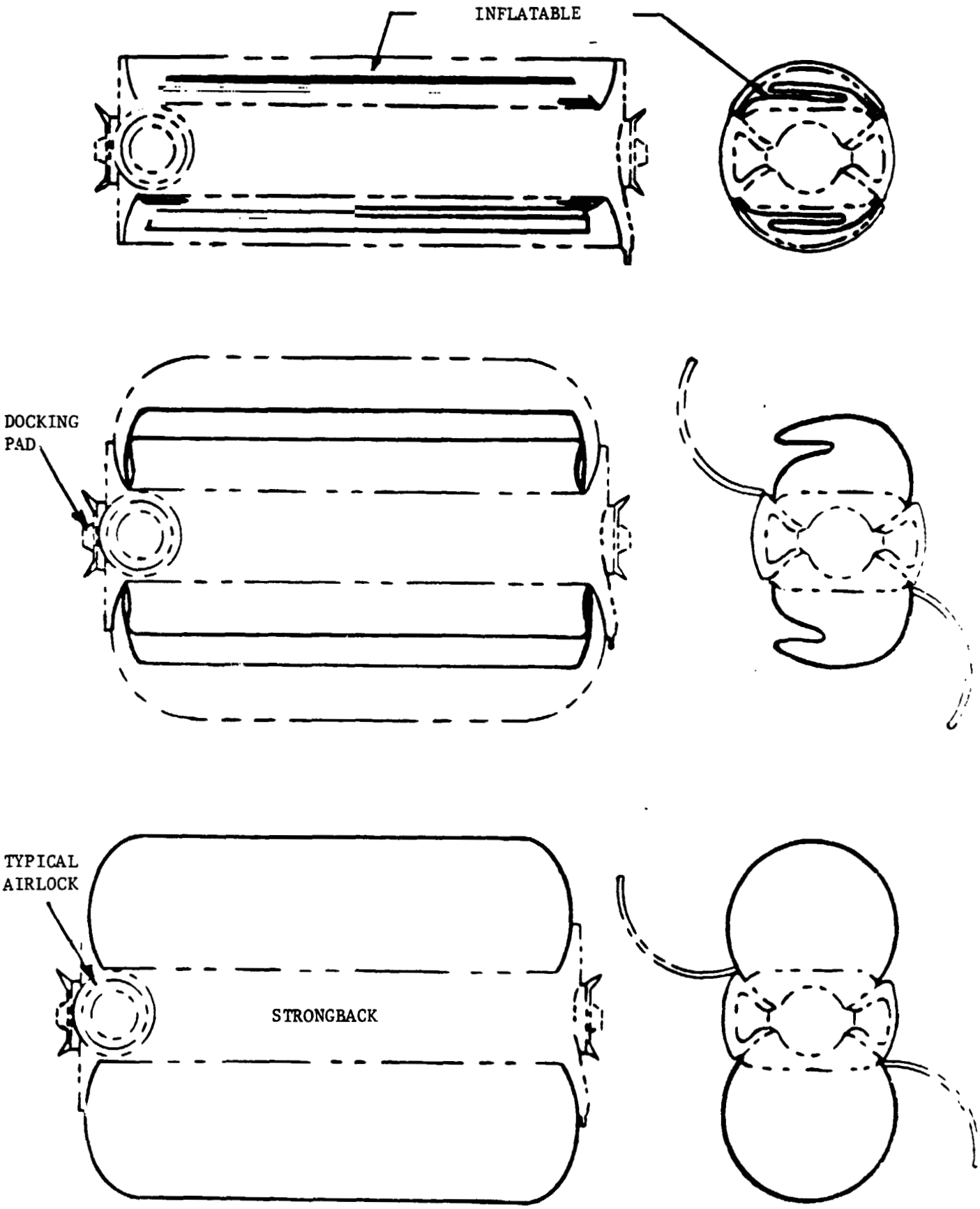

FIGURE IIF-5 HABITAT INFLATABLE SHELL FROM PACKAGED TO DEPLOYED CONDITION

G. ADDITIONAL CONSIDERATIONS

Many other subsystem and system ideas and concepts for non-metallic structures have been discussed with cognizant space engineers and scientists in government and industry. The following list is given for information only, since funding and schedule limitations of the program do not permit a detailed design analysis:

1) A Storage Volume external of the Space Station habitat
2) A Debris or Junk Enclosure external of the Space Station habitat
3) Attachable work stations for special or isolated projects
4) Safe Haven Structures

Some of these ideas seem similar; however, no one solution will serve all of the above goals. Once a space station design becomes a reality, specific requirements for some of the above ideas will evolve.

Studies of space stations or free flying platforms have indicated a need for "safe-haven" provisions. Reference 6 suggests an external inflatable volume or a temporary volume enclosed with inflatable bulkheads. Reference 12 indicates that in a free-flying platform type of configuration, not attended by orbiter, crew safety must be assured by the provision of a dedicated safe haven, containing sufficient life support capabilities to assure crew survival until rescue by orbiter. At least 2 discrete, emergency safe haven habitable volumes are to be provided at all times and provisions for rescue of the crew from an isolated "safe haven" by orbiter ought to be made.

The Lunar Shelter (Stay Time Extension Module, STEM) developed by GAC during Apollo days may readily be adopted to the "safe-haven" concept for space stations. (Reference 13)

SECTION III -- PERFORMANCE PARAMETERS

A. MICROMETEOROID PROTECTION OF INFLATABLE/DEPLOYABLE STRUCTURES

The selection of flexible polyurethane foam as a micrometeoroid barrier for inflatable/deployable structures is based on company-sponsored hypervelocity particle impact tests conducted at the Illinois Institute of Technology and tests conducted at the RTD facility in Dayton. As a result of these tests (0.0045-gram particles at 22,000 ft/sec and 0.005 gram particles at 30,000 ft/sec), it was concluded that foam of 1.2-pcf density was equivalent to a single sheet of aluminum of 15 times the mass per unit area. Thus, a two-inch thickness of 1.2 pcf foam is considered equivalent to an aluminum sheet 0.53-cm thick (1.44 gm/cm^2) with respect to penetration resistance. Based on preliminary analysis, the probability of zero penetration for a 30-day period will exceed 0.999.

Figure IIIA-1 summarizes the types of materials tested for Goodyear for micrometeoroid protection systems to be used with inflatable or flexible structures in space. These data can be used as a starting point if additional tests are required for the hangar as well as the manned habitat application.

The average cumulative total meteoroid flux-mass model for 1 A.U. has been essentially the same for the last twenty years. For this reason the foam micrometeoroid protection system is still a viable approach.

The density of the foam barrier was increased in development studies from 1 to 2 lb/cu ft to provide a non-flammable material. Even though the material density was increased, the effectiveness of the material as a barrier to particle penetration was not increased. Thus the material provided equivalent penetration protection for equivalent thickness, independent of material density.

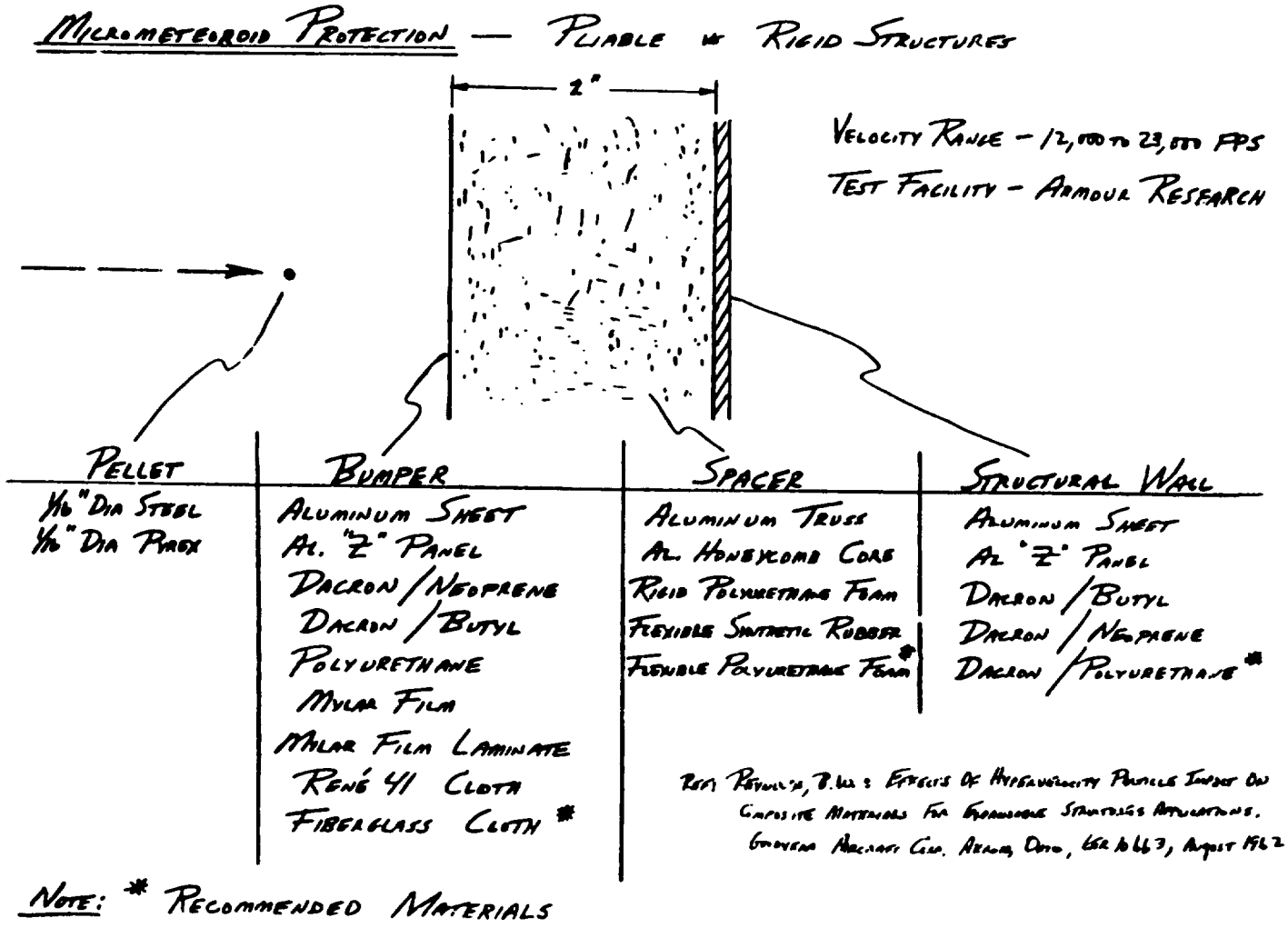

REF: PETTINOS, P.D.: EFFECTS OF HYPERVELOCITY PARTICLE IMPACT ON COMPOSITE MATERIALS FOR GUIDANCE STRUCTURES APPLICATIONS, GOODYEAR AEROSPACE CORP. AKRON, OHIO, GER 16663, AUGUST 1962

FIGURE IIIA-1. SUMMARY OF MATERIALS TESTED FOR MICROMETEOROID PROTECTION SYSTEM

For the expandable rigidized materials concept, a different type of barrier material is provided. This is a flexible urethane mesh (Scott Foam 10 PPI) of 1.8 lb/cu ft density. While the function of this material is primarily to act as a micrometeoroid barrier, it also serves as a basic mechanism for rigidization of the structure. The mesh material is an ideal substrate for impregnation with gelatin resin, which serves as a rigidizing agent. The normally flexible mesh material when impregnated may be rigidized by vacuum curing of the resin, thereby providing a rigid wall structure. With respect to particle penetration protection, this material provides the same protection for an equivalent thickness as the flexible foam material used in the elastic recovery materials concept. (Reference 4).

It is likely that additional tests will have to be made on representative hangar materials with and without rigidization to determine resistance to penetration by micrometeoroids and space debris.

GAC is proposing a shell material for the manned habitat both with and without foam at this time. It is believed that the shell thickness alone is adequate to protect the astronaut from the micrometeoroid flux as presently postulated; however, only additional testing can answer this question.

The one inch thickness of foam was considered to be adequate during the design of the D-21 Expandable airlock. Since the assumed micrometeoroid flux has essentially remained the same for the last 10 to 15 years, GAC firmly believes that adequate protection is provided for the corresponding foam material design for the manned habitat.

B. LEAKAGE RATE PREDICTION AND CONTROL FOR INFLATED STRUCTURES IN SPACE

Leakage can generally be attributed to the gas permeability of the basic fabric and the mechanical interface between the flexible and rigid structure. Development goals are generally in the range of 0.25 to 0.50 lb/day and/or two to three percent of the volume per day for large volume structures. Goodyear has been exposed to this problem in the tire industry for a long time. At the present time, tires with an initial pressure of 30 - 35 psig, a 1.95 cu ft volume and a surface area of 825 sq. in. show a pressure loss of 1.7 psi/month. The best tire technology predicts a future value of 0.5 psi/mo. pressure drop for this same tire. The following air losses can be predicted for these pressure drops as --

$$\Delta w = 0.017 \text{ lbs/mo} = 10^{-4} \text{ lbs/ft}^2\text{/day for 1.7 psi pressure loss}$$

and

$$\Delta w = 0.005 \text{ lbs/mo} = 2.95\,(10^{-5}) \text{ lbs/ft}^2\text{/day for 0.5 psi pressure loss}$$

A space habitat would likely retain a constant pressure at all times rather than let the pressure decrease because of leaks. This constant pressure situation was analyzed for the flex section and tire designs and it was found that the leak loss increases an insignificant amount because of the low pressure losses involved in the first place.

A typical flexible habitat with a surface area of 1315 ft^2 therefore, using the 1.7 psi loss condition, has a leakage of 0.13 lbs/day. This is less than the 0.5 lbs/day leakage allowable for the habitat itself. No leakage is anticipated at the bead interface of tires since this is considered an unacceptable design. This same design philosophy must be chosen for a flexible inflatable habitat structure.

A typical bead-type interface between a flexible structure and a rigid structure is shown in Figure IIIB-1. Many times 'O' rings are incorporated to eliminate leaks at the interface; however, this becomes

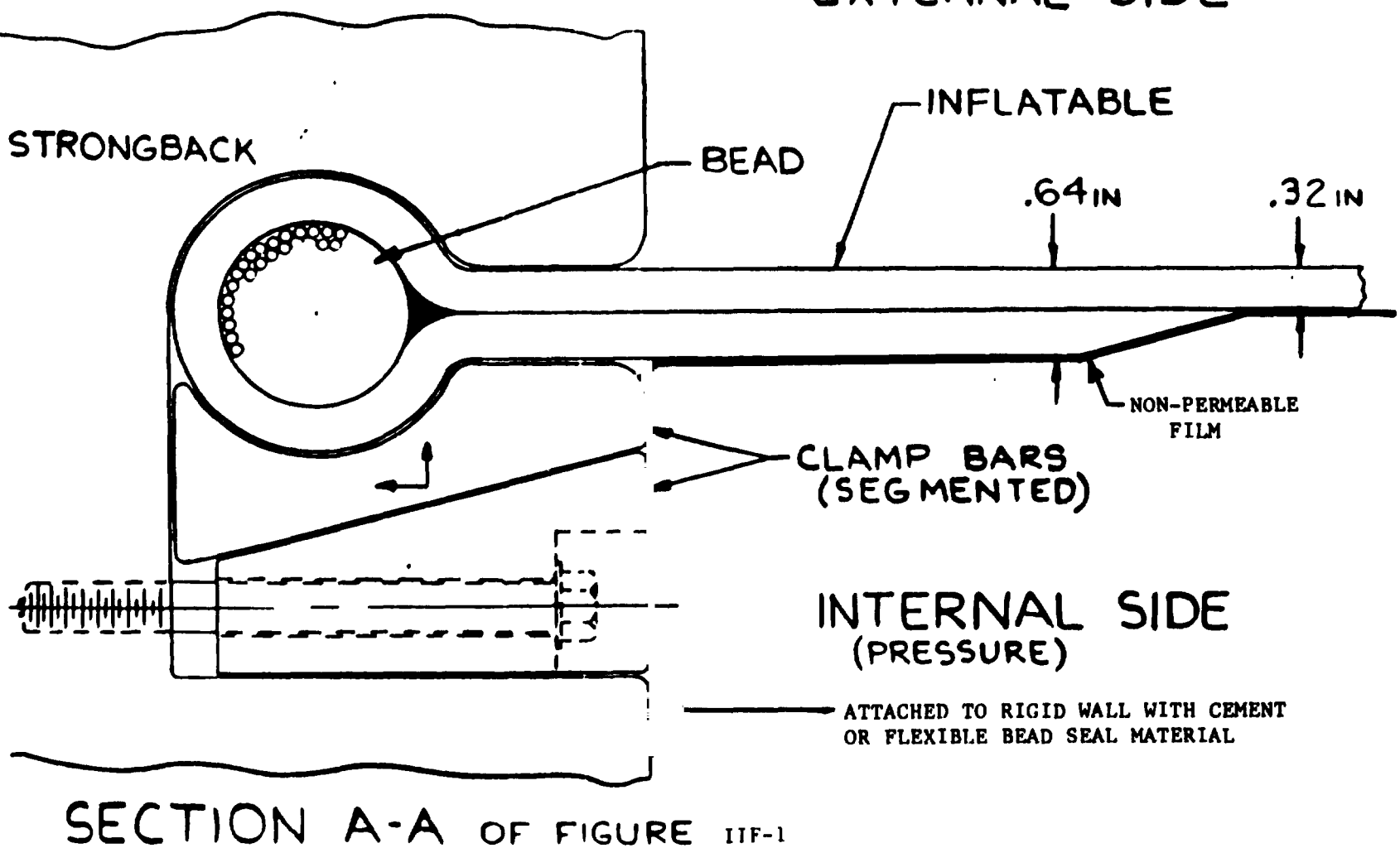

SECTION A-A OF FIGURE IIF-1

FIGURE IIIB-1 INFLATABLE SHELL/STRONGBACK INTERFACE CONNECTION SEALING METHOD

GOODYEAR AEROSPACE
GAC 19-1615

difficult when irregular paths are experienced. For this reason by attaching film to the rigid surface inboard of bead section the potential leakage path of the bead is eliminated. Pressure inside the habitat will help film in its sealing action also. Excess material should be provided in bead-crotch area to prevent film from taking any stretching loads resulting from the habitat internal pressure.

For initial pressures of 14.7 psig, the tire would experience even lower leak losses. Conservative estimates indicate that the predicted leakage for the space habitat of 0.13 lbs/day would be 8 times lower with the initial pressure being 14.7 psig rather than 30 psig, and the external environment the vacuum of space.

Since leakage depends on the geometry of the expandable structure in addition to the material itself, actual test data is necessary to enhance predictions for the prototype. For further precautions, a non-permeable flexible film or low permeable inner elastomer liner compatible with the environment involved could readily be incorporated.

Tests were conducted on flex element (XA30A553) material to ensure that the two plies of each of the materials were completely bonded together and that no residual MEK was trapped in the elastomer. No irregularities, no debond, nor blisters were noted before, during or after the specimen tests. Zero permeability was measured for the materials over an extended period with Helium gas, thus showing that the material leak rate was less than 30 SCCM for differential pressures of 14.9 psig.

For this reason, multiple layers of the above material should also offer zero permeability. The biggest problem area is usually the mechanical interface. Recognizing this goes a long way towards solving the potential leakage problem.

GAC had to determine whether the shuttle flex section leak test data met the specification requirement that at 14.9 psig constant internal pressure the leakage would not exceed 0.116 lbs/ day. The test was conducted allowing the internal pressure to decrease with time as a consequence of the leakage while the specification is for a leak rate at a constant internal pressure of 14.9 psig.

GAC developed a mathematical model of the system as tested with emphasis of the leakage process which permits the pressure to decrease with time. GAC then validated the mathematical model by comparison with the measured test data.

The basic idea was to determine the decreasing pressure vs time history for a system with initial pressure of 14.9 psig, which would satisfy the 0.116 lbs/day leak rate when at a constant internal pressure of 14.9 psig.

The test was modeled as shown:

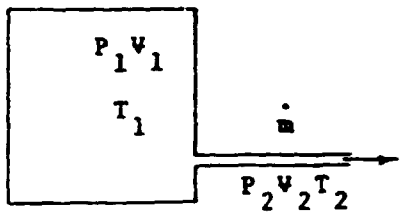

$$P_2 = P_{atm}$$

The test section is a closed container with mass leaking (flowing) out through very small openings. The fluid flow is of very low velocity and the area through which it flows is very small. The flow is then of low Reynolds Number and therefore viscous and laminar. This condition can be modeled as shown above by a closed pressure vessel (C.V.) with a long, thin tube through which the leakage fluid passes.

Since the control volume is a pressure vessel, compressibility effects should be considered. The flow through the tube is dominated by viscosity. Since viscosity is not strongly affected by pressure, neglect compressibility effects for this simple model.

From continuity

$$\dot{m}_{\text{out of C.V.}} = \dot{m}_{\text{through tube}} \qquad (1)$$

Equation of State in C.V. is

$$P_1 V_1 = m R_1 T_1 \quad .$$

where P = Pressure (lb/Ft^2)

V = Volume (Ft^3)

m = mass (slugs)

R = gas constant ($1716 \frac{Ft\text{-}lbs}{Slug\text{-}^\circ R}$)

T = Temperature ($^\circ R$)

Assume V_1 and T_1 are constant for the test.

Therefore $$\frac{dm}{dt} = \frac{dP_1}{dt}\left(\frac{V_1}{RT_1}\right) \quad . \qquad (2)$$

Assume flow in tube is steady and laminar, i.e., Hagen-Poiseuille flow. (H.P.)

Therefore solution of the H.P. flow gives, for volume of fluid through tube per unit time

$$V_o = \frac{\pi r_o^4}{8\mu} \frac{P_1 - P_2}{L} \qquad (3)$$

where r_o = radius of tube (ft)

L = length of tube (ft)

μ = dynamic viscosity of fluid $\left(\frac{lb_F - sec}{Ft^2}\right)$

P_1 = Pressure upstream of flow (lb/Ft^2)

P_2 = Pressure downstream of flow (lb/Ft^2)

For $\dot{m}$ multiply equation (3) by ρ. Since the mass flow of interest is that which is exiting the tube, use ρ_2 (ambient density).

Then mass flow through tube becomes

$$\dot{m} = \frac{\rho_2 \pi r_o^4}{8\mu L} (P_1 - P_{atm}) . \qquad (4)$$

Substitute equation (2) and equation (4) for equation (1)

$$\frac{dP_1}{dt} = \frac{\rho_2 \pi R T_1 r_o^4}{8\mu V_1 L} (P_1 - P_{atm}) . \qquad (5)$$

Equation (5) is of the form

$$\frac{dP_1}{dt} = k (P_1 - P_{atm})$$

where $$k = \frac{\rho_2 \pi R T_1 r_o^4}{8 \mu V_1 L} \qquad (6)$$

Now we redefine variables.

$$\bar{P} = (P_1 - P_{atm}).$$

Therefore $$\frac{d\bar{P}}{dt} = \frac{dP_1}{dt}$$

or $$\frac{d\bar{P}}{dt} = \gamma \bar{P}$$

and $$\frac{d\bar{P}}{\bar{P}} = \gamma\, dt \qquad (7)$$

whose solution is $$\bar{P} = C e^{\gamma t} .$$

@ $t = 0$ $\quad \bar{P} = (P_1 - P_{atm}) = 30.3$ in Hg

Therefore $\quad 30.3 = C e^{0}$

or $\quad C = 30.3$ in Hg,

and $$\bar{P} = 30.3\, e^{\gamma t} \qquad (8)$$

γ of equation (8) is actually the k of equation (6). Now we computed some values of γ for various Δt intervals from the experiment to verify that γ is in fact a constant.

Integrate equation (7)

$$\int_{\bar{P}_1}^{\bar{P}_2} \frac{d\bar{P}}{\bar{P}} = \int_{t_1}^{t_2} \gamma\, dt$$

$$\ell n\, \bar{P}_2 - \ell n\, \bar{P}_1 = \gamma(t_2 - t_1) .$$

From the test data where the flex section was pressurized to 30.3 in Hg gage initially, pressures at various times were noted over a 19.5 hour period.

for $t = 6$ hr to $t = 8$ hr:

$$\ln 27.12 - \ln 27.87 = 2\gamma \qquad \gamma = -.01364$$

for $t = 12$ hr to $t = 14$ hr:

$$\ln 24.87 - \ln 25.55 = 2\gamma \qquad \gamma = -.01349$$

for $t = 0$ to $t = 9$ hr

$$\ln 26.72 - \ln 30.3 = 9\gamma \qquad \gamma = -.01397$$

Several values of Equation (8) were plotted using $\gamma = -.01397$ and the conclusion is that mathematical model and data agree.

By substitution of equations (4) and (6) (and noting that $\gamma = k$), γ can be expressed as

$$\gamma = \frac{\dot{m}}{\Delta P} \frac{R T_1}{V_1} \tag{9}$$

where $\Delta P = (P_1 - P_{atm})$

The general form of the decreasing Pressure-Time expression becomes

$$\bar{P} = P_o e^{-\left[\frac{\dot{m}}{\Delta P} \frac{R T_1}{V_1}\right] t} \tag{10}$$

E-10-1517-711)
REF: EOI 380

where P = Gage pressure at any time

P_o = Initital gage pressure

t = Time

and $\dot{m}$, $\left.\frac{dP_1}{dt}\right|_{initial}$, $\left(\frac{r_o^4}{L}\right)$ are interrelated as per equations (4) and (5).

We will now use the mathematical model to determine the experimental $\dot{m}$ corrected to constant pressure in the flex element. Initial conditions are P_1 = 30.3 In. Hg gage, V_1 = 4.7541 cu. ft. and T_1 = 70°F or 530°R.

Using the experimental value of γ and equation (9) gives the experimental value of $\dot{m}$.

$$\dot{m} = \frac{-.01397 \frac{1}{Hr}\ 2145.6 \frac{lb_F}{F^2}\ 4.7541\ F^3\ 32.174 \frac{lbm}{slug}\ \frac{24\ Hr}{Day}}{1716 \frac{ft\ lb_F}{slug\ °R}\ 530\ °R}$$

$\dot{m}$ = −.121 lbm/day at constant P = 14.9 psi

This exceeds specification value of $\dot{m}$ = −.116 lbm/day.

Equation (10)can be used to determine a decreasing pressure-time curve which reflects an acceptable $\dot{m}$.

From equation (9), using $\dot{m} = -.116 \frac{lbm}{day}$

E-10-15(7-71)
REF: EOI 380

$$\gamma = \frac{-.116 \frac{\text{lbm}}{\text{day}} \frac{1 \text{ day}}{24 \text{ Hr}} \frac{\text{slug}}{32.174 \text{ lbm}} 1716 \frac{\text{ft lb}_F}{\text{slug } ^\circ\text{R}} 530 \ ^\circ\text{R}}{2145 \frac{\text{lb}_F}{F^2} \ 4.7541 \ f^3}$$

$$\gamma = -.01339 \frac{1}{\text{Hr}}$$

Equation (10) becomes

$$\tilde{P} = 30.3 \ e^{-.01339 \ t} \quad , t \text{ in hr.} \qquad (11)$$

This equation defines a decreasing pressure vs time curve for a flex section system which will meet the specification value of $\dot{m}$ = 0.116 lbm/day leak rate when under a constant pressure 14.9 psig.

It should be noted that the term in brackets in equation (10) (which is γ) is in units $\frac{1}{\text{hr}}$. This results in the term $e^{-\gamma t}$ being dimensionless. Therefore, the pressure terms $\tilde{P}$ and P_o, can be expressed in whatever units are conve.ient (in. Hg, psi, etc.).

The development of equation (10) indicates that the physics of the problem are understood and adequately modeled by the expression. The equation enables leak test data taken under decreasing pressure conditions to be converted to a constant pressure case.

C. RIGIDIZATION OF FLEXIBLE STRUCTURES IN THE SPACE ENVIRONMENT

Goodyear has tried many methods of rigidization on items like simple balloons, inflatable antennas and inhabited structures for space applications. Some of the successful techniques for rigidizing these membranes can be summarized as follows:

- °ULTRA VIOLET-SENSITIVE RESINS OR ELASTOMERS
- °THERMAL SENSITIVE RESINS OR ELASTOMERS
- °PLASTICIZER BOIL OFF
- °VAPOR PHASE CATALYSIS
- °YIELD MEMBRANE - METALLIC FOIL, WIRE GRID, FILM-FOIL LAMINATE
- °PREDISTRIBUTION OF UNACTIVATED FOAM ON DEPLOYABLE SURFACE

Goodyear also investigated foam-in-place techniques for such space bodies as antennas, solar concentrators, radar decoys and similar structures. Several representative tests were conducted in vacuum chambers to pin-point problem areas. No qualified systems were manufactured since prototype equipment showed excessive weight for space payloads of that era.

Much work was done on rigidization of expandable structures in the 1960's by Government and industry to enhance deployment of larger satellites for the small missiles of the day.

GAC conducted a research and development program for optimization of chemically rigidized expandable structure techniques for manned space structure applications, (Reference 4). A survey of 12 candidate resin systems was made under the Materials Survey task, (see Tables IIIC-I and IIIC-II) resulting in a recommendation to AFAPL for use of the reversible-type gelatin resin system with companion

Resin	Process	Catalyst	Temperature for Rigidization
Gelatin	Plasticizer boil-off	None	Wide range
Urethane	Cross linking initiated by water vapor	Optional amine catalyst (Amine vapor may be mixed with water vapor.)	Limits above and below room temperature not defined
Epoxy	Cross linking initiated by amine vapor	Optional - several possible candidates, e.g., triphenyl phosphite	Limits above and below room temperature not defined
TEGDMA	Catalyzed polymerization[a]	Amine accelerator plus peroxide catalyst	Minimum between 32° and 70°F
N-VC	Catalyzed polymerization[b]	Acid gas, e.g., N_2O_4	Initiates at 70°F
CPBU	Catalyzed cross linking	Peroxide catalyst and/or heat	120° to 350°F
N-VC/CPBU	Catalyzed polymerization[b]	Suitable catalyst undefined (see Reference 13)	Dependent on catalyst
GMA	Plasticizer boil-off	None	Above 60°F
FA	Catalyzed polymerization[b]	Acid gas, e.g., HCl	From -50° to +250°F
Phenoxy	Solvent boil-off	None	Wide range
PVA	Solvent boil-off	None	Wide range
Hydron	Plasticizer boil-off	None	Wide range

[a] Rigidization initiated by accelerator addition. (Catalyst added in original formulation.)

[b] Rigidization initiated by catalyst addition.

TABLE IIIC-I - RIGIDIZING PROCESSES AND TEMPERATURES FOR CANDIDATE RESINS

Resin	Polymer Softening Point	Resin Shelf Life	Blocking Problems*
Gelatin	Up to 390°F; dependent on residual water content	Long time	None with proper formaldehyde treatment
Urethane	Up to ≈250°F; cure dependent	Several months in anhydrous storage at 70°F or below (in Butyl acetate solution)	Probably controlled by residual solvent
Epoxy	High if well cured	Several months as two-package system	Probably severe and not controllable by solvent addition to epoxy
TEGDMA	High if well cured	30-day shelf life with oxygen atmosphere below 80°F (*Ref 6, D-22 Experiment*)	Unknown other than D-22 Experiment
N-VC	Up to 390°F	Probably long time.[b] No H_2O sensitivity	Unknown until a binder is defined
CPBU	Very high after high temperature cure	Not established (Similar to TEGDMA?)	Non-tacky B-stage (*Ref 13*)
N-VC/CPBU	Not defined	Not established	Unknown
GMA	185° to 210°F	Long time[b]	Unknown
FA	Very high	Long time[b]	Probably serious
Phenoxy	Approx 212°F	Long time[b]	Probably serious
PVA	185°F	Long time[b]	Probably controllable
Hydron	170° to 200°F	Long time[b]	Serious

*Blocking, or self-adhesion of resin-coated surfaces, could seriously hamper deployment of a packaged structure before rigidization.

[b]Based on observations of bottle or similar type of container storage.

TABLE IIIC-II - POLYMER SOFTENING POINT AND STORAGE PROPERTIES FOR CANDIDATE RIGIDIZING RESINS

mesh core type of resin carrier. Instructions for step-by-step fabrication processing were given for the reversible-type gelatin resin system and its companion mesh core resin carrier as applicable to the D-21 Airlock Experiment type of expandable structure. Formulas were developed for the effects of core rigidity on beam deflection and bending stresses of a gelatin-rigidized mesh core sandwich construction as applied to the D-21 airlock structure micrometeoroid barrier. This work is applicable to the rigidization system proposed for the OTV hangar herein.

The primary objective of this program was to maximize the structural efficiency of the most promising candidate resin systems and to obtain a structural analysis method to permit reliable analytical evaluation of chemically rigidized resin/carrier systems. In addition, an attempt was made to achieve the important associated objective of developing practical fabrication techniques for manufacturing expandable, rigidized, manned space structures.

The basic function of protection from micrometeoroid penetration is provided by the use of a flexible polyurethane mesh core material. This material is impregnated with gelatin resin during the structure fabrication process. Continued flexibility of this layer during the packaged configuration is retained by maintaining the total composite wall material in a sealed condition. Once orbital conditions have been attained and the structure deployed, the material wall cavity is vented to vacuum, allowing the gelatin-resin moisture to escape, which results in rigidization of the foam material layer. Approximately one hour is required for the structure to rigidize into its final expanded configuration, with material compressive rigidity values in the range of about 10 psi.

Twelve systems for chemical rigidization were considered during the resin survey. The advantages, disadvantages, and complexities of the candidate resin systems were evaluated using step-by-step fabrication technique logic.

The reversible-type gelatin resin system with its companion mesh core (Scott foam) structure was selected as the most promising resin/carrier composite. It was strongly recommended that this composite be further evaluat .d for use as a rigidization system in expandable manned space structures.

Two novel resin systems, Hydron and poly (vinyl alcohol) on a mesh core substrate, were found to somewhat parallel the properties of the gelatin system, and with further development work, could possibly offer an alternate candidate rigidized resin system.

Aerospace applications of chemically rigidizable composites will presumably require tight packaging of structures built in whole or in part of the composites. It is of first importance that during package storage no adhesion (blocking) shall develop between two resin coated surfaces in contact that might later interfere with deployment. Blocking problems have been encountered with many commercial polymers, particularly linear polymers. It is necessary to assume that the problem could arise with most resins and that no general solution would exist; rather, a specific remedy would need to be found in each case.

It appears from early experiments that some control of rate of water evaporation from a structure being rigidized in space would be required to avoid too much evaporative cooling too soon. With fixed venting, about an hour might be required for a controlled rigidization with certain geometrical factors of volume per vent. Some continuing weight loss might be expected over the first 24 hours.

The resin/carrier composite selected and recommended for use in the design of chemically rigidized expandable structures for space is a gelatin-impregnated resilient mesh core system. This system, which may be

repeatedly rigidized or flexibilized by loss or gain of a few percent of water weight, possesses much greater adaptability in fabrication technique logic than resin systems that rigidized non-reversibily by polymerization. Reliability through packaging and storage appears very good. Strength for the gelatin system at elevated temperatures is also very good.

Rigidization due to overpressure/yielding has proven very effective for thin-skin structures such as balloons, antennas, solar collectors, space mirrors and similar bodies. This method is not considered appropriate here since a structural sandwich is required to take the loads expected from the astronauts while performing maintenance functions. Interface loads between the rigidized hangar and the space structure during even minor maneuvers must be considered during the design.

The sandwich structure must withstand combined compressive and flexural stresses due to the applied astronaut working loads. The fabric faces cannot carry compressive stresses unless they are stabilized to prevent buckling. This stability is provided by the core of the sandwich. A flexible foam core does not exhibit enough compressive stiffness to stabilize the faces. A foam core may be rigidized by impregnation with the proper materials or by inflation.

Some self-expanding can be expected for a flexible core sandwich as defined in the D21 Airlock, the STEM, and similar applications. The hangar has other requirements which necessitate augmentation of the elastic recovery concept. In order to supply a working surface for the astronaut, rigidization of the foam core is necessary as mentioned above. When a housing is provided for living quarters, an experiment or just a tunnel to traverse from one rigid habitat to another, the flexible core system can be made to work.

Time-load tests conducted on small samples of a typical micrometeoroid barrier foam layer were used to ascertain the maximum length of time the proposed shelter or airlock type material could be packaged with a high reliability of elastic recovery deployment when unpackaged. Figure IIIC-1 shows the recovery characteristics of the foam under vacuum conditions and for varying temperatures. (Reference 14). From Figure IIIC-1 it can be seen that the packaged structure must be insulated against extreme cold if full recovery is to be achieved. The material was packaged to 20 percent of its relaxed thickness for a period of 24 hours under vacuum conditions. It may be necessary to pressurize the foam sandwich structure to expedite deployment before rigidization becomes effective.

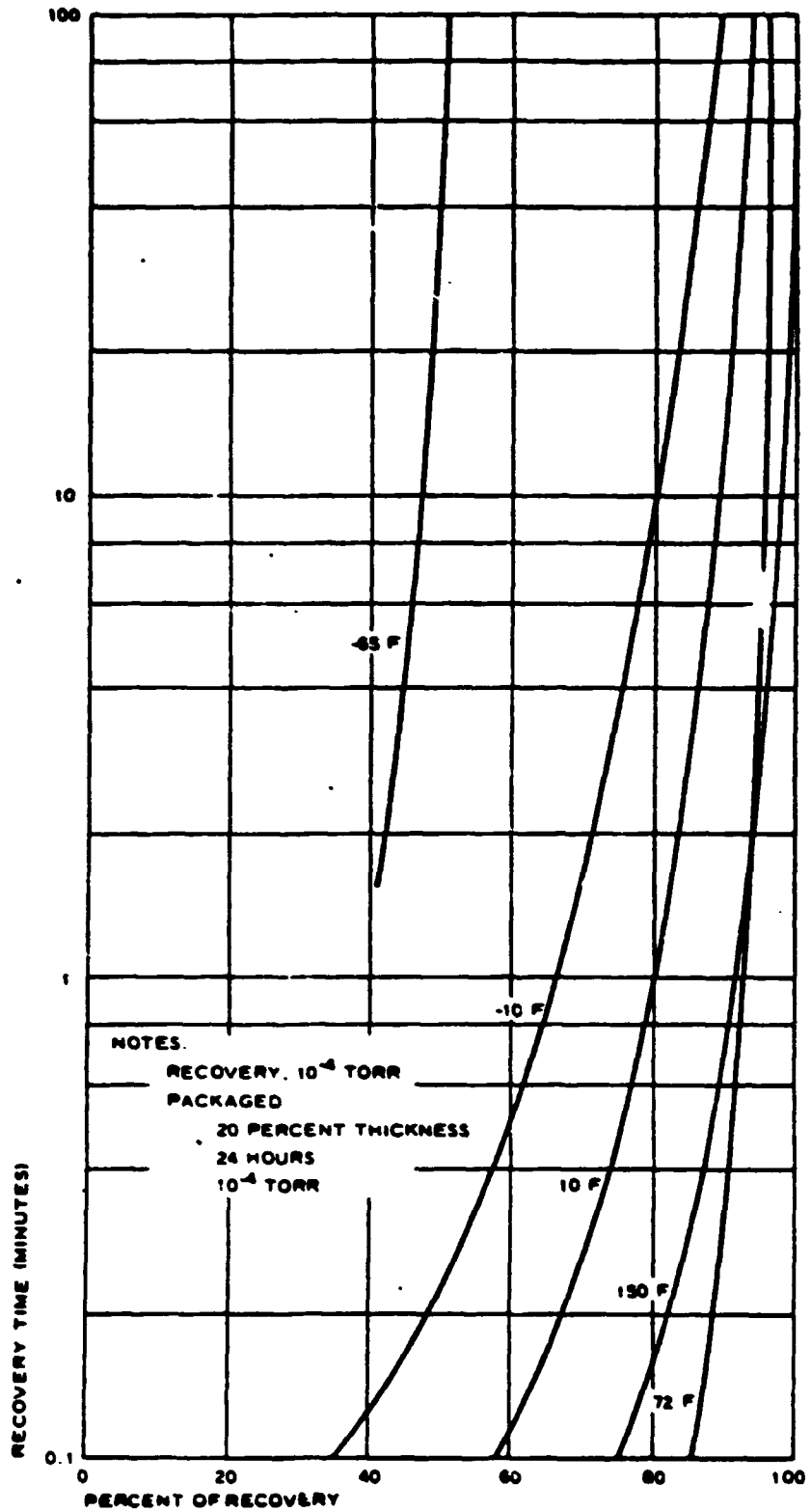

FIGURE IIIC-1 — Foam Thickness Recovery versus Time

D. FLAMMABILITY AND OFFGASSING

Since fluorocarbons have been tested successfully in the past for flammability and offgassing, it is believed that Viton is a good choice for an elastomer. The above items in conjunction with the fact that the early flex element development units made by McDonnell Douglas had used Viton and had been approved by NASA led to the selection of Viton as the elastomer for the Goodyear flex element. Due to processability, the specific Viton selected was Viton B-50. The formulation used was:

Viton B-50	= 100 pts	parts by weight
Maglite Y	= 15 pts	
Carbon Black	= 15 pts	
Diak 3	= 3 pts	

Several combinations of elastomer and cloth were submitted to NASA via MDTSCO for evaluation. The results showed that the Viton B-50 elastomer and Nomex cloth would pass the flammability and offgassing test as called out in NHB8060.1A by being subjected to the following autoclave cure, post cure and vacuum bakeout.

Cure	300 degree F 50 psi 22 in Hg (Vacuum) 1 hour
Post Cure	24 hours at 300 degree F
Vacuum Bakeout	24 hours at 250 degree F and pressure of 30 mm Hg, absolute

This is a basic material proposed for the inflatable shell of a habitat module; therefore, it is anticipated that all flammability and offgassing requirements of such a program can be met.

Figure III-D-I summarizes the types of flammability and offgassing tests that NASA requires for components and subsystems of space structures along with the acceptance criteria.

ACCEPTABLE - NON-COMBUSTIBLE OR SELF-EXTINGUISHING WITHIN 6 INCHES/10 MINUTES

ODOR EVALUATION - ACCEPTANCE FOR AVERAGE RATING OF 2.5 OR LOWER (FIVE MEMBER PANEL)

MEMBERS RATING	TEST CONDUCTOR'S RATING
UNDETECTABLE	0
BARELY DETECTABLE	1
EASILY DETECTABLE	2
OBJECTIONABLE	3
IRRITATING	4

MAXIMUM ALLOWABLE LEVEL OF TOTAL ORGANICS (EXCLUDING WATER) $\leq$ 100 MICROGRAMS/GRAM OF SAMPLE

MAXIMUM ALLOWABLE LEVEL OF CO IN TESTED CONFIGURATION $\leq$ 25 MICROGRAMS/GRAM OF SAMPLE

TOXICITY LEVEL - RECORD INORGANIC GAS LEVELS (HCN, NH_3, HCL)

TOTAL MAX LOSS (TML) $\leq$ 1.0 PERCENT (24 HRS., 125°C, 10^{-6} TORR)

MAXIMUM VOLATILE CONDENSABLE MATERIAL (VCM) CONTENT $\leq$ 0.1 PERCENT

FIGURE IIID-I - FLAMMABILITY AND OFFGASSING TESTS
NASA REPORTS NHB8060.1A / SP-R-0022A

E. LIFETIME FOR NON-METALLIC MATERIALS

None of the environmental conditions which the spacelab tunnel flex element must withstand were very severe. Most any elastomer could survive the operational environment imposed on the flex element. There were, however, two significant requirements that led to the selection of Viton as the elastomer: 10-year life and offgassing/ flammability requirements. Viton is known for its long life at elevated temperatures; and since there was no elevated temperature requirement on the flex element, the life would be well in excess of ten years. (Elevated temperature is used for accelerated aging testing of rubbers). Characteristic dry heat resistance of vulcanizates of Viton in continuous service is considered to be greater than three years at 400°F.[1]

For comparison, conventional elastomers would be brittle after one day at 400°F.[2]

Other characteristics of Viton which make it an excellent selection are:

Weatherability[3] - 6 years' exposure in Florida: excellent - no cracks

Fungus resistance[3] - 30 days' exposure to four groups of commonly occurring fungi (MIL-E-5272C): no attack

In addition, a test was run to verify that the 40 degree F temperature requirement was well above the low temperature capability of the Viton formulation used. This test, the Scott Brittle Point, established a temperature of approximately -25 degrees F as the low temperature capability of the formulation.

[1] "Answers to questions frequently asked about 'Viton'." VT-000.2 (RI) by DuPont.

[2] DuPont Viton® Fluoroelastomer, Bulletin E-10764.

[3] "Type of Viton® Fluoroelastomer", VG1-111 by DuPont (A-73643).

GAC quotes their elastomeric products as good for ten years under reasonable, uncontrolled storage conditions. This includes such items as diaphragms, seals, pillow type tanks, dunnage bags, fuel cells, flotation bags, uprighting bags, impact attenuators and similar structures. After storage, these products can give five years of service, generally. Diaphragms and seals usually give 18 to 20 years of service.

Until further tests are conducted, it is believed that the Viton B-50 elastomer has the best chance to meet the desired 20 year lifetime.

F. CRACK PROPAGATION PREVENTION

The purpose of the leak before burst test was to demonstrate that the design of the flex element is stable under limit conditions with readily detectable damage. This test was performed after flight cycle 200. (Reference 15)

The leak before burst test involved inducing a 0.5 inch cut completely through the flex element while at an internal pressure of 15.9 psig. The cut was oriented perpendicular to the yarns of the ply that was loaded.

The blade used was double edged, 0.5 inch wide, and came to a point. It was mounted on a pneumatic actuator such that once the blade penetrated the unit, it could be withdrawn and the pressure maintained for 4 minutes. The leak-before-burst test was filmed for documentation. Visual examination of the cut after the test revealed that the cut did not grow beyond the initial cut length.

The design was stable under limit pressure and deplacement conditions when a readily detectable damage consisting of a 1/2 inch slit through both plies was intentionally inflicted on the unit. This represented a successful completion of the leak-before-burst test.

GAC also investigated the effect of a hole large enough to permit the escape of four pounds of air per hour under a pressure of 15.9 psi. The area of the hole was that of a circle having a diameter of 0.075 inches (0.00442 sq. in.). It was found that the 1/2 inch slit was considered more critical than the hole size of 0.00442 sq. inches and therefore became the design criteria.

A secondary test added as part of the safe life testing involved the imposition of a 0.5 inch cut through a single ply of the flex element. This cut was induced at the end of cycle 196 and was perpendicular to the yarn direction of the outer ply. Due to the uncertainty involved with making a knife cut and being sure of cutting completely through one of the plies without imposing any damage to the second ply, it was decided to remove an area of the outer ply for 0.5 inch keeping the width of the removed area as short as possible. This was accomplished by removing single yarns at a time. The damage was located as shown in Figure IIIF-1 and labeled "D." A small leak resulted from imposing this damage. Cycles 197 through 200 were conducted with no change in appearance or leakage.

Three more intentional damage areas were added to the flex element, after cycle 200 giving a total of five. (See Figure IIIF-1). Damage "F" was located at the point where a double fold occurred repeatedly during the negative pressure phase of the safe life test. Damages "G" and "H" were located on maximum internal bending areas (under negative pressure). Damages "F" and "H" represented cuts parallel to the yarn direction. These were accomplished by removing a single yarn 0.5 inches in length. Damage "G" represented a cut perpendicular to the yarn direction.

After these damage areas were imposed, the flex element was pressurized to 15.9 psig and the damage areas checked for leaks. There was no leakage at any of the three new areas. Damage "D" was still leaking at the same rate as when it was initially induced. The flex element then underwent 4 more flight cycles (201-204) with leak checks conducted after each cycle. None of the damage areas grew as a result of the 4 flight cycles and there was no change in leakage. This represented a successful completion of the damage susceptibility test.

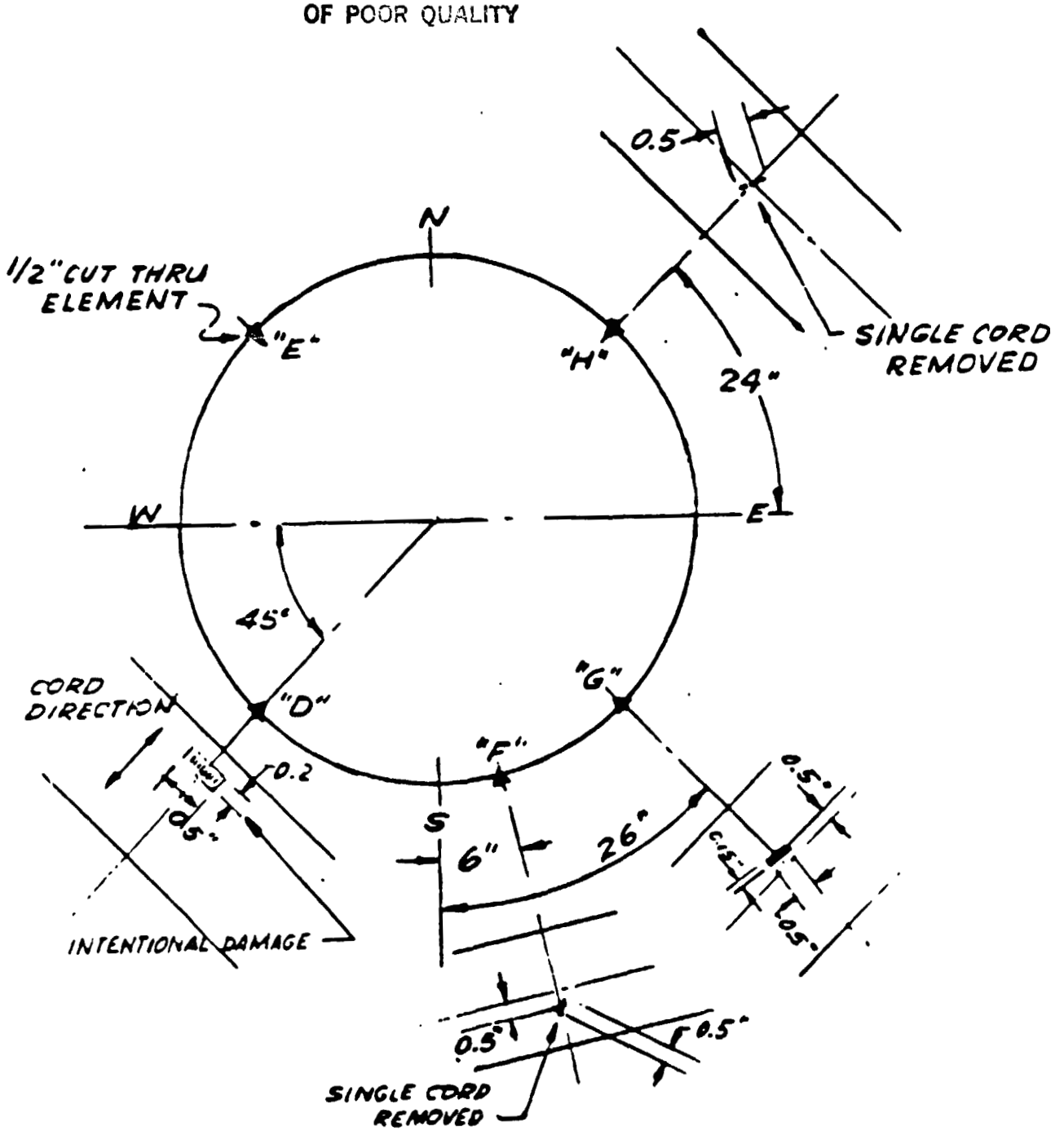

FIGURE IIIF-1 -- LOCATION OF INTENTIONAL DAMAGE AREAS ON THE STT FLEXIBLE ELEMENT

The method of analysis to determine the critical slit length was that developed by Hedgepath for a flat sheet in NASA TN D-882 "Stress Concentration in Filamentary Structures" and modified by Topping to take account of curvature in GER 15879, "The Critical Slit Length of Pressurized Coated Fabric Cylinders." More information can be obtained from Reference 5.

G. IMPACT DETECTION/REPAIR

Analyses have been performed by previous contractors of vehicle leakdown rates to determine how much time an astronaut would have to find a puncture leak and repair it. (Reference 16) Figure IIIG-1 shows the results of this analysis. For an extremely small hole of 0.003-in. diameter, which would be very difficult to find, it would take approximately 90 days for the pressure to leak down from 11 psi to 8 psi. For a considerably larger hole of 0.10-in. diameter, that can probably be found by sound, approximately two hours are required for the same pressure decay. The study has shown that an astronaut should have adequate time to find and plug a leak before the cabin pressure leaks down to a dangerous level.

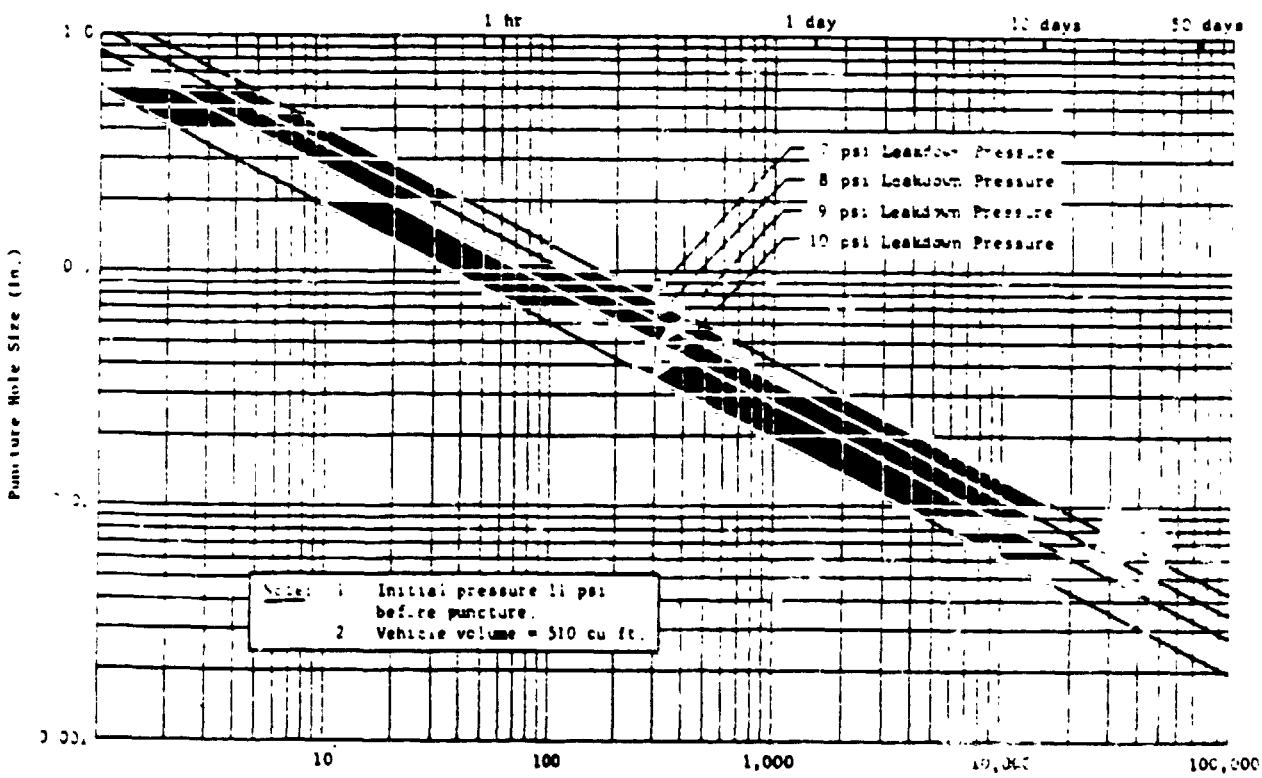

Figure IIIG-1 -- TIME IN MINUTES TO LEAK DOWN TO PRESSURE

GAC performed analyses on the puncture problems with the Lunar Stay Time Extension Module (STEM). (Reference 14). The data is introduced here as information and indicates the type of analysis which will be made, as updated, on any habitat structure during a development program.

Decompression of the STEM may occur by perforation of the shelter wall with micrometeoroids, by accidental puncture from within or by failure of the O-rings in the airlock doors to seal properly when the astronauts enter or leave the shelter. Inside the shelter, the astronauts may be in "shirt sleeves" or in their space suits with helmets removed, so the time for the shelter pressure to drop from 5 psi to 3-1/2 psi, still an acceptable oxygen pressure for sustaining life, was calculated as a function of hole size in the shelter wall. A brief study of how the astronauts would protect themselves during decompression was also made.

Based on Environmental Hazards Analysis (Paragraph D), (Reference 14) in this section, the size of the hole in the sealing bladder of the shelter and the probability of puncture by primary micrometeoroids was calculated with the following principal parameters:

(1) Representative Micrometeoroid Mass Density $\rho = 0.5$ gm/cm^3.

(2) Critical Micrometeoroid Mass$_c$ = 2.33×10^{-3} gm. This mass penetrates the foam barrier in the shelter wall but not the sealing bladder.

(3) Approximately 2/3 of the shelter-airlock surface of 450 ft^2, or 300 ft^2, is estimated to be subject to primary micrometeoroid impact. STEM mission exposure parameter for primary micrometeoroid defined as the product of the exposed surface of the shelter and the stay time is

$$300 \times 8 = 2400 \text{ ft}^2 \text{ days}$$

(4) The probability that the shelter wall will not be punctured is a function of the mass of the primary micrometeoroids which are assumed to have a "Poisson" distribution. The mission exposure parameter yields a zero puncture probability of 0.9996.

(5) From the mass density and the critical mass of the primary micrometeoroid, we find the volume of the critical micrometeoroid to be

$$2.33/.5 \text{ X } 10^{-3} = 4.66 \text{ X } 10^{-3} \text{ cm}^3$$

With the assumption that the micrometeoroids are spheres and that the puncture in the shelter wall is twice the diameter of the micrometeoroids, we obtain:

Critical Micrometeoroid diameter = 0.208 cm., and

Hole diameter = 0.416 cm = 0.16"

When considering flow-through a puncture in the shelter wall, decompression time depends on the nature of the flow through the puncture. Five types of flow were considered.

a. Adiabatic Choked Flow. The adiabatic choked flow exists in a nozzle at or above the critical pressure ratio. Flow is at sonic velocity. It occurs only where the hole diameter is greater than the wall thickness. In the STEM shelter with a two-inch thick wall, we do not expect to have punctures larger than two inches in diameter. This type of flow is therefore not considered.

b. Isothermal Frictionless Flow. The isothermal frictional flow may occur in openings where the diameter is much less than the length of the opening. This is not considered here since there is always friction. Isothermal frictionless flow is mainly a criterion defining the upper limit of isothermal flow discussed next.

c. Isothermal Flow with Friction. The isothermal flow, with friction, occurs where the length of the flow channel is much greater than its diameter.

This flow occurs in relatively slow pressure transients (slow leaks) where the temperature of the escaping gas remains constant by heat exchange with its surroundings.

d. Adiabatic Flow with Friction. The adiabatic flow, with friction, occurs where the length of the flow channel is much greater than its diameter. Adiabatic flow occurs in relatively fast pressure transient such as in explosive decompression, where the temperature varies adiabatically with the pressure.

e. Isothermal Free-Molecular Flow. The isothermal free molecular flow occurs where the initial hole diameter is very small. This flow does not apply to punctures considered here.

Decompression times, as a function of hole diameter in the shelter wall, were calculated as outlined in Reference 17. It was assumed that the automatic atmospheric control system was not making up any loss in oxygen gas during decompression. The oxygen makeup system will be monitored, activating an alarm signal when excessive oxygen is fed into the shelter. This alarm will give the astronauts the choice of maintaining oxygen pressure within the shelter, if at all possible, or shutting off the oxygen feed lines to preserve the oxygen supply before locating the leak and fixing it. This analysis is based on the astronauts stopping the oxygen flow immediately after the alarm. The factor ϕ, shown later under "Nomenclature and Formulas," is therefore zero which gives the fastest decompression possible.

At the beginning of decompression, the shelter has a 5 psi oxygen pressure. A 3-1/2 psi oxygen pressure is assumed to be the lowest safe limit for the astronauts to function normally. The elapsed time for the 1-1/2 psi pressure has been calculated as follows:

Nomenclature and Formulas

V = Volume of shelter = 400 ft^3

$\gamma = \frac{C_p}{C_v} = \frac{\text{Molar heat capacity at constant pressure}}{\text{Molar heat capacity at constant volume}}$,

= 1.4 isothermal flow

= 1.2, 1.4 and 1.8 adiabatic flow

$f_1(\gamma) = \sqrt{\left[\frac{2}{\gamma+1}\right]^{\frac{\gamma+1}{\gamma-1}}}$

T_o = 530° R temperature of shelter atmosphere °R

m = 30 molecular weight of shelter atmosphere lb/mole

$\phi = \frac{F_F + \epsilon}{F_L}$ where F_F mole rate flow of oxygen added to the shelter, ϵ mole rate flow change due to metabolic process and operation of the carbon dioxide removal system, F_L = mole rate flow of shelter atmosphere due to leakage. For fastest decompression $F_L \gg F_F + \epsilon$ and $\phi \approx 0$.

C_D = 0.9 coefficient of discharge ranging from 0.60 for sharp edge orifices to 0.94 for a converging nozzle with a 15° divergence in the nozzle throat. C_D = 0.9 gives conservative discharge values.

A = Area of puncture in ft^2

$\alpha = 223\left[\frac{C_D A}{V}\right]\sqrt{\frac{T_o}{m}}\, f_1(\gamma)\ \text{sec}^{-1}$

P_o = Shelter atmosphere pressure 5 psi before puncture occurs.

P = 3-1/2 psi Minimum oxygen pressure at which astronauts are still physically able to function normally

t = Time in minutes in which the shelter pressure drops from 5 psi to 3-1/2 psi.

$$\frac{P}{P_o} = e^{-\alpha T} \text{ for isothermal decompression } (\phi = 0)$$

$$\frac{P}{P_o} = \left[1 + \frac{\gamma - 1}{2}\alpha T\right]^{\frac{2\gamma}{1-\gamma}} \text{ for adiabatic decompression .}$$

The time for the pressure to drop from 5 psi to 3-1/2 psi has been shown as a function of hole diameter in Figure IIIG-2. For a micrometeoroid puncture of 0.9996 probability, 15 to 30 minutes would elapse before the atmospheric pressure becomes critical. This should give the astronauts sufficient time to take remedial action.

Figure IIIG-2 also shows that very little time elapses before the atmospheric pressure becomes critical if there are larger holes. For a 1/2" diameter hole, the elapsed time is only from 1-1/2 to 3 minutes. The importance of proper sealing of the airlock doors must be stressed.

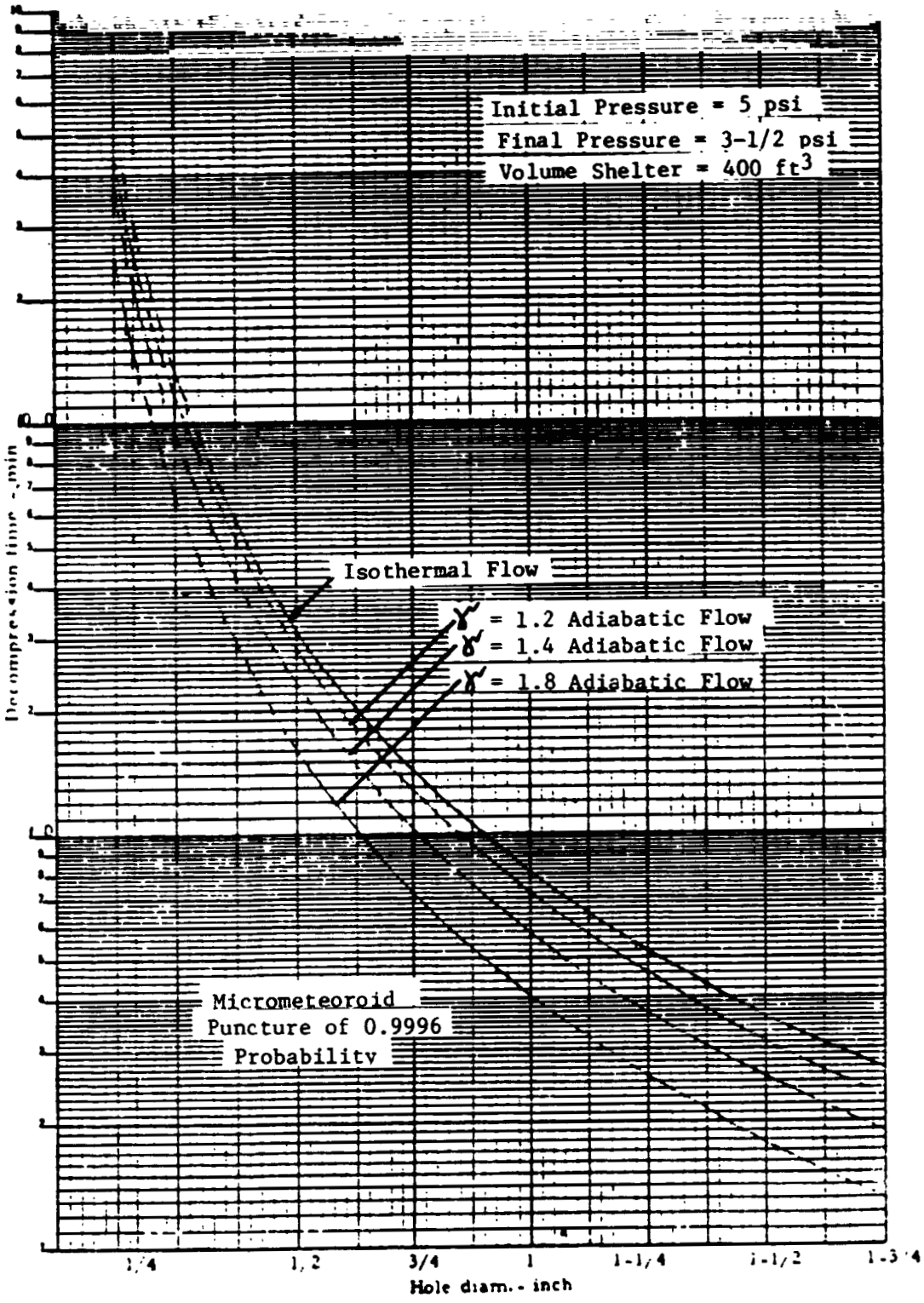

FIGURE IIIG-2 -- DECOMPRESSION TIME AS A FUNCTION OF HOLE DIAMETER

H. EFFECTS OF ATOMIC OXYGEN

Several reports of this special discipline have been received and it was found that reference 18 summarizes the results to date and cites earlier references of value. Test data obtained with the shuttle orbiter indicated a surface recession of 380 to 500 microns for organic films. Goodyear has no data on the effects of atomic oxygen on polymeric coated cloth. It is suggested that such space approved materials as Viton B-50/Nomex and Acousta 200 fabric be tested in future shuttle flights to obtain basic data.

It is important to point out that non-metallic space structures will undoubtedly be protected with micrometeoroid barriers and multi-layer insulation for most manned space applications; therefore, no critical problems with atomic oxygen are anticipated. This philosophy was considered acceptable when discussed with prominent scientists in this field.

I. EFFECTS OF SPACE DEBRIS

Recent studies have indicated that man-made debris in earth orbit could be a safety problem for space questions in the near future. References 19 and 20 show the observed debris flux as a function of orbital altitude. Reference 19 also predicts the cumulative flux in 1995 between 600 and 1100 km altitude. The maximum potential collision risk occurs near 850 km (460 nautical miles), the altitude favored for sun-synchronous operations (Reference 20).

Reference 19 indicates that the space shuttle with an average cross section of 250 M^2 and an operational altitude of almost 300 km has a current collision probability of about 1×10^{-4}/yr. This is less than the probability of an accidental death on earth (5×10^{-4}/yr, of which half is from traffic accidents). This risk is considered acceptable for the present shuttle operation. However, this acceptability will decrease with time, larger structures and higher altitudes.

Some protection can be provided against smaller debris by the use of shielding. Prevention of debris formation is the most effective approach to this problem.

GAC does not consider debris to be a near-term problem to the proposed unpressurized hangar concept, nor the smaller pressurized manned habitat based on these early considerations.

SECTION IV -- POTENTIAL SHUTTLE FLIGHT EXPERIMENTS

A. EXPANDABLE AIRLOCK

GAC qualified an expandable airlock experiment for use on the Skylab Vehicle under contracts with both NASA and the US Air Force. Appendix A is a copy of a paper which summarizes the background conditions that led to the D-21 expandable airlock experiment definition, the objectives of the experiment, and a technical discussion of the proposed experiment. This paper was taken from Reference 13 and shows the state of the art of inflatable space structures circa 1970. This information, along with similar data, is presented herein to offer the reader a viable background in one document for interchange and comparison of ideas and concepts.

The most significant environmental change is the present use of 14.7 psig air mixture vs 5 psig oxygen pressure within the space vehicles. Therefore a new structural layer will be required for the airlock expandable material.

Through the use of the shuttle, a flight demonstration of the elastic recovery structure concept can further the development of expandable structures for manned space flight.

Reference 21 shows in detail how the D-21 airlock experiment was to validate the use of expandable structures technology for airlock designs. Expandable airlocks were considered to conserve weight and storage volume during launch and to permit a maximum use of internal volume of orbiting laboratories by minimizing gas losses during repeated decompression and compression cycles for egress and ingress maneuvers. A few summary charts from Reference 21 have been added to Appendix A to offer a better insight into the expandable airlock concept.

The EPT foam used in the bladder construction governs the lower limits of materials flexibility for the overall materials composite. The material retains sufficient flexibility for dynamic deployment at temperatures as low as -100 F. Embrittlement occurs at about -110 F.

SECTION V -- POTENTIAL TETHERED EXPERIMENTS FROM SHUTTLE

After reviewing references 22 and 23, it became apparent that large non-metallic space structures provided a good tethered experiment from the shuttle by using the tethered satellite system presently being developed by NASA. The ultimate goal would be to tether a 100 meter diameter balloon from the shuttle. As depicted on Figure V-I, a 30 ft. diameter balloon is recommended at this time to review and solve the most important technical problems and permit an early experiment.

Inflatable structures are ideal for tether missions which utilize the outer atmosphere (90 to 200 km) as either a test bed for the thermal stability of structures and materials or as a hypersonic "wind tunnel" facility to test aerodynamic models. (See Figure V-1 insert). Large structures can be deployed from small packing volumes to determine drag and explore solar sailing, power production, optical experiments, etc.

Based on past experience, the conductive balloon materials which can be considered for the 30 ft. balloon are summarized in Table V-I. The material characteristics are indicated along with the balloon's weights and volumes. The package volume is assumed as 3.75 times the balloon material volume. An additional 5 percent is included in the balloon surface for seams which makes the balloon surface areas around 3000 ft^2. Incidentally, the weight and volume of the 100 meter diameter balloon is 120 times the weight and volume of the 30 ft. diameter balloon.

Table V-II indicates typical deployment/inflation systems used with balloon satellites. The pressurized gases and sublimation techniques have been used effectively for over twenty years. For extremely large structures, the pressurization system becomes heavy and cumbersome. It may be necessary to consider a balloon material which has a predetermined memory to deploy and rigidize.

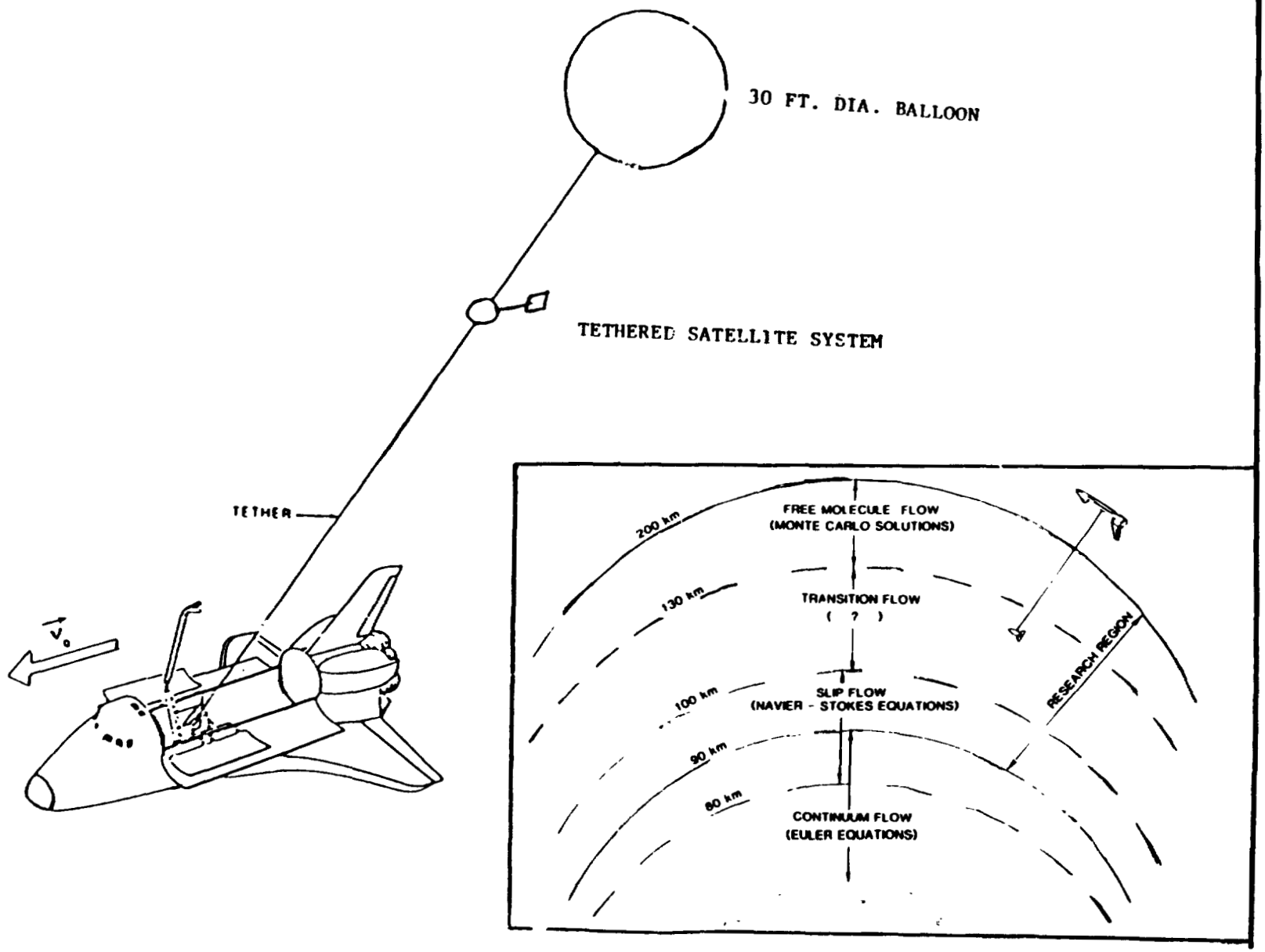

FIGURE V-1 - BALLOON EXPERIMENT WITH TETHERED SATELLITE SYSTEM

1. ALUMINIZED MYLAR WITH AL WIRE GRID CEMENTED ON SURFACE

   0.25 MIL MYLAR FILM, 5 MIL ALUM WIRE, 1/2 INCH SPACING

   BALLOON MATERIAL VOLUME = 141.9 IN^3

   BALLOON WEIGHT = 8.8 LBS

   BALLOON PACKAGE VOLUME = 532 IN^3

2. FILM-FOIL LAMINATE LIKE ECHO II

   0.18 MIL ALUM FOIL ON EACH SIDE OF 0.35 MIL MYLAR FILM

   BALLOON MATERIAL VOLUME = 324 IN^3

   BALLOON WEIGHT = 23 LBS

   BALLOON PACKAGE VOLUME = 1215 IN^3

3. ALUMINIZED MYLAR WITH NITINOL WIRE CEMENTED TO SURFACE

   0.25 MIL MYLAR, 5 MIL WIRE, 1/2 INCH SPACING

   BALLOON MATERIAL VOLUME = 141.9 IN^3

   BALLOON WEIGHT = 13.3 LBS

   BALLOON PACKAGE VOLUME = 532 IN^3

TABLE V-I - TYPICAL MATERIAL FOR 30 FT DIAMETER BALLOON/TETHERED EXPERIMENT

1. PRESSURIZED GASES - NITROGEN, HELIUM

   USED EFFECTIVELY FOR BALLOON SIZES UP TO 30 FT DIAMETER.

2. SUBLIMATION POWDERS/EVAPORATING LIQUIDS

   USED SUCCESSFULLY WITH ECHO BALLOONS.

   GOOD FOR VERY LARGE BALLOONS - 135 FT DIA, LARGEST TO DATE.

3. NITINOL MEMORY MATERIAL AS WIRE GRID

   MUST BE DEPLOYED IN SUNLIGHT.

   THREE DIMENSIONAL MODELS DEPLOYED IN SOLAR SIMULATOR.

   ELIMINATES NEED FOR PRESSURIZATION SYSTEM.

   ALLOWS DEPLOYMENT OF ODD-SHAPES NOT JUST BODIES OF REVOLUTION.

TABLE V-II - TYPICAL DEPLOYMENT/INFLATION SYSTEMS FOR BALLOON SATELLITES

SECTION VI -- CONCLUSIONS AND RECOMMENDATIONS

Flexible, non-metallic structures can perform successfully in applications where flexibility and expandability are requirements. This performance has been demonstrated in space applications by the Spacelab/Shuttle transfer tunnel experiment and the parachute recovery system used to land the Viking spacecraft on the planet Mars.

This report, along with the references noted, describes the state-of-the-art of non-metallic materials and fabrication techniques. The development of a space platform during the next ten years will encourage applications of large structures to enhance communication and energy transfer. Non-metallic, deployable structures can have wide application in structures of the future.

The discovery of improved flexible materials and fabrication techniques presents new opportunities for design applications of space structures. Development work may be required to optimize the use of these new materials and fabrication techniques for space applications. The use of higher pressures for manned vehicles will dictate smaller deployable structures than were considered 20 years ago in order to maintain adequate safety factors in the flexible materials and joints.

One concept described in this report, the deployable/rigidized hangar, has enough merit for early consideration during space station development. The proposed method of rigidization and its implementation should be investigated. In addition, the foam/gelatin, double-surface wall should be tested for effectiveness against micrometeoroids. A scale model of the hangar concept should be built for packing and deployment testing to minimize future problems with prototype structures.

C-2

The Tethered Satellite System (T.S.S.) presently under development would be an excellent experiment to test inflatable/deployable/rigidized structure concepts. Large structures can be deployed from small packing volumes thus offering an optimum way to determine drag and explore solar sailing, power production, optical experiments, etc.

Packaged structures carried in the Shuttle cargo bay could be deployed near the Shuttle in space to investigate non-metallic structures for such applications as large antennas, solar collectors, optical surfaces, long booms, etc.

Representative non-metallic materials considered for space applications should be assigned a spot on the NASA Long-Duration Exposure Facility (LDEF) to determine performance characteristics. This data could be used to establish potential material lifetimes to corroborate accelerated lifetime tests on Earth.

It is important to point out that non-metallic space structures will undoubtedly be protected with micrometeoroid barriers and multi-layer insulation for most manned space applications; therefore, no critical problems with atomic oxygen are anticipated. This philosophy was considered acceptable when discussed with prominent scientists in this field.

In order for non-metallic structures to become widely accepted in space applications, it is necessary for cognizant government and industry leaders to know what has been considered in the past and how this relates to unique applications of the future.

SECTION VII -- REFERENCES

1. Innovative Structures for Space Applications: Goodyear Aerospace Corporation Brochure, GAC 19-1563 Rev A, November 1982

2. Space Station Concept Development Group OMV/OTV/Satellite Servicing Workshop. Unpublished Paper, Martin-Marietta, Denver, Colorado, November 14, 1983.

3. Development of Deployable Structures for Large Space Platform Systems. Interim Report Volume I. Report No. SSD82-0121-1, NASA/MSFC Contract NASA 8-34677, August 1982, Rockwell International Space Operations/ Integration and Satellite Systems Division.

4. Cordier, K. L.: Optimization of Chemically Rigidized Expandable Structure Techniques. AFAPL-TR-70-19, Goodyear Aerospace Corporation, Akron, Ohio, April 1970.

5. Preliminary Study to Adapt Inflatable Structures to a Space Station Manned Habitat and an Orbit Transfer Vehicle (OTV) Hangar. GAC study for Rockwell International, Downey, CA. GAC 19-1585, February 1983, Goodyear Aerospace Corporation, Akron, Ohio. Prime Contract NAS8-34677.

6. Space Station Crew Safety Alternatives Study, Interim Briefing. Rockwell International, Shuttle Integration and Satellite Systems Division. Contract NAS1-17242, 13 September 1983, Report No. SSD 83-0106.

7. Mikulas, Martin M., Jr.: Space Station Structural Design. Unpublished Paper. NASA, Langley Research Center, Presented at the Space Station Technology Workshop, Williamsburg, VA, March 28 - 31, 1983.

8. Space Station Crew Safety Alternatives, Midterm Briefing. Rockwell International, Shuttle Integration and Satellite Systems Division. Contract NAS1-17242, May 1983. Report No. SSD83-0064.

9. Study of Large Flexible Tunnel for Shuttle/Payload Interface. Goodyear Aerospace Corporation, Akron, Ohio. MSFC Contract NAS8-28951, 22 November 1972, Report No. GER-15834.

10. Design and Fabrication of a Flexible Tunnel for Sortie Lab. Goodyear Aerospace Corporation, Akron, Ohio. MSFC Contract NAS8-30297, January 1974, Report No. GER-16060.

11. Andrews, D. G., Caluori, V.A. and Bloetscher, F: Optimization of Aerobraked Orbital Transfer Vehicles. AIAA 16th Thermophysics Conference. June 23-25/ Palo Alto, California. AIAA-81-1126. (Also Horton, T. E.: Thermophysics of Atmospheric Entry. Progress in Astronautics and Aeronautics. Volume 82, Martin Summerfield, Series Edition.)

12. Spacelab Follow-On Development, Medium Team Study. Volume I - Executive Summary Part B. Prepared for ESA/ESTEC under Contract No. 4714/81/F/HEW (SC), Aeritalia Report No. MT-AI-RP-001, March 1982.

13. Transactions 3rd Aerospace Expandable and Modular Structures Conference, Air Force Aero Propulsion Laboratory (Sponsor), WPAFB, Dayton, Ohio, May 16 - 18, 1967. AFAPL TR 68-17

14. Lunar Stay Time Extension Module (STEM), Final Report, Goodyear Aerospace Corporation, Akron, Ohio, Contract NAS 1-4277, GER 12246, 21 August 1965.

15. Safe Life and Leak Before Burst Test Report for STT Flexible Element. Goodyear Aerospace Corporation, Akron, Ohio, C. O. No. 78016033. Report No. GAC 19-1250, May 1979.

16. AFAPL-TR-65-108 Aerospace Expandable Structures Conference Transactions, May 1965, Pg. 367 - 368.

17. Shaffer, A.: Analytical Methods for Space Vehicle Atmospheric Control Process, Part I and II. ASD Technical Report 61-162, Wright-Patterson Air Force Base, Ohio, December 1961.

18. Leger, L.J., Visentine, J. T. and Kuminecz, J. F.: Low Earth Orbit Atomic Oxygen Effects on Surfaces. NASA-LBJ Space Center, Houston, Texas, AIAA 22nd Aerospace Sciences Meeting, January 9 - 12, 1984, Reno, Nevada, AIAA-84-0548.

19. Kessler, D. J.: Sources of Orbital Debris and the Protected Environment for Future Spacecraft. Journal of Spacecraft and Rockets, Vol. 18, No. 4, July - August 1981, Page 357, (also AIAA 80-0855R).

20. Reynolds, Robert C., Rice, Eric E. and Edgecombe, Donald S.: Man-Made Debris Threatens Future Space Operations. Physics Today. September 1982.

21. Expandable Airlock Experiment (D-21), Final Definitive Experiment Plan (DEP), Goodyear Aerospace Corp., Akron, Ohio, GER 13036 Rev A, 1 June 1967

22. The Tethered Satellite System. Final Report from the Facility Requirements Definition Team. NASA Contract NAS8-33383. Center for Atmospheric and Space Sciences, Utah State University, Logan, Utah. May 1980. (No Report Number)

23. Bekey, Ivan: Tethers Open New Space Options. NASA Office on Space Flight. Astronautics and Aeronautics, April 1983, pp 33 - 40.

APPENDIX A

EXPANDABLE AIRLOCK EXPERIMENT FOR THE SIVB WORKSHOP

TABLE 3-I - D-21 EXPANDABLE AIRLOCK DESIGN SUMMARY

PHYSICAL CHARACTERISTICS

WEIGHT	185.59 LBS
PACKAGED VOLUME (LAUNCH)	17.5 FT^3
EXPANDED VOLUME (ORBIT)	78 FT^3
SIZE	60 INCH X
HATCH	34 INCH DIA
DESIGN PRESSURE	3 1/2 PSIG

COMPONENT SUMMARY

- PACKAGING ASSEMBLY
  - RESTRAINT SYSTEM
  - RELEASE SYSTEM
- AIRLOCK STRUCTURE ASSEMBLY
  - EXPANDABLE STRUCTURE
  - TERMINAL RINGS
- HATCH ASSEMBLY
  - HATCH STRUCTURE
  - HINGE & LATCH HARDWARE
  - EMERGENCY EGRESS
- PRESSURE BULKHEAD ASSEMBLY
  - BULKHEAD STRUCTURE
  - AIRLOCK CONTROL PANEL
  - VENT SYSTEM
- PRESSURIZATION SYSTEM
  - INITIAL DEPLOYMENT
  - PROOF PRESSURE
  - INGRESS-EGRESS
  - 15-DAY TEST
- TELEMETRY DATA SYSTEM
  - AIRLOCK WALL SURFACE TEMPERATURES
  - AIRLOCK PRESSURE
- MOUNTING STRUCTURE ASSEMBLY
- REMOTE CONTROL PANEL
  - INSIDE NASA AIRLOCK MODULE (A/M)

TABLE 3-II - D-21 EXPANDABLE AIRLOCK WEIGHT SUMMARY

AIRLOCK		81.27
EXPANDABLE MATERIAL	39.53	
TERMINAL RING (2)	9.17	
CLOSING RINGS (2) OUTER SURFACE	3.11	
HATCH ASSEMBLY	19.78	
PRESSURE BULKHEAD	6.68	
SEALS (2)	3.00	
PACKAGING		13.48
PACKAGING RESTRAINT AND RELEASE	5.71	
MOUNTING STRUCTURE	7.77	
PRESSURIZATION		64.68
150 IN^3 STORAGE BOTTLES (6)	30.54	
INFLATION GAS N_2	7.06	
BOTTLE SUPPORTS	4.20	
PYROTECHNIC GAS RELEASE VALVES (5)	1.15	
DRAIN FITTINGS (6)	2.28	
CHARGING VALVES (5)	.60	
PRESSURE RELIEF VALVE	.40	
VENT VALVE MANUAL (2)	3.00	
VENT VALVE ELECTRIC	5.50	
VENT VALVE - EMERGENCY EGRESS	1.50	
MANIFOLD, TUBING & FITTINGS	8.45	
INSTRUMENTATION AND CONTROLS		25.16
TELEMETRY SENSORS (6-TEMP, 2-PRESS)	.65	
HARD LINE SENSORS (5)	1.25	
BATTERIES (2)	2.00	
CONTROL PANELS (2)	4.40	
PRINTED CIRCUIT BOARDS (14)	3.34	
CIRCUIT BOARD HOLDERS	2.93	
POWER SUPPLY WIRING (12V)	1.64	
PYROTECHNIC PIN PULLERS AND WIRING	3.06	
WIRING AND RECEPTACLES	5.89	
LBS TOTAL		184.59

Table 3-IV - Structural Characteristics

DESIGN PRESSURE	3-1/2 PSI
SAFETY FACTOR	3
STRUCTURAL APPROACH	FILAMENT WIND
STRUCTURAL MATERIAL	8-MIL DIA STAINLESS STEEL CABLE
UNIT WEIGHT	.109 LB/1000 FT
ULTIMATE	300,000 PSI
"E" MODULUS	30×10^6 PSI
WINDING ANGLE	30°
WINDING AREA	77 FT^2
TOTAL WEIGHT	4.2 LB

FOLDING EFFECTS

SINGLE CABLE WITH SHARP 180° CREASE FOLD
15% DECREASE IN ULTIMATE

PRESSURE BLADDER BACKING SHARP 180° PACKAGING FOLD
1000 CYCLES - NO DEGRADATION

Table 3-V Environmental Compatibility - Expandable Material

TOXICITY: NON-DETECTABLE

O_2 COMPATIBILITY: 5 PSI AT 200°F

FLAME RESISTANCE: .3 MIL ALUM FOIL FLAME BARRIER

THERMAL CHARACTERISTICS

MAX TEMPERATURE

OUTER SURFACE MATERIALS	+300°F
INNER SURFACE MATERIALS	+250°F

MIN TEMPERATURE

DEPLOYMENT FLEXIBILITY	-100°F
EXPANDED STATIC	-150°F

VACUUM EFFECTS

1/2 % WEIGHT LOSS AT 10^{-6} TORR

SPACE RADIATION

MATERIAL TOLERANCE	10^7 RAD
EXPECTED DOSE (1-YEAR)	10^5 RAD

MICROMETEOROIDS

P_0 = .9999 . . . . . FOR 30 DAYS

EXPANDABLE AIRLOCK EXPERIMENT FOR THE SIVB WORKSHOP

F. Forbes,* L. Jurich,** and A. Cormier*

assisted by

G. Reid,† L. Manning,** and J. Williams‡

INTRODUCTION

The purpose of this technical paper is to describe the D-21 expandable experiment scheduled for orbital flight testing on the NASA SIV Workshop Flight AAP-2. This paper summarizes the background conditions that led to the D-21 experiment definition, the objectives of the experiment, and a technical discussion of the experiment.

With the rapid advancement in space technology, the United States will be orbiting a series of manned space laboratories from which astronauts can perform various experiments and tasks. Some of these experiments and tasks will necessitate astronaut extra-vehicular activity (EVA). An airlock system will be necessary to alleviate the repeated decompression and compression cycles imposed on the laboratory work area during egress and ingress maneuvers associated with EVA. An expandable airlock would minimize weight and volume requirements imposed on the vehicle and would permit maximum utilization of the internal volumes already available in these laboratories and spacecraft.

Since 1960, considerable Air Force in-house work has been performed on various expansion and rigidization systems, including gelatin rigidized structures and expandable self-rigidizing honeycomb. Additionally, a number of contractual efforts were initiated to investigate expandable elastic recovery material concepts. The level of contract efforts included basic materials research, design and fabrication studies, and construction and ground tests of full-size prototype structures.

Several contract efforts monitored by NASA also have resulted in the successful construction and test of large expandable space structures. These

---

*Space Technology Branch of Air Force Aero Propulsion Laboratory, Wright-Patterson AFB, Dayton, Ohio.

**Astronautics Programs Department, Goodyear Aerospace Corporation, Akron, Ohio.

†6570th Aerospace Medical Research Laboratory, Wright-Patterson AFB, Dayton, Ohio.

‡NASA Langley Research Center, Hampton, Va.

99 — 114

structures, based on the elastic recovery materials approach, were successfully demonstrated, tested, and then evaluated in vacuum chamber deployment tests. As an outgrowth of this development, two structure concepts have emerged: (1) the chemically rigidized structure concept (see Figure 1) and (2) the elastic recovery materials technique (see Figure 2).

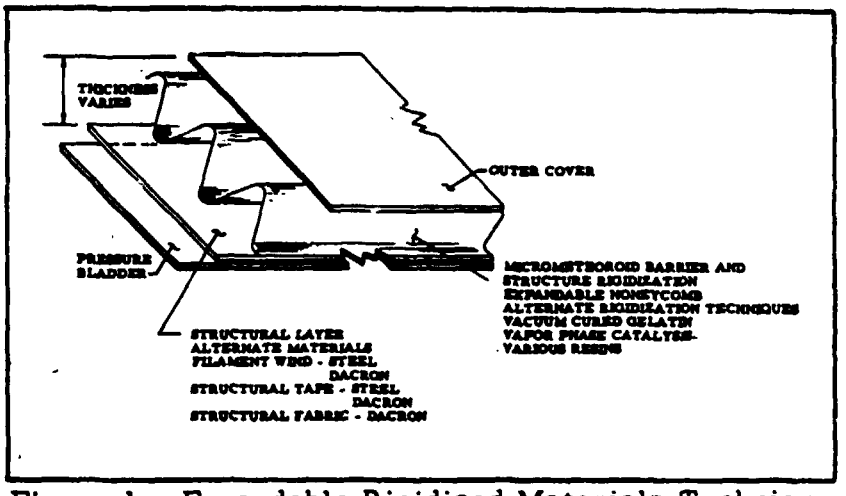

Figure 1 - Expandable Rigidized Materials Technique

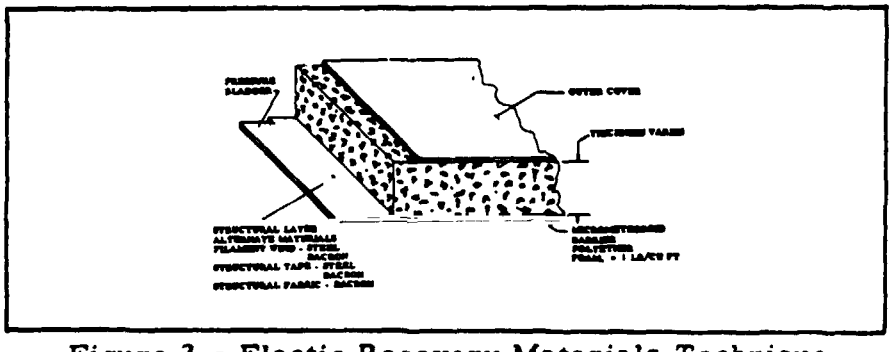

Figure 2 - Elastic Recovery Materials Technique

Both structure techniques are designed to do essentially the same job. The chemically rigidized approach, however, provides an added capability of structure rigidization subsequent to deployment in orbit. The chemical system is more complex and, therefore, has not been so extensively developed as the elastic recovery approach has.

The elastic recovery materials technique rests on a solid background of development. Technology is at a point where the next logical and needed step is a manned orbital flight demonstration. Extensive development of this materials technique conducted by both NASA and the Air Force in the form of full-scale prototype structure fabrication and testing is summarized below. Because of these programs, the Air Force has selected, as a basis for the D-21 flight experiment, the elastic recovery concept.

A crew transfer tunnel was developed by the Goodyear Aerospace Corporation under contract to the Space Technology Branch of the Air Force

Aero Propulsion Laboratory (AFAPL). The tunnel structure is 4-ft wide and 12-ft long, integrated with a rigid metal honeycomb slab structure 3-ft wide and 12-ft long, along one side. Successful structural, gas leakage, packaging, and deployment tests were conducted on the full-scale structure along with extensive materials environmental compatibility testing.

A Stay Time Extension Module (STEM), an integrated lunar shelter airlock, was developed by Goodyear Aerospace under contract to the NASA Langley Research Center. The shelter is 7-ft in diameter and 13-ft long, with an integral airlock 7-ft in diameter and an additional 4-ft long. The test program included structural evaluation, gas leakage, packaging, and deployment.

A retractable airlock was developed by the Whittaker Corporation for the Langley Research Center. This airlock design is 4-ft in diameter and 7-ft long and incorporates a mechanism for retracting the structure when it is not in use.

These advances in elastic recovery materials technology clearly indicated that the next logical step was a manned orbital flight demonstration. Therefore, an expandable airlock system was defined and submitted for approval to both the Department of Defense (DOD) and NASA for flight experiment. In September 1966, the expandable airlock flight experiment was formally approved and designated D-21. This approval was followed in December by a competitive contract award to Goodyear Aerospace for developing the D-21 experiment hardware.

SCOPE OF D-21 EXPERIMENT

The D-21 experiment probably is the most extensive program to have been implemented in the manned application of expandable structures technology. The scope of the D-21 airlock program extends fro.. initial human factors evaluations to establishing size and geometry of the a rlock structure to final retrieval of data and definition of experiment results subsequent to orbital testing.

Human Factors

One of the first tasks to be implemented was intensive human factors testing to establish the baseline definition of the experiment design. Testing was conducted by AFAPL and the Air Force Aero Medical Laboratory to establish optimum geometry requirements for the D-21 airlock design and to establish the minimum hatch size consistent with the Apollo space suit and use of a PLSS (Portable Life Support System). Neutral buoyancy tests were conducted in the underwater facility at Wright-Patterson AFB (WPAFB) to establish optimum maneuvers of ingress/egress and to define locomotion aids necessary for these maneuvers and, therefore, for the orbital experiment.

Step-by-step procedures have been established for the overall experiment. These procedures have been defined in a "time line" established for the experiment; about three hours of EVA are required of each of two astronauts to perform the overall experiment. It is expected that the time line

and experiment procedures will be continually refined as crew training is implemented. The proposed training plan includes using both underwater facilities and the KC-135 zero "g" airplane to implement practice maneuvers of the experiment procedures prior to flight.

Hardware Requirements

The experiment plan was established by AFAPL in conformance with experiment guidelines stipulated by the NASA Manned Spacecraft Center (MSC). This plan calls for the developing and extensive qualification testing of experiment hardware used specifically for this purpose. Additional experiment hardware also is required to support astronaut crew training in conformance with experiment procedures stipulated in the experiment plan. This hardware will consist of airlock mockups (of both rigid and expandable materials) to be used both underwater and in the KC-135 to simulate zero "g" maneuvers in experiment procedures. Duplicate sets of flight hardware will be required as the primary and backup flight units. All hardware, except that used for training, must comply with the NASA requirements of NPC-200-2 and NPC-200-3 for quality control and inspection.

Documentation and Design Reviews

Documentation will be required substantially beyond the requirements normally associated with a research and development project. In addition to the usual status reports normally required, documentation in various forms consistent with the experiment requirements and schedules will be submitted for review and approval throughout the program. These documentation forms will include (1) definitive experiment plan, (2) failure mode and effects analysis, (3) qualification test specifications and procedures, (4) qualification test status and final report, and (5) quality control plan and inspection system.

In addition to the documentation stipulated above, periodic design reviews will be held to ensure final integration of the D-21 experiment with the flight vehicle and subsequent implementation of the experiment during flight. These reviews will include (1) initial design review, (2) design certification review, (3) qualification test design review, (4) postqualification test design review, (5) acceptance review, and (6) flight readiness review.

Test Requirements

Extensive ground testing will be required prior to flight acceptance of the D-21 experiment. This testing will be performed on one set of flight design hardware fabricated specifically for this purpose. The test program is directed toward attaining two objectives: (1) to ensure compliance with manned mission requirements and (2) to ensure a high probability that the experiment will succeed.

The test program will be conducted on an integrated assembly of the D-21 hardware. Testing will be environmental in nature and will simulate

the three categories of environment expected: earth environment, spacecraft environment, and space environment. Testing under the first two categories will be performed with the D-21 hardware in a packaged configuration (see Figure 3). Space environment testing will be performed with the D-21 in both a packaged configuration and in a deployed configuration (see Figure 4). Space environment testing also will include the functional aspects of the D-21 experiment defined by the experiment procedures.

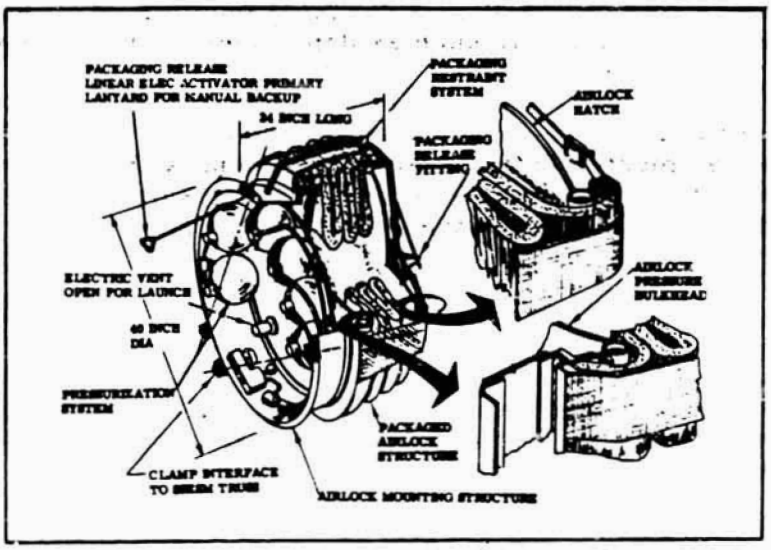

Figure 3 - D-21 Packaged Configuration

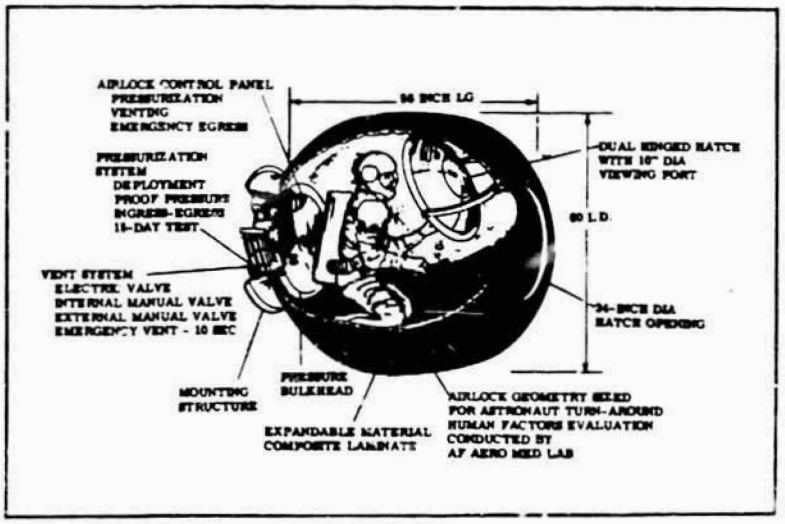

Figure 4 - D-21 Expanded Configuration

Experiment Data

Data from the D-21 orbital experiment will be obtained via telemetry,

motion picture coverage, and voice recordings. The D-21 airlock will be instrumented for temperature and pressure data via telemetry to establish the leak rate of the D-21 airlock in orbit.

Biomedical data will be obtained during astronaut ingress/egress demonstration of the D-21 airlock to evaluate the airlock design relative to the dynamics of ingress/egress and human factors suitability.

Motion picture coverage will permit visual monitoring of the key functional phases of the experiment, such as deployment of the structure and the ingress/egress demonstration.

Voice recordings will be obtained during the entire period of the functional phases of the experiment. These recordings, along with other methods of data return, will permit a thorough assessment of the results of the D-21 experiment. Evaluation and analysis of the experiment results will be published in a final report.

SIVB MISSION OBJECTIVES

Fundamentally, the objective of the SIVB mission is to evaluate the feasibility of using the empty shell of the spent SIVB stage to support crew operations for a 30-day orbital mission.

The SIVB orbital workshop mission will consist of two flights. AAP-1 is manned and AAP-2 is unmanned and is launched five days later. Rendezvous and docking will occur at an approximate orbital altitude of 260 naut mi followed by the 30-day operational mission. The basic orbital hardware of AAP-2 consists of the SIVB spent stage, an airlock support module for subsystem support of the spent SIVB (such as stage pacification, environmental control system, power, and communications), and a multiple docking adapter (MDA) for subsequent linkup of the Apollo Command Service Module (CSM) and resupply modules.

Corollary experiments (such as D-21)will be carried on AAP-2, either in the MDA or on the airlock support module. All experiments will be performed during the 30-day mission period and will be integrated into an overall time line for overall experiment procedures.

Figure 5 shows an artist's concept of the expanded configuration of the D-21 airlock deployed from its mounting location atop one of the four truss structures used to support the airlock support module. The experiment is located external to the thermal curtain used to shield the support module subsystems and is near the EVA panel, thus providing astronauts access to the experiment.

D-21 FLIGHT EXPERIMENT OBJECTIVES

The objective is to obtain the maximum amount of data for use in future airlock designs. These data must necessarily be obtained under a constraint

Figure 5 - D-21 Airlock Deployed from Mounting Location

of minimum astronaut participation considering the large number of individual experiments to be performed on NASA Flight AAP-2. Specifically, the objectives of the experiment are as follows:

1. To ascertain the ability of expandable structures to withstand the boost and launch phase of a typical mission profile with subsequent successful deployment in orbit

2. To validate the successful performance of expandable materials in operational use when subjected to the total orbital space environment

3. To evaluate structure packaging techniques and deployment dynamics

4. To evaluate space environment effects on expandable materials after prolonged exposure (six months)

5. To demonstrate the compatibility of expandable elastic recovery materials in airlock designs with the dynamics of astronaut ingress/egress

6. To establish design parameters and requirements for elastic recovery airlocks for future manned orbital laboratories

7. To provide a baseline from which to extrapolate the application of expandable structures technology to other uses such as crew transfer tunnels, space shelters, and controlled maintenance stations and storage depots

TECHNICAL DISCUSSION OF D-21 EXPERIMENT

The experiment total flight package consists of four distinct units of hardware: (1) the integrated D-21 airlock package, (2) a control panel mounted inside the NASA airlock module (AM) for remote control of the experiment, (3) a wiring harness interconnecting the D-21 package with the remote control panel, and (4) a container for earth return of material specimens.

The D-21 airlock package, shown in Figure 4 and in an exploded view in Figure 6, is comprised of the following subassemblies: (1) packaging system, (2) airlock structure assembly, (3) hatch assembly, (4) pressure bulkhead assembly, (5) pressurization system, (6) telemetry data system, (7) electrical system, (8) mounting structure assembly, and (9) experiment control system.

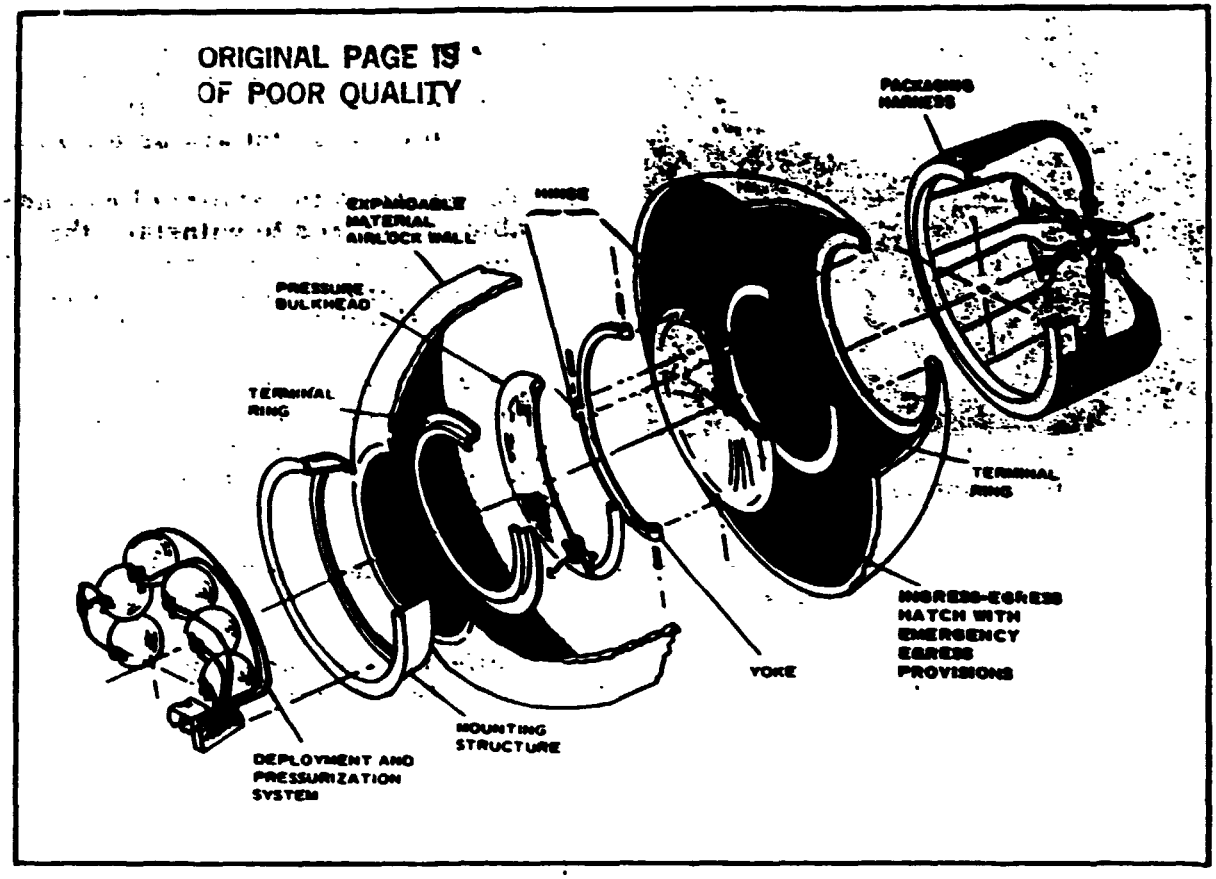

Figure 6 - D-21 Airlock (Exploded View)

Packaging System

The packaging system consists of a series of flexible nylon straps located around the periphery of the mounting base to restrain the expandable portion of the airlock structure in a packaged configuration (see Figure 3). The restraining straps terminate at a release fitting located at the apex point of the package. To deploy the airlock structure to its expanded configuration, provisions are incorporated to release the restraint system either by remote control (electric actuator located in mounting base structure) or by a manually actuated lanyard located on the D-21 airlock package. Provisions are incorporated into the packaging design to position and retain the restraining straps after the airlock is deployed. These straps are secured to the wall structure to lie along the contoured airlock wall material after expansion until full and final geometry has been attained.

Airlock Structure Assembly

The structural assembly consists essentially of the expandable structure material comprising the airlock wall, which is intimately bonded and joined with rigid structure design terminal rings.

The terminal rings, at each end of the airlock configuration, are fabricated of light gage aluminum sheet material. The function of these rings is to provide a rigid termination to the flexible material of the airlock and also to provide a smooth flat surface for hatch and pressure bulkhead seals. The rings are nonstructural in the sense that no tension load transfer occurs between the wall structure and the rings themselves. The rings do, however, function as a load path (via the seals) to transfer hatch and pressure bulkhead pressure loads into the reacting expandable structure.

The expandable portion of the airlock structure uses the elastic recovery materials technique to permit folding and packaging of the structure into a small compact configuration for launch. Once in orbit, the airlock is deployed to its full expanded configuration by the recovery action of the wall material and augmented by low level pressure (less than 0.5 psi) for final shaping. After final shaping, the inherent stiffness of the wall structure will ensure final shape rigidity even under zero pressure conditions.

Basically, the structure wall is a four-layer composite of flexible materials in accordance with Figure 7 and as described below.

Pressure Bladder - The pressure bladder is a laminate of three individual sealant layers with an inner layer of 0.3-mil aluminum foil. The inner sealant layer is a laminate of nylon film-cloth. This layer is bonded with polyester adhesive to a second layer of closed-cell EPT foam 1/16-in. thick. The outer sealant is a nylon film-cloth laminate coated with a polyester resin. The total weight of the bladder composite is 0.159 psf and is independent of design pressure.

Structural Layer - The filament winding manufacturing process is used for the structural layer and provides near the optimum in lightweight load-carrying flexible structure. The structure layer will be wound with three 0.0036-in. stainless steel wires interlaced with a rayon yarn in a winding pattern of 32 hoop filaments and 29 longitudinal filaments per inch.

Micrometeoroid Barrier - Micrometeoroid protection is achieved by a one-inch layer of flexible polyester foam. Flexible foam of 1.2 psf density has been selected as suitable barrier material, based on hypervelocity particle impact tests. While the primary function of the foam would be to act as a micrometeoroid barrier, it also serves as a deployment aid. During packaging, the foam layer would be compressed to about 10 percent of its original thickness and restrained by the packaging canister. Upon deployment in orbit, the canister would be released and the elastic recovery characteristics of the foam would help shape the airlock to its fully expanded volume.

Outer Cover Layer - The outermost layer of the composite wall structure encapsulates the wall to provide a smooth base for the application of a thermal coating. Inasmuch as the outer cover would encapsulate the composite wall, it would serve as an aid in packaging the structure prior to launch. By a vacuum technique, the wall thickness can be compressed from the fully expanded thickness to about 1/4 in., suitable for folding and subsequent packaging in the canister. A passive thermal control coating would be applied to maintain material temperatures within acceptable limits.

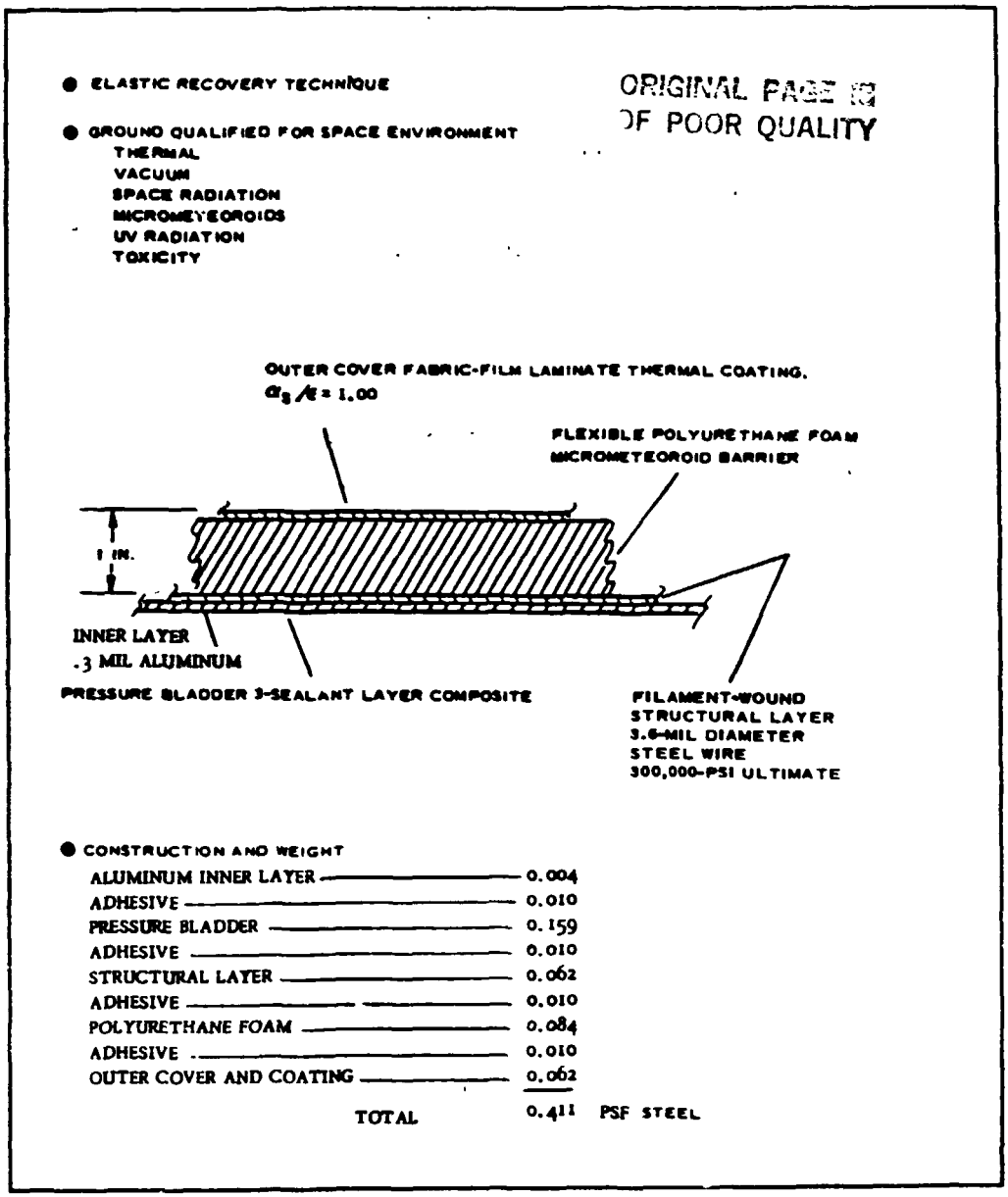

Figure 7 - Expandable Materials Approach

The structural approach being used in the D-21 design is based on a filament winding technique as indicated above. The structural characteristics of this technique are summarized in Table 1.

The compatibility of the expandable materials approach with respect to operations in a space environment has been tentatively established with extensive ground testing. Table 2 presents the environmental compatibility characteristics of the selected materials approach. The materials capability indicated appears to be well within the range of expected environmental conditions without constraining the basic Saturn-Apollo SIVB flight in any way.

TABLE 1 - STRUCTURAL CHARACTERISTICS

Item	Characteristic
Design pressure	3-1/2 psi
Safety factor	3
Structural approach	Filament wind
Structural material	8-mil diam stainless steel cable
Unit weight	0.109 lb/1000 ft
Ultimate	300,000 psi
"E" modulus	30×10^6 psi
Winding angle	30 deg
Winding area	77 sq ft
Total weight	4.8 lb
Folding effects	
Single cable with sharp 180-deg crease fold	15 percent decrease in ultimate
Pressure bladder backing with sharp 180-deg packaging fold	1000 cycles, no degradation

Hatch Assembly

The hatch assembly shown in Figure 4 consists of a basic dome and compression ring structure; a dual yoke-type hinge and latch hardware; hatch separation provisions for emergency egress; and a 10-in. diameter viewing port. The hatch latches and seals against the terminal ring and can be operated either from the interior or exterior of the airlock.

The basic pressure dome and compression ring structure is fabricated of aluminum and is separable from the overall hatch assembly as a provision for emergency egress. Although the emergency egress feature of the hatch is not required for the experiment procedures as now stipulated, this feature will be incorporated into the hardware design to be available if needed. Controls to separate and jettison a portion of the hatch under emergency conditions are provided at three locations:

1. At the interior of the D-21 airlock on the airlock control panel

TABLE 2 - ENVIRONMENTAL COMPATIBILITY

(EXPANDABLE MATERIALS)

Item	Characteristic
Toxicity	Nondetectable
Oxygen compatibility	5 psi at 200 F
Flame resistance	0.3-mil aluminum foil flame barrier
Thermal characteristics	
Maximum temperature (F)	Outer surface materials, +300; inner surface materials, +250
Minimum temperature (F)	Deployment flexibility, -100; expanded static, -150
Vacuum effects	One-half of one percent weight loss at 10^{-6} Torr
Space radiation	Material tolerance, 10^7 rad; expected dose (one year), 10^5 rad
Micrometeoroids	P_0 = 0.9999 for 30 days

2. At the interior of the D-21 airlock on the mounting base structure
3. Inside the NASA AM on the remote control panel

Actuation of any of these three controls activates pyrotechnics that first vent the airlock down in 10 sec and then jettison the hatch dome structure. Figure 8 presents the schematic functioning of the emergency egress system. Figure 9 shows the diagram of the vent valve used to effect 10-sec venting. This valve is located on the pressure bulkhead and is not part of the hatch assembly. Figure 10 shows how jettisoning of the dome structure is incorporated into the hatch design.

The dual hinge arrangement shown in Figure 4 permits the hatch, in opening or closing, to slide along the interior wall of the airlock rather than sweeping out in a fixed arc as with a single-hinge design. The advantage of the design is the lesser volume swept out in hatch operation, which allows greater usable volume in the airlock. Two latches are provided on the hatch and are located 180 deg apart and 90 deg from the yoke-hinge attachments. The hatch can be jettisoned with the latches in either the open or closed positions.

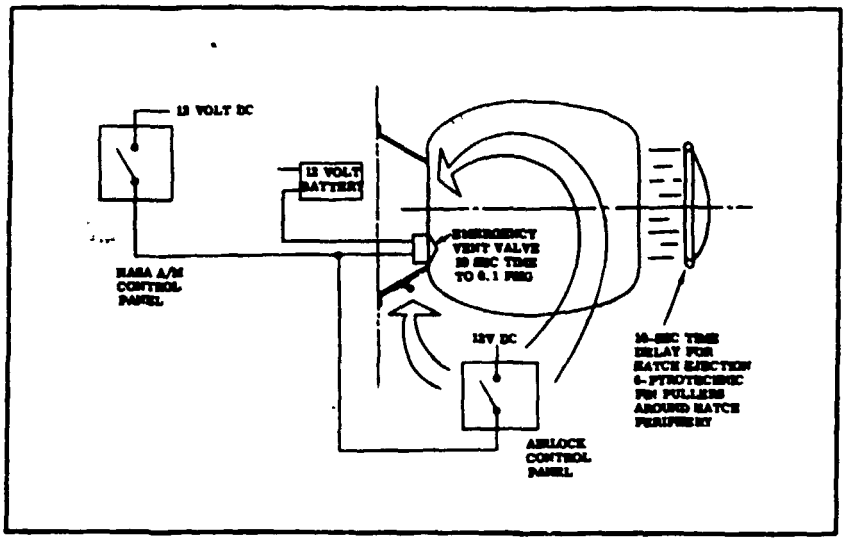

Figure 8 - Emergency Egress System

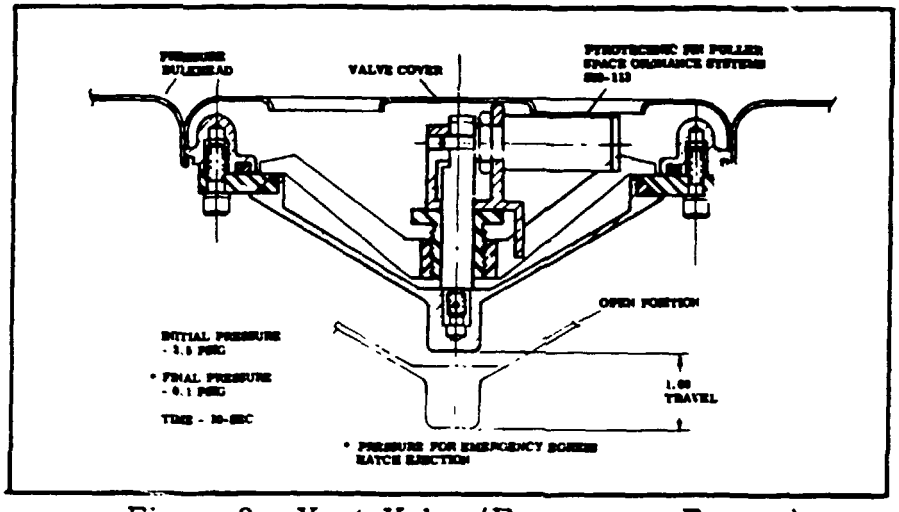

Figure 9 - Vent Valve (Emergency Egress)

The hatch also incorporates a 10-in. diameter viewing port. This port is located off center of the pressure dome to clear the hatch handles. Handles are provided at the center of the pressure dome on both sides. The handle is used to actually open and close the hatch, with latches used only for initial opening or final closing of the hatch.

Pressure Bulkhead Assembly

The pressure bulkhead assembly shown in Figure 4 consists of a basic dome and compression ring structure of aluminum, similar in concept to the dome structure of the hatch. The bulkhead assembly seal and connection is made at the 34-in. diameter terminal ring of the airlock structure and also

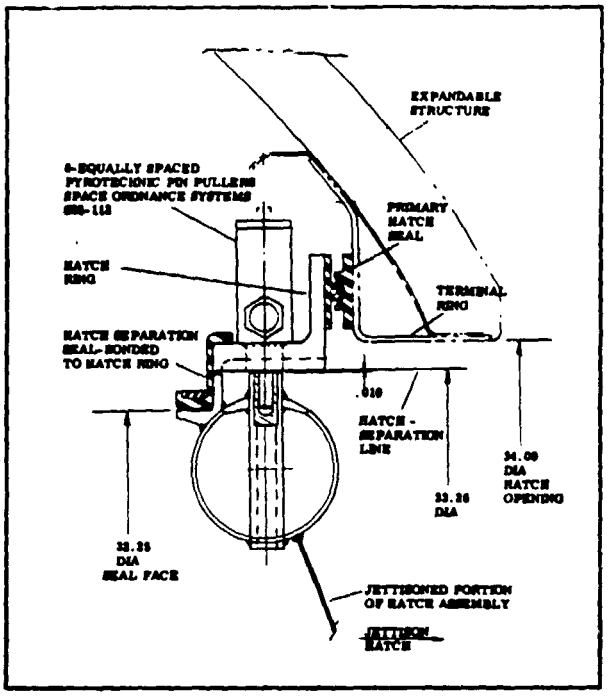

Figure 10 - Emergency Egress Hatch

attached to this ring with six equally spaced bolts. Provisions are incorporated into this assembly for a control panel; a future connection for an astronaut umbilical; and subsystem connection requirements for pressurization, venting, electrical wiring, and instrumentation.

Subsystem Interface Connection - The bulkhead design provides an eight-inch diameter connection pan and plate adjacent to the control panel for interfacing exterior subsystem requirements with the interior of the D-21 airlock. The opening of this pan is provided with a cover plate that is flush with the pressure dome contours.

The pan depth is approximately five inches, with equipment-mounting bosses located on the lower surface and around the periphery. The following equipment provisions are incorporated into this pan connection design:

1. A one-inch diameter manual vent valve located under the pan cover plate. The operating handle for this valve is above the cover plate accessible to the astronaut and adjacent to the control panel.

2. A one-inch hose connection at the bottom of the pan. This connection is used for a vent line to an exterior manual vent valve located on the exterior surface of the mounting structure for the D-21 airlock.

3. A 3-1/2-in. emergency vent valve submerged within and located on the lower surface of the pan (see Figure 9).

4. A one-inch diameter pressure relief valve set at 3-1/2 psig and mounted on the exterior surface of the pan face.

This valve is normally "locked" inoperable when not in use. The purpose of this valve is to limit airlock pressure to 3-1/2 psig and to eliminate excessive pressure buildup from astronaut suit dumping of excess oxygen and water (umbilical rate of 7.9 lb per hour).

5. A one-inch diameter pressure relief valve set at 5.25 psig and also mounted on the exterior surface of the pan face. This valve limits airlock pressure to a proof pressure level.

6. A one-inch diameter electric motor-driven vent valve. This valve is mounted on the exterior surface of the pan face and controlled either from within the D-21 airlock or from the remote control panel.

7. A 1/4-in. connection is provided on the lower pan surface for a pressure line tie to the airlock pressurization system.

8. A 1/4-in. connection is provided on the exterior periphery of the pan for the manifold connection of two pressure transducers to monitor airlock pressure.

9. Three electrical connectors are provided on the periphery of the pan to interface the exterior and interior electrical and instrumentation systems integrated into the D-21 airlock.

Pressurization System

The pressurization system for the D-21 experiment consists of six 150 cu in. high-pressure gas storage bottles charged with nitrogen. The gas is released from each storage bottle through a pyrotechnic valve to flood the airlock to a specific level of pressure established by a predetermined charge in the bottle. Gas flow from any pyrotechnic valve is directed through a common manifold fitting and then through a 1/4-in. supply line to the inlet fitting on the pressure bulkhead of the airlock. All elements of the pressurization system, including pressure storage bottles, pyrotechnic valves, and manifold fitting, are supported off the mounting base structure assembly.

Controls for gas release are located either inside on the D-21 airlock control panel or on the remote control panel located within the NASA AM. These controls are established for conducting the D-21 experiment and include pressurization provisions for deployment, proof pressure, astronaut ingress/egress, and a final 15-day test.

Deployment - Release of the airlock canister restraint is actuated by a switch located on the remote control panel in the airlock module. A mechanical backup system manually operated at the base of the D-21 airlock also is provided. An initial deployment of the structure is partially effected upon

release of the restraint system. Final deployment is achieved through pressurization by release of nitrogen from the 485 psig nitrogen storage bottle. Figure 11 shows the deployment system and method of control.

Proof Pressure - As soon as the airlock has been fully deployed, it is pressurized to a 5-psig proof level from two of the pressure bottles manifolded together for this purpose. The proof pressure level is to be held for about 30 min and then vented. Figure 12 shows the proof pressurization system and the method of control.

Ingress/Egress - Individual pressurization is provided for two cycles of astronaut ingress/egress. This portion of the pressurization system is shown in Figure 13. Pressurization controls are provided both within the D-21 airlock package and within the NASA AM.

15-Day Test - The pressurization system also provides for a 15-day pressure test during which time pressure and temperature data will be obtained via telemetry for determining long-time leak rates of the airlock experiment. Provisions for this pressurization also are shown in Figure 13.

Venting Provisions - Four distinct venting provisions are incorporated in the D-21 experiment design:

1. Manual Vent - A one-inch diameter manual vent valve is located within the D-21 airlock adjacent to the D-21 control panel.

2. Electric Vent - A one-inch diameter electric motor-driven vent valve is located on the exterior of the pressure bulkhead assembly. This valve is switch controlled from either the D-21 control panel or from the remote control panel located in the NASA AM.

3. Manual Vent - Another one-inch diameter manual vent valve is located exterior to the D-21 on the outside surface of the airlock base structure. This valve is provided as a backup to the electric vent in case of malfunctioning.

4. Emergency Vent - A 3-1/2-in. diameter vent valve (see Figure 9) is provided for rapid venting as an emergency feature. This valve is used only in conjunction with the emergency egress feature of the hatch design.

Telemetry Sensors

Pressure and temperature data will be monitored during the course of the D-21 experiment using the NASA support module telemetry system. Eight sensors will be provided, two for airlock pressure and six for surface temperature of the expandable material wall structure.

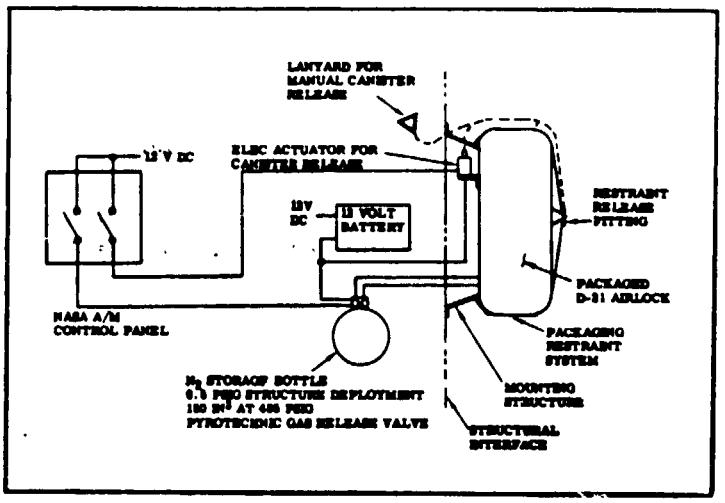

Figure 11 - Pressurization Cycle (0.5 psig)

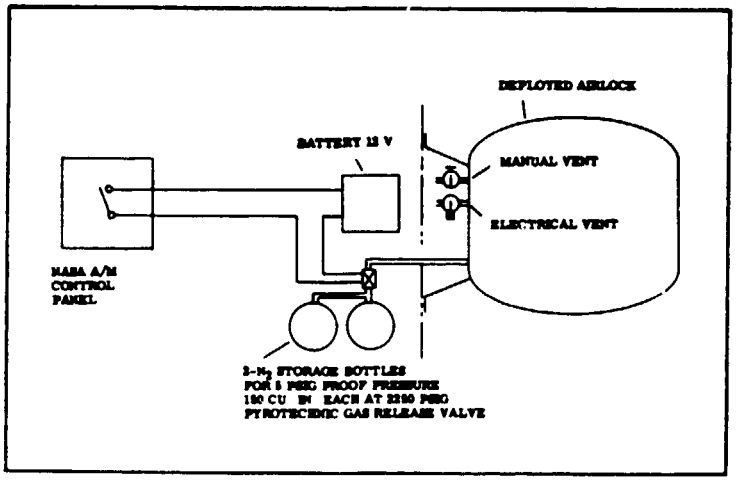

Figure 12 - Pressurization Cycle (5.0 psig)

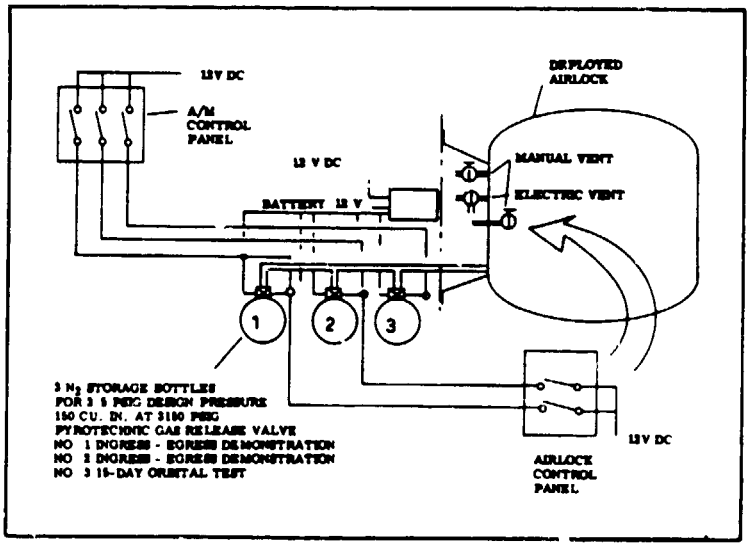

Figure 13 - Pressurization Cycles (3.5 psig)

The pressure transducers will be mounted on the airlock pressure bulkhead and will have a range of zero to 6 psig. Accuracy of these sensors is expected to be about ±4 %.

Two temperature sensors (thermistors) will be mounted on the interior surface of the expandable wall structure located at the midpoint of the structure and 180 deg apart. The range of these sensors is -50 to +150 F, with an expected operational range of 50 to 100 F.

Four additional temperature sensors (also thermistors) will be attached to the exterior surface of the expandable wall material. These will be located 90 deg apart around the periphery of the airlock. The range of these sensors is -150 to +250 F. The operational range expected is -125 to +250 F.

Electrical System

Power for the D-21 experiment will be supplied from a self-contained battery pack and from the 28-v power source of the NASA support module. The self-contained power source will be a dual pack of nickel-cadmium batteries. These batteries will supply power only for the pyrotechnics included in the D-21 design and will be used for no other purpose.

The NASA support module will provide all remaining power requirements for the D-21 experiment including telemetry power, lighting, vent valves, canister release, and control panel lighting. Table 3 presents the power profile for the D-21 experiment for various operating modes.

Mounting Structure

The mounting base structure shown in both Figures 3 and 4 is contructed of light gage aluminum sheet. The basic geometry is a cylindrical shell 34 in. in diameter and 10 in. high. Stiffener rings are provided at each end of the shell, with axial stiffeners located circumferentially around the shell.

The mounting structure provides the physical integrating function for all hardware components of the experiment. The airlock structure assembly is attached to one ring face of this structure with 24 equally spaced bolts. All subsystems exterior to the airlock itself are located within and supported on the mounting shell structure.

The physical interface between the D-21 experiment and the NASA support module is at the face of the mounting structure opposite the airlock. The mounting interface will include provision for 24 equally spaced bolts to provide optimum mounting load distribution. Physically, this interface will be made at the McDonnell Company in St. Louis, where the D-21 experiment will be installed and integrated with the NASA support module.

Experiment Control System

Controls for conducting the D-21 airlock experiment are provided in three locations:

1. A remote control panel located inside the NASA AM

TABLE 3 - POWER PROFILE (SUPPORT MODULE POWER SOURCE)

Operating mode	Duration (min)	Average load (amps)		Total load (amps)			
		Remote control panel	D-21 airlock	Average	Peak	Peaks/ mode	Peak duration
Experiment, on	5	0.36	0.50	0.86	. . .	. . .	. . .
Telemetry calibration	5	0.36	0.58	0.94	. . .	. . .	. . .
Canister release	5	0.40	0.50	0.90	1.10	1	1 min
Pressure system armed	10	0.44	1.56	2.00	. . .	. . .	. . .
Deploy	5	0.36	1.64	2.00	3.00	2	1 sec
Proof pressure	30	0.40	1.69	2.09	3.09	2	1 sec
Ingress No. 1	40	0.44	3.86	4.30	5.30	2	1 sec
Ingress No. 2	40	0.48	3.99	4.47	5.47	2	1 sec
Start 15-day test	5	0.52	2.04	2.56	3.56	1	1 sec
15-day pressure test	15 days	0.16	0.42	0.58	. . .	. . .	. . .
Final vent	1 sec	0.16	0.42	0.58	1.58	1	1 sec

2. The D-21 control panel located inside the D-21 airlock and mounted on the pressure bulkhead

3. Emergency and/or backup controls mounted on the exterior surface of the D-21 airlock mounting base structure

The remote control panel provides the principal control method for conducting the D-21 experiment. Located in the pressurized environment of the airlock module, this control panel location will still permit implementation of the D-21 experiment in the event that possible limitations may be imposed on EVA.

The control panel located inside the D-21 airlock will not be used during the D-21 experiment. This piece of hardware is redundant to the experiment as now planned but is included in the experiment design and hardware to permit future pressurized ingress/egress demonstrations.

Backup controls are provided exterior to the D-21 and located on the base support structure. The purpose of these controls is to ensure implementation of experiment sequence performance in the event of possible malfunction of the primary control system operated from the remote control panel.

Remote Control Panel - The remote control panel will be located within the airlock section of the NASA AM. This panel, along with appropriate interconnect wiring to the D-21 experiment, will be supplied and installed by McDonnell in conformance with overall experiment design requirements. This panel, diagrammed in Figure 14, incorporates the following controls and indicators:

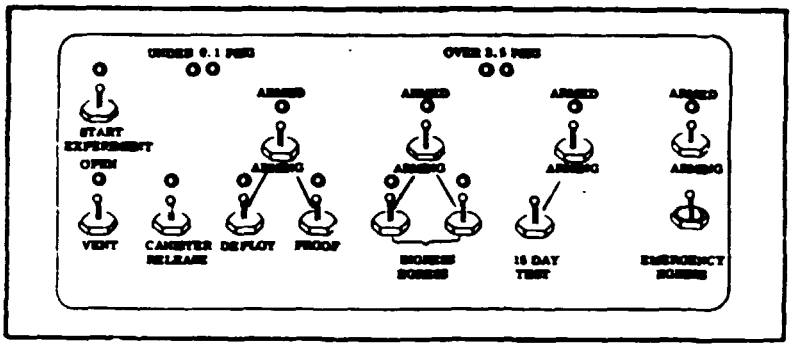

Figure 14 - Remote Control Panel

1. START EXPERIMENT switch to energize panel lighting and indicators on all control panels, the electrical vent control, and the pressure and temperature telemetry sensors in the D-21 airlock

2. VENT switch to control the electrical airlock vent. An indicator light is on when the airlock vent valve is open

3. CANISTER RELEASE switch to release the airlock restraints system, which permits the airlock to deploy

4. ARMING switch to arm the pyrotechnic gas release valves of the pressurization system. An indicator light will come on when the system has been armed

5. DEPLOY switch to actuate pyrotechnic valve for release of gas to deploy the airlock

6. PROOF switch to actuate pyrotechnic valves for release of gas from two bottles into the airlock for proof pressure test

7. D-21 LIGHTS switch to illuminate the interior of the D-21 airlock. Two 21-candle power lamps are provided for this purpose

8. INGRESS/EGRESS switches, one for each ingress/egress pressurization, to actuate pyrotechnic release valves to release gas into the D-21 airlock for two ingress/egress tests

9. 15-DAY TEST switch to actuate pyrotechnic release valve to release gas into the D-21 airlock for the 15-day pressure/exposure test

10. High-pressure dual indicator light that goes on when pressure in the D-21 airlock exceeds 3.5 psig, the normal operating pressure

11. Low-pressure dual indicator light that goes on when pressure in the D-21 airlock is less than 0.1 psig, at which time the airlock hatch can be opened

12. An emergency egress system is provided for rapid venting and subsequent jettisoning of the D-21 airlock hatch. An ARMING switch is provided for arming the squibs of the emergency vent valve and the emergency jettison of the airlock hatch. An EMERGENCY EGRESS switch activates the emergency airlock vent and jettisons the airlock hatch.

D-21 Airlock Internal Control Panel - This panel, shown in Figure 15, is located inside the D-21 airlock and is mounted on the pressure bulkhead assembly and has the following controls:

1. VENT switch to control operation of the electrical airlock vent

2. ARMING switch to arm the pyrotechnic valve squibs of the two ingress/ingress pressurizing gas bottles

3. INGRESS/EGRESS switches to release gas into the D-21 airlock for the two ingress/egress tests

4. High-pressure dual indicator lights that go on when pressure in the D-21 airlock exceeds 3.5 psig, the normal operating pressure

5. Low-pressure dual indicator lights that go on when pressure in the D-21 airlock is less than 0.1 psig, at which time the airlock hatch can be opened

6. MANUAL VENT to vent mechanically the airlock in case of malfunction of the electrically operated vent

7. EMERGENCY EGRESS has the same function as those controls provided on the remote control panel

Backup Controls - In addition to the experiment controls, there also are some local backup controls provided on the exterior surface of the D-21 supporting base structure. A diagram of these controls is shown in Figure 16, with the following functions:

1. MANUAL RESTRAINT RELEASE to release the airlock canister restraint in case of malfunction of the electrical restraint release.

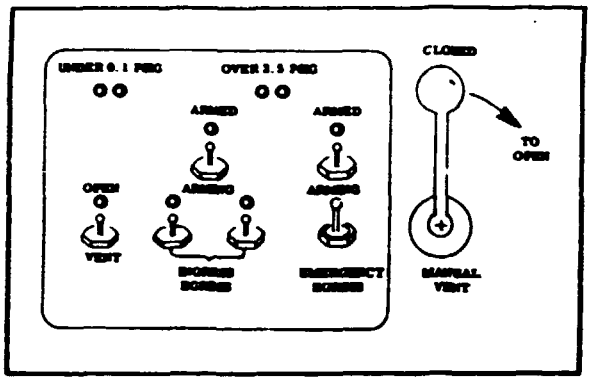

Figure 15 - D-21 Airlock Internal Control Panel

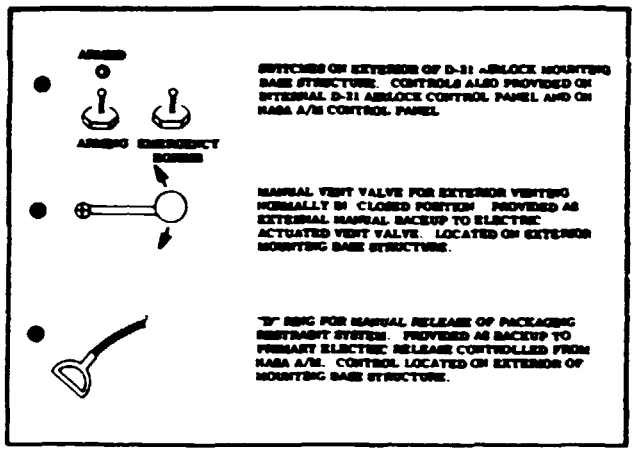

Figure 16 - Miscellaneous External Controls of D-21 Airlock

2. MANUAL VENT VALVE, located on the exterior of the airlock base, to vent the airlock from outside in the event of malfunction of the electrically operated vent.

3. EMERGENCY EGRESS has the same function as those controls provided on the remote control panel.

EXPERIMENT PROCEDURES

Procedures for conducting the D-21 experiment have been established consistent with attaining the objectives stipulated for the orbital test demonstration.

Deployment will be demonstrated to evaluate the effects of launch and boost on structure packaging and to evaluate deployment dynamics on the airlock structure. Proof pressure will next be tested to ensure and to establish structural integrity prior to initiating manned operations.

Astronaut ingress/egress will be demonstrated to evaluate the compatibility of expandable elastic recovery materials in airlock designs with the dynamics involved in operational use. The objective is to determine if material stiffness is adequate for airlock designs and to evaluate the effects of stiffness on ingress/egress performance by the astronaut.

A 15-day long-term exposure test will be conducted with the airlock under pressure. Multiple objectives of the D-21 program will be achieved by this test sequence in the experiment procedures. First, the test results will be used to evaluate the performance of expandable materials in operational use when subjected to the total combined effects of the orbital environment. Second, the test results will be used to establish parameters and requirements for future specific airlock designs. Third, this 15-day test will be used to establish a baseline from which other applications of expandable structures technology can be extrapolated.

The final sequence in the experiment procedures is a revisitation mission six months subsequent to the initial launch. The purpose of this final phase is to evaluate space environment effects on expandable materials after prolonged exposure. This evaluation will consist essentially of earth return of a material specimen with subsequent laboratory analysis.

The procedures to be followed in conducting the D-21 airlock experiment are presented as a functional sequence diagram in Figure 17 and in the experiment procedures summary below. The total elapsed time required to conduct the overall experiment is estimated at 191.4 min. The total EVA requirements for each of two astronauts required to perform the experiment are estimated at 166.1 min.

The experiment procedures are to be conducted in three distinct time periods or phases:

1. Phase I - Deployment and structural test demonstration
   a. Total elapsed time - 52.8 min
   b. Total EVA (each of two crewmen) - 30.9 min
2. Phase II - Astronaut ingress/egress demonstration
   a. Total elapsed time - 93.1 min
   b. Total EVA (each of two crewmen) - 91.8 min
3. Phase III - Postenvironment exposure examination
   a. Total elapsed time - 45.5 min
   b. Total EVA (each of two crewmen) - 43.4 min

A revisitation mission to the SIVB orbital workshop will be conducted approximately six months subsequent to the initial experiment. During this visit, another postenvironment exposure examination will be conducted in accordance with the procedures and time estimates stipulated for Phase III.

The experiment procedures summary follows:

1. Phase I - Deployment (EVA 30.9 min, elapsed time 57.8 min
   a. Depressurize AM
   b. Crewman Number 1 (CM1) moves to anchoring station outside thermal curtain and photographs

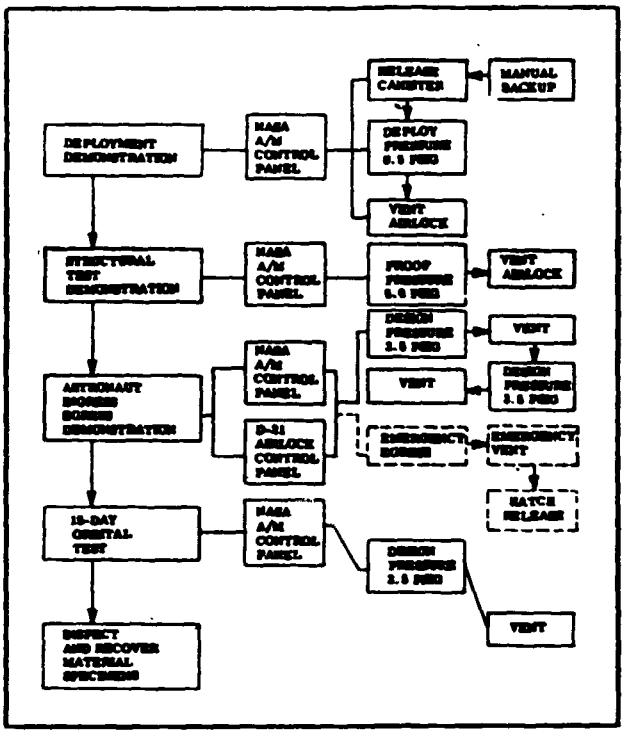

Figure 17 - Experiment Procedures Diagram

deployment while CM2 controls deployment from inside the AM

c. CM1 visually inspects D-21

d. CM1 photographs D-21 as CM2 initiates proof-pressure test

e. CM1 returns to AM

f. AM is sealed and repressurized

g. Proof pressure test will continue for at least 30 min before Phase II begins

2. Phase II - Ingress/egress demonstration (EVA 91.8 min, elapsed time 93.1 min

a. Depressurize AM

b. CM1 moves to anchoring station outside thermal curtain

c. CM1 photographs D-21 as CM2 activates depressurization valve from inside AM

d. CM1 moves to D-21 and works hatch between pressurization cycles initiated by CM2 and examines seal during D-21 pressurization

e. CM1 and CM2 both move to anchoring station where camera is transferred to CM2

f. CM2 photographs CM1 during two ingress/egress cycles conducted without D-21 pressurization

g. Both CM1 and CM2 return to AM

h. AM is sealed and repressurized

3. Phase III - Postenvironment exposure examination

a. Depressurize AM (EVA 43.4 min, elapsed time 45.5 min)

b. CM1 moves to anchoring station and photographs D-21 as CM2 activates D-21 depressurization switch

c. CM1 moves to D-21 and visually examines interior and exterior surface and actuation at hatch, photographing where appropriate

d. CM1 receives sample patches and returns to AM

e. AM is sealed and repressurized

4. Revisitation

a. Same as a. above

b. CM1 moves to anchoring station and photographs D-21

c. Same as c. above

d. Same as d. above

e. Same as e. above

DATA AND INSTRUMENTATION

Data from the D-21 experiment will be obtained from all sources available on the SIVB flight. These data will include photographic coverage, astronaut voice recordings, biomedical data pertaining to ingress/egress maneuvers, and airlock temperature and pressure data via telemetry.

Photography (16 mm Color)

Movie coverage of the D-21 experiment is requested. Table 4 gives this film coverage. Movie coverage by portable hand-held cameras is desirable. Photographic coverage will be effected from either the MDA or the Apollo CSM if viewing areas are appropriate. Fixed camera mounting also can be used. However, this method is least desirable.

TABLE 4 - MOVIE COVERAGE OF D-21 EXPERIMENT

Experiment period	Time (min)	Frames per second
Airlock canister release	1	16
Pressure deployment	5	6
Ingress/egress demonstration	30	1
Postenvironment inspection, end of 15-day test	3	1

Voice Recording

A voice recording of astronaut comments concerning the D-21 experiment is being requested. The recording will cover all phases of EVA appropriate to the experiment procedures. The total period involved is 191.4 min; recording has been requested to cover the entire period.

Biomedical Data

Biomedical data have been requested during the astronaut ingress/egress portion of the D-21 experiment. No special data are required. Only those data normally recorded during the SIVB orbital workshop flight will be obtained.

Telemetry data follows:

Telemetry

1. Data channels (eight analog data items can be commutated)
   a. Two pressure
   b. Six temperature
2. Temperature (inner surface of D-21 airlock)
   a. Two sensors 180 deg apart
   b. Range - -50 to +150 F
   c. Operating range - 0 to 100 F
   d. Accuracy - ±1 percent
   e. Vendor - Yellow Springs Instrument Company, Part No. 427
3. Temperature (outer surface of D-21 airlock)
   a. Four sensors 90 deg apart
   b. Range - 150 to 250 F
   c. Operating range - 125 to 250 F

d. Accuracy - ±1 percent

e. Vendor - Rosemont Engineering, similar to Part No. 118L (Goodyear Aerospace Specification Control 66QS1293)

4. Pressure of D-21 airlock

a. Two sensors on pressure bulkhead

b. Range - 0 to 60 psig

c. Accuracy - ±4 percent

d. Vendor - Fairchild Controls, similar to Part No. TP-200-948A491 (Goodyear Aerospace Specification Control 66QS1294)

5. Sensor output signal range (all channels)

Zero to 5 v, dc

6. Data channel frequency response

Two cycles per second (minimum)

7. Data sampling rate

a. Continuous (from start of experiment to start of 15-day test)

b. 5 sec/4 hr (first two days of 15-day test)

c. 5 sec/12 hr (remaining 13 days of 15-day test)

SUMMARY OF DEVELOPMENT SCHEDULES AND TESTS

The hardware development schedule is shown in Figure 18. Four sets of experiment hardware will be fabricated in addition to two mockup units that will represent the packaged and deployed hardware configurations. The first hardware unit will be used for qualification testing. This test unit will be shipped to WPAFB after qualification tests have been completed for continued structural testing to destruction. The second hardware unit will be used during astronaut training for experiment procedures.

Two flight units will be fabricated. These are scheduled for delivery 1 March and 1 April of 1968. Flight hardware along with aerospace ground equipment will be shipped to McDonnell for final integration of the D-21 experiment.

Table 5 shows the sequence of testing to be performed and the facility where testing will be done. All space environment testing will be conducted at AEDC (Arnold Engineering Development Center). Table 6 summarizes the specific types of space environment tests to be performed. These tests all will be performed under vacuum conditions with varying thermal environment and airlock pressures to simulate the extremes of the conditions anticipated for the D-21 experiment.

Qualification test requirements for the D-21 experiment represent a

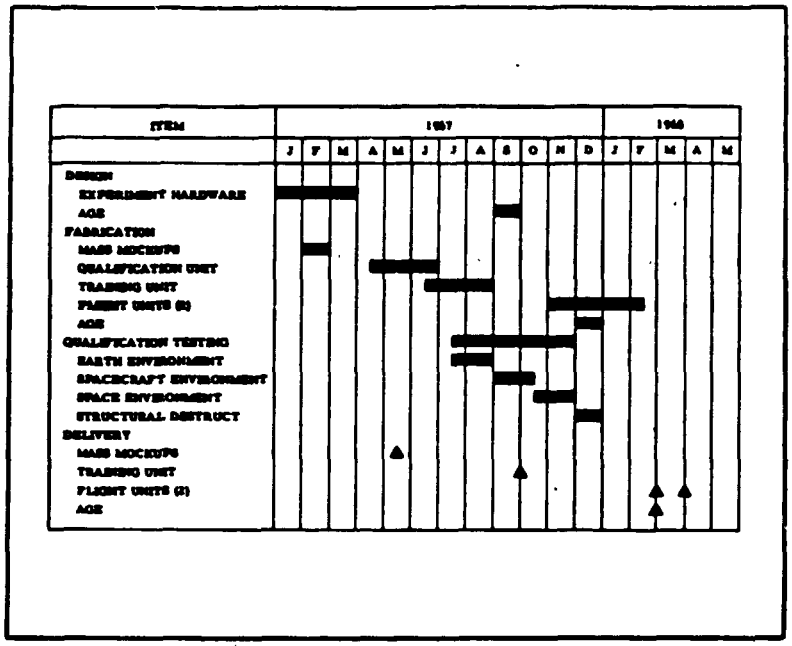

Figure 18 - Hardware Development Schedule

TABLE 5 - TEST SEQUENCE AND FACILITY

Test	Test facility
Functional-operational	Goodyear Aerospace
Humidity	Goodyear Aerospace
High temperature	Goodyear Aerospace
Low temperature	Goodyear Aerospace
EMI compatibility	Goodyear Aerospace
Electrical compatibility	Goodyear Aerospace
Magnetic fields	Goodyear Aerospace
Salt fog	Wylie Labs
Acoustic noise	Wylie Labs
Shock	Goodyear Aerospace
Acceleration	AEDC
Vibration	AEDC
Space environment	AEDC
Fungus	Wylie Labs

TABLE 6 - SPACE ENVIRONMENT TESTS

Test	Airlock pressure	Environmental conditions	Conditions
Launch	Packaged	Vacuum	Packaged airlock installed in test chamber. Maximum available vacuum applied to chamber in two-minute time span.
Operational	0	Vacuum: 1×10^{-6} mm Hg Temperature: -65 F	Airlock, in a packaged configuration, to be placed in the space chamber and required conditions obtained. Canister to be ejected and unit deployed and inflated.
Endurance	0	Vacuum: 1×10^{-6} mm Hg Temperature: -150 F	With zero pressure in airlock, subject unit to environment for 12 hr.
Cycling	0 to 5.25 psi	Vacuum: 1×10^{-6} mm Hg Temperature: -150 F	Cycle pressure in the airlock 30 times. Minimum internal temperature is -50 F.
Endurance	5.25 psi	Vacuum: 1×10^{-6} mm Hg Temperature: -150 F	With 5.25 psi in airlock, proof pressure unit for 12 hr and conduct leak test. Minimum interval temperature is -50 F.
Endurance	0	Vacuum: 1×10^{-6} mm Hg Solar radiation	With zero pressure in airlock, subject unit to solar radiation impinging on top surface of airlock.
Cycling	0 to 5.25 psi	Vacuum: 1×10^{-6} mm Hg Solar radiation	Cycle pressure in the airlock 30 times. Solar radiation impinging on side surface of airlock. Maximum internal temperature is +150 F.
Endurance	5.25 psi	Vacuum: 1×10^{-6} mm Hg Solar radiation	With 5.25 psi in airlock, proof pressure unit for 12 hr and conduct leak test. Solar radiation impinging on side surface of airlock. Maximum internal temperature is +150 F.
Emergency egress	. . .	Vacuum: 1×10^{-6} mm Hg Temperature: -150 F	Operate emergency egress system.

comprehensive and extensive testing program. Successful completion of this program will be a significant achievement in itself and certainly will indicate successful performance of the D-21 airlock in orbit.

CONCLUSIONS

Conclusions of the D-21 experiment follow:

1. Flight demonstration of the elastic recovery structure is the next logical and needed step in the timely development of the expandable structures for manned space flight applications.

2. The D-21 experiment hardware can meet the space experiment schedule and requirements.

3. The experiment procedures as defined will achieve all the experiment objectives.

APPENDIX B

LUNAR STEM TYPE ELASTIC RECOVERY MATERIAL

The shelter-airlock structure was fabricated primarily to demonstrate: structural integrity under a 5 psi design pressure; packaging of the structure in a simulated launch canister and deployment subsequent to unpackaging. To meet these objectives, a representative prototype of the shelter-airlock structure was fabricated reflecting the proposed STEM design. No attempt was made to optimize, from a weight standpoint, the "hard structure" components such as rings, frames, door and hatch. The flexible portion of the structure did however duplicate the proposed design with the exception that thermal conductivity characteristics were eliminated. This deviation from proposed design, however, did not affect either folding or packaging characteristics, so that the major objectives of the fabrication model were not compromised.

The flexible shelter and airlock utilized a flexible filamentary structure to withstand the principal loads. A filament-winding technique, like that used in the construction of fiberglass motor cases, was used. The shelter structure consisted of two sets of continuous windings. A hoop wrap over the cylindrical portion carried most of the hoop tension there. The curved ends were constructed by means of a geodesic, or nearly geodesic, set of windings on a prescribed surface whose shape depended on a prescribed surface determined by the ratio of inner to outer diameter of the ends. The end wrap filaments carried some of the hoop tension.

The airlock structure utilized only a single set of continuous windings. The winding was oriented in an angular wrap to carry both circumferential and meridional loads.

The five-psi atmosphere was retained in a three-ply bladder that was bonded to the inside of the structure. A flexible foam thermal-meteoroid shield was bonded to the outside of the structure. The airlock was fabricated by the same technique.

After fabrication, the two mudules were bolted together through the hatch rings with an "O" ring employed at the interface to prevent leakage in the joint. A circular step-through hatch provided access to the main shelter whil' an elliptical opening permitted a walk-in entry to the airlock.

The shelter-airlock included a composite wall, shelter and airlock entries, and a terminal bulkhead.

a. Composite Wall. The composite wall material for the shelter-airlock structure, as shown in Figure 28, was divided into four individual layers and described in the following paragraphs.

(1) Pressure Bladder. The pressure bladder, bonded to the inner surface of the structural layer, served as a gas barrier for pressure tightness. The bladder, as shown in Figure 29, was a three-layer lamination of flexible sealant materials. The outer layer was a close-woven nylon cloth. The sandwiched layer was a 1/16 inch thickness of vinyl foam and the inner layer was a mylar film-cloth laminate. To facilitate construction, the pressure bladder was laid up on the shelter and airlock filament winding mandrels applying first the inner laminate of cloth and film. This was followed by the layup of the foam center and the third laminate of nylon cloth. All three laminates were made with longitudinal panels equally spaced around the circumference of the mandrels. Seams for the individual layers had a 1-inch lap joint. The splice pattern for all three laminates were staggered to prevent fabric build-up in local areas.

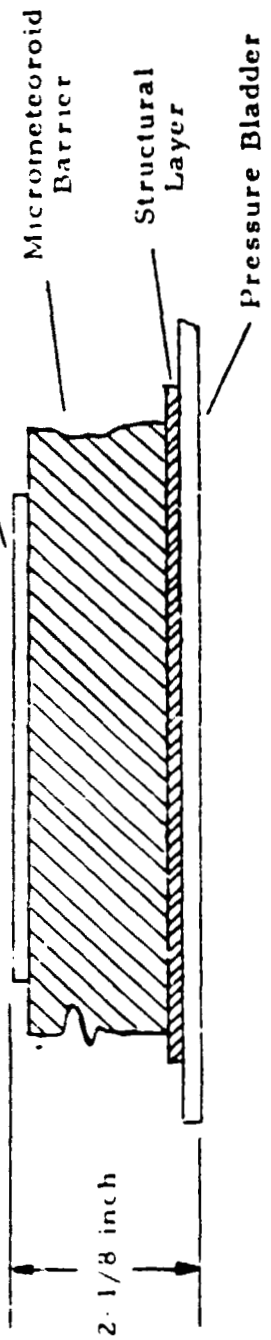

Construction and Weight

Pressure Bladder	0.126
Structural Layer	0.200
Micrometeoroid Barrier	0.200
Polyester Adhesive	0.027
Outer Cover	0.060
	0.613 Lb/Ft^2

Vacuum Test (10^{-6} MM HG)

Off-Gassing	2.6 Percent Weight Loss
Stabilized in Approx.	20 Hr

FIGURE 28. COMPOSITE WALL FOR LUNAR STEM

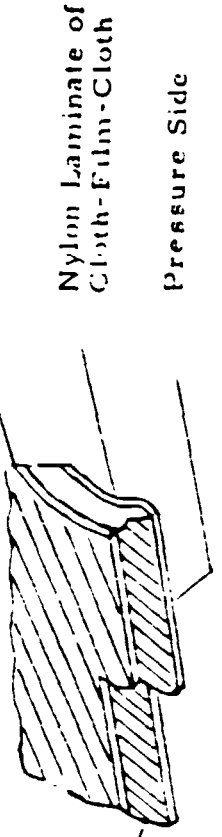

Construction

3-Layer Laminate

Inner Nylon Laminate	0.015
Polyester Adhesive	0.027
Closed-Cell Vinyl Foam	0.042
Polyester Adhesive	0.027
Outer Nylon Cover	0.015
	0.126 Lb/Ft^2

Permeability

1.0 × 10^{-4} Lb/Ft^2-Day at 5 PSI — 0.03 Lb/Day

Shelter Permeability

Toxicity

No Toxic Contaminants Detected

Vacuum Test (10^{-5} MM HG)

Off-Gassing	6.25 Percent Weight Loss
Stabilized in Approx	66 Hr

FIGURE 29. PRESSURE BLADDER FOR LUNAR STEM

(2) Structural Wall. Upon completion of fabrication for the pressure bladder, the filament structure was wound for the composite wall. The winding was performed on the bladder-covered mandrels after the end rings for filament termination had been bonded to the bladder and attached to the form. This procedure, for ring installation after bladder fabrication, served three functions. First, the load-carrying rings sandwiched between the bladder and the filament-wound structure provided a double bonded attachment. Second, the tendency of peel action was eliminated between the pressure barrier and the ring. And third, the windings of the case could be epoxy bonded directly to the ring preventing possible filament angle shift.

A material description of the structural (flexible) filaments follows.

Type 302, 3-strand stainless steel cable

Cable diameter	0.008 in.
Strand diameter	0.0036 in.
Ultimate tensile stress	300,000 psi
Design ultimate	255,000 psi
Safety factor	3
Design pressure	5 psi

To provide a bond between the structural layer and pressure bladder, the cables were wet wound with an elastomer onto the mandrels. The pattern for the shelter was a combination of circumferential and angular longitudinal wraps. The windings for the case were composed of 40 longitudinal, wound at 10-1/2 degree angle, and 76 circumferential cables per inch. For balanced in-plane dome contour on the shelter, a geodesic 20 degree head was employed on the hatch-ring end of the shelter. An 11 degree geodesic head was configured for the terminal end.

The structural wall weighed 0.200 lb/ft^2 with a breakdown of 0.150 lb/ft^2 for the material and 0.050 lb/ft^2 for the bonding substance. Results of a vacuum test (1.8×10^{-6} mm Hg) on the structural layer were:

(1) Off-gassing, 0.66 percent weight loss
(2) Stabilized in approx. 21.5 hr.

(3) Micrometeoroid Barrier. The micrometeoroid barrier was a 2-inch thick flexible foam bonded to the filaments. The polyurethane open-cell flexible foam barrier had a density of 1.2 pcf and weighed 0.2 lb/ft^2.

The selection of flexible polyurethane foam as a micrometeoroid barrier was based on company-sponsored hypervelocity particle impact tests conducted at the Illinois Institute of Technology. As a result of these tests (0.0045-gram particles at 22,000 ft/sec), it was concluded that foam of 1.2-pcf density was equivalent to single sheet aluminum of 15 times the mass per unit area. Thus, a two-inch thickness of 1.2 pcf foam was considered equivalent to an aluminum sheet 0.53-cm thick (1.44 gm/cm^2) with respect to penetration resistance. Based on analysis, the probability of zero penetration for a 30-day period would exceed 0.999. The slabs of polyurethane were patterned and applied much the same as the vinyl foam for the bladder. In the cylindrical section, panels were made of longitudinal straps equally spaced around the circumference of the structure. The domed ends and airlock were tailored to match the contour. Panels were butt spliced and bonded together at the edges to form a micrometeoroid barrier, an insulating shell and a protective spacer to alleviate sharp bends in the structural filaments during the packaged phase. Results of a vacuum test (4.8×10^{-6} mm Hg) on the barrier material were

(1) Off-gassing, 0.4 percent weight loss
(2) Stabilized in approx, 1.5 hr

The foam micrometeoroid barrier is an effective insulator (K = 0.156). Accordingly, the conductivity of the foam must be increased. The proposed technique was to use five-mil diameter copper filaments imbedded in the foam and oriented normal to the thickness layer. About 26 filaments/inch^2 would be required for K = 1.46. This construction is shown schematically in Figure 66.

(4) Outer Cover. Application of the outer cover to the foam completed the composite wall construction. The material and installation duplicated that of the inner laminate on the pressure bladder. Panels were also patterned in the same manner, providing for a one-inch lap splice. The basic difference between the inner laminate of the bladder and foam cover was the surface coating for temperature control. Although the cover served primarily as a thermal barrier, it also functioned as a protective surface for the foam. In addition for packaging, the sealant laminate permitted evacuation of the meteoroid barrier thereby reducing the total wall thickness from approximately a 2-1/2 to a 1/2 inch thickness. Results of a vacuum test (4 X 10^{-6} mm Hg) on the outer cover were

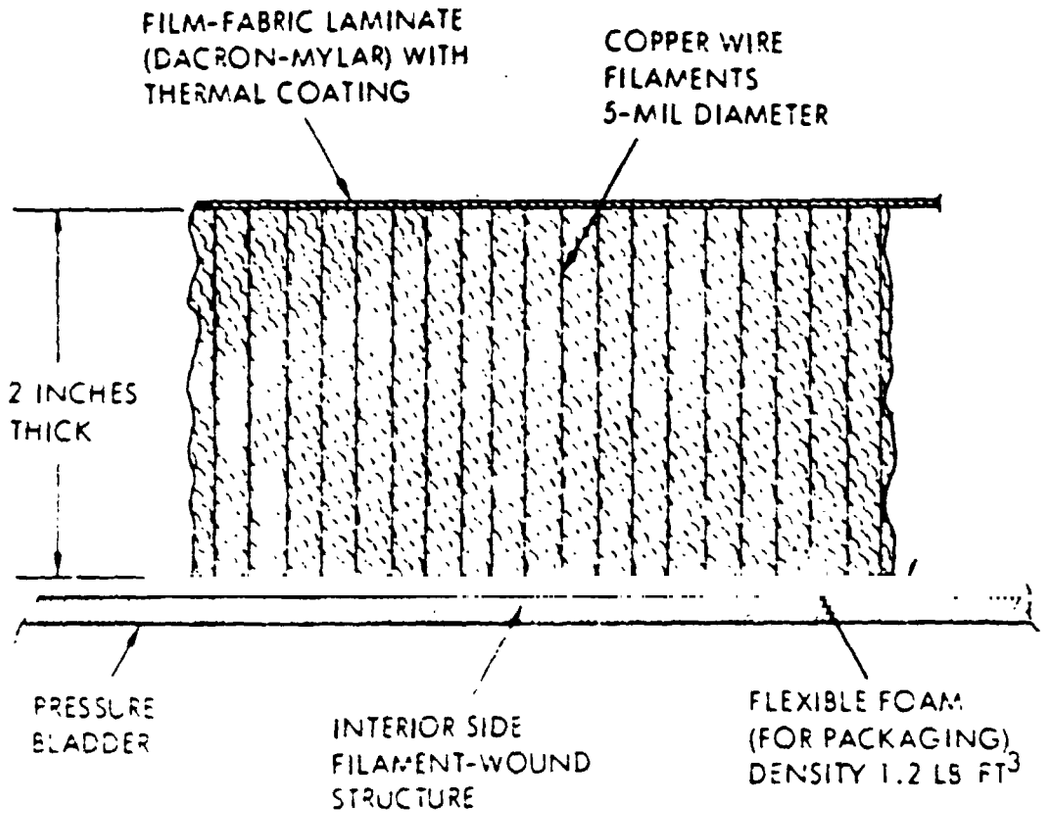

NOTES

1. Filament Winding for Structural Loads
2. Pressure Bladder for Gas Tightness
3. Flexible Polyurethane Foam for Micrometeoroid Protection
4. Copper Wire Filaments (Imbedded in Molded Foam) for Thermal Conductivity Requirements
5. Exterior Surface Coated for Thermal Control ($\alpha_s/\epsilon_s = 0.25$)

FIGURE 66. DIAGRAM OF SHELTER WALL CONSTRUCTION FOR LUNAR STEM

(1) Off-gassing, 3.5 percent weight loss

(2) Stabilized in approx. 1.5 hr

A sketch of the outer cover is shown below.

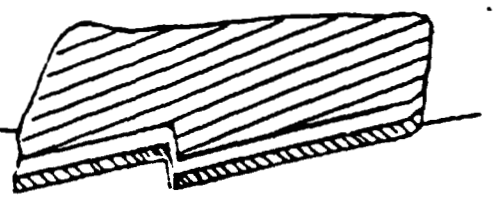

Thermal Characteristics (Test)

α = 0.176
ϵ = 0.651
α = 0.21

Coating Degradation (Vacuum and U-V Tests)

Time	Increase in (α_s/ϵ)
23 Days	8 Percent
67 Days	38 Percent

Tests on the composite wall material and its component layers under vacuum conditions were used to evaluate off-gassing effects on the material physical properties (Table XXVIII). An initial off-gassing was encountered, resulting from boil-off of plasticizers and volatile solvents, with a neglible weight loss, which subsequently leveled off.

Tests were made to assure that no toxic by-products, such as those used in the pressure bladder polymer type materials, were given off while under the deployment environment of 5 psia O_2 atmosphere. A survey of toxic materials known to be used in the pressure bladder material construction was made, and found to be Toluene-diisocyanate (TDI). Although carbon monoxide was not

Table XXVIII. Vacuum Off-Gassing - Composite Wall Materials

Material	Percent Weight Loss	Time to Stabilize	Vacuum Level
Total Composite	2.63	40-Hrs	10^{-6} mm
Outer Cover	.36	1.5	4×10^{-6}
2-Inch Foam	.39	1.5	4.8×10^{-6}
Structural Layer	.66	20.5	1.8×10^{-6}
Pressure Bladder	6.3	96.0	10^{-6}

known to be contained, tests for it were also included. The test procedure for collecting traces of any toxic gases was to place the test material in a pressure vessel that was evacuated and subsequently pressurized to 5 psia with O_2. The test material was exposed for 24 hours, prior to chemical analysis of the toxic gases, and all were found to be below the threshold limit values for atmospheric contaminants, established for occupational exposure. The values as determined by calorimeter type chemical tester or mass spectrometer are ahown in Table XXIX.

Table XXIX. Threshold Limits for Atmospheric Contaminants

Gases	Test Result Value (PPM)(1)	Threshold Limit Value (PPM)(2)
Toluene	200.0	200.0
Xylene	200.0	200.0
Methyl Ethyl Ketone	200.0	200.0
Methulene Chloride	200.0	500.0
Toluene-diisocyanate	0.01	0.02
Carbon Monoxide	25.0	100.0

(1) Note that the values shown are minimum sensitivity values of the instruments used in testing. In all cases, no trace of the contaminants were found, therefore, proving if there were minute traces of contaminants, the concentration is below the threshold limit value.

(2) American Conference of Governmental Industrial Hygienists, 1963, or National Bureau of Standards.

APPENDIX C

FLEX SECTION FOR THE SPACELAB CREW TRANSFER TUNNEL

Goodyear Aerospace Corporation (GAC) analyzed, designed, developed and qualified the flex section for the transfer tunnel between the NASA Space Shuttle Orbiter Crew Cabin and the Space lab module located in the payload bay of the shuttle under subcontract to McDonnell Douglas Technical Services Company (MDTSCO). The Space lab Transfer Tunnel (STT) flex sections constitute a non-rigid connection of the tunnel to minimize STT section loads at the Space lab and orbiter interfaces resulting from axial, lateral, torsional and rotational displacements caused by installation, thermal gradients and maneuvering.

Figure A-1 shows the general location of the two flex sections within the crew transfer tunnel as it connects between the orbiter crew cabin and the Space lab. Also shown is the side view of the flex section along with a cross-section defining all the major components. Each flex section consisted of one flexible element, two inner and outer rings, two negative pressure rings, one debris shield and one electrical bonding strap. Figure A-2 shows five flex section flight units (standing vertical), the qualification test unit (foreground) and two spare flex elements on the table in the GAC Fabric Manufacturing facility.

The flexible element consists of two plies of fabric, steel beads and fillet. The fabric consists of Nomex undirectional cloth coated with Viton B-50 elastomer with each ply biased at ± 15 degrees to the flex element centerline. Overall thickness of the composite is approximately 0.11 inches with the individual thickness of the Nomex being approximately 0.025 inches. Each ply of Nomex is coated on each side with approximately 10 mils of Viton. A ten mil thickness of Viton is added to the inner and outer surfaces during the lay-up. The fabric plys are wrapped around the beads in the same direction with fillets added to the outer diameter of the beads to ensure a smooth transition during wrapping.

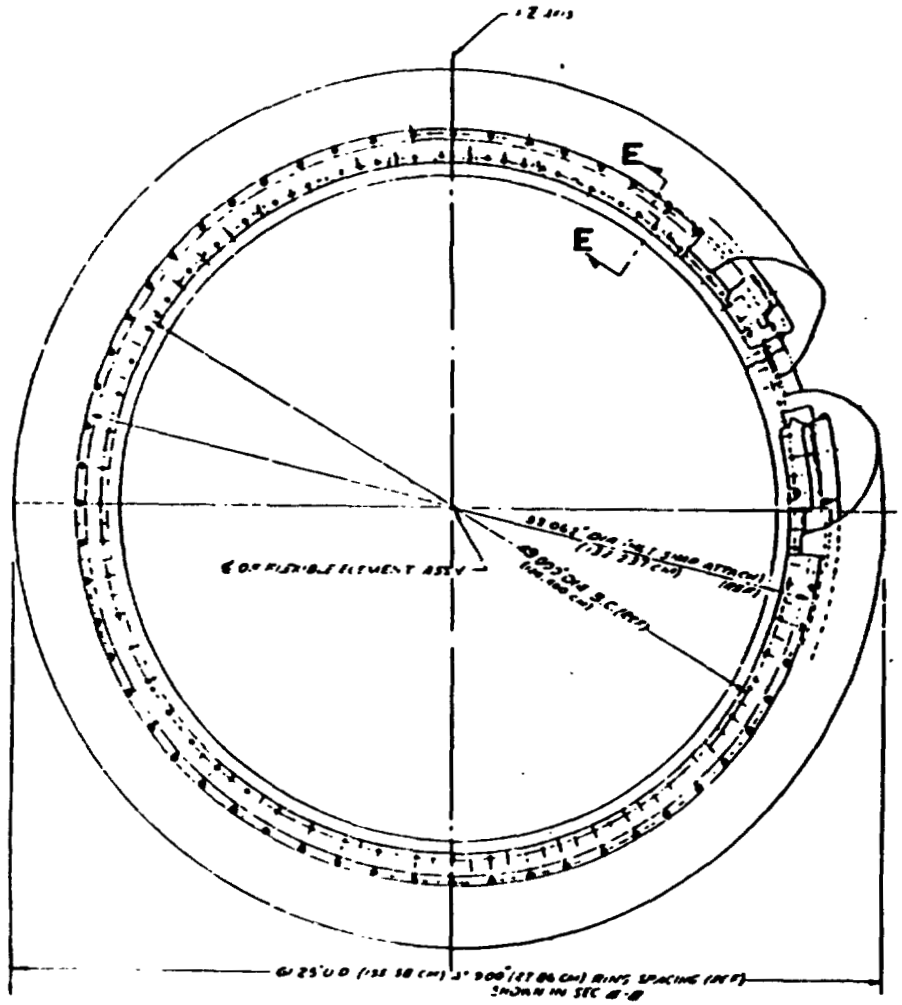

FLEXIBLE ELEMENT ASSY
or
FLEX SECTION

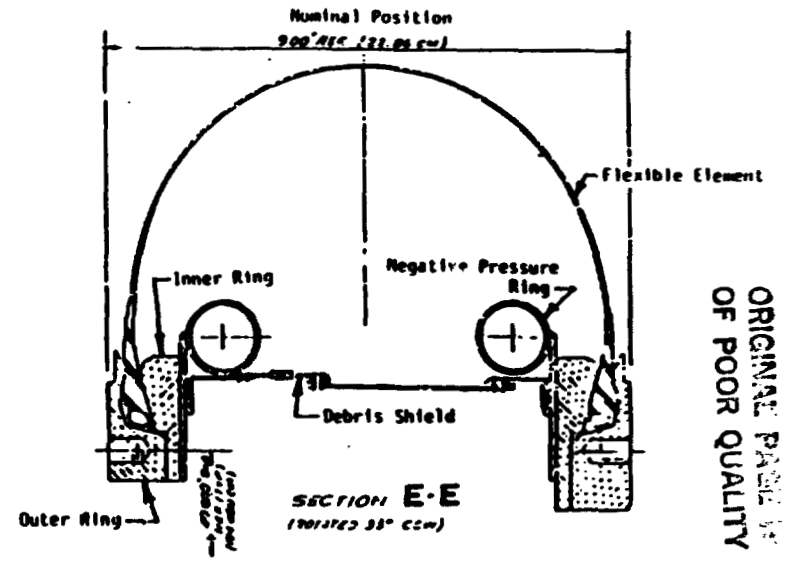

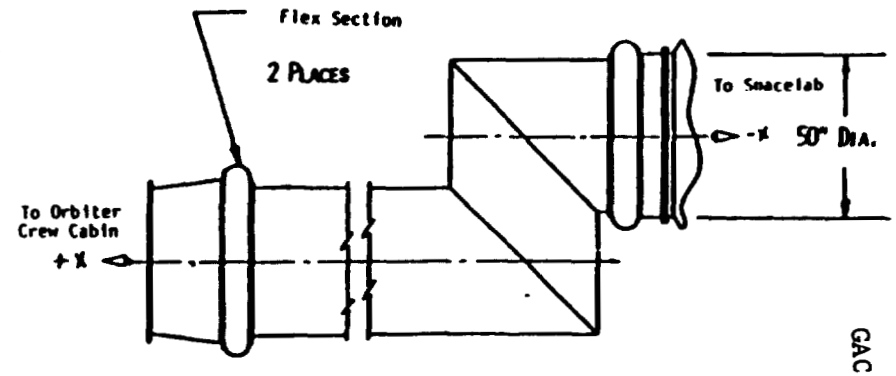

CREW TRANSFER TUNNEL

GAC 19-1615

FIGURE A-1. SCHEMATIC OF CREW TRANSFER TUNNEL AND FLEX SECTION CONCEPTS

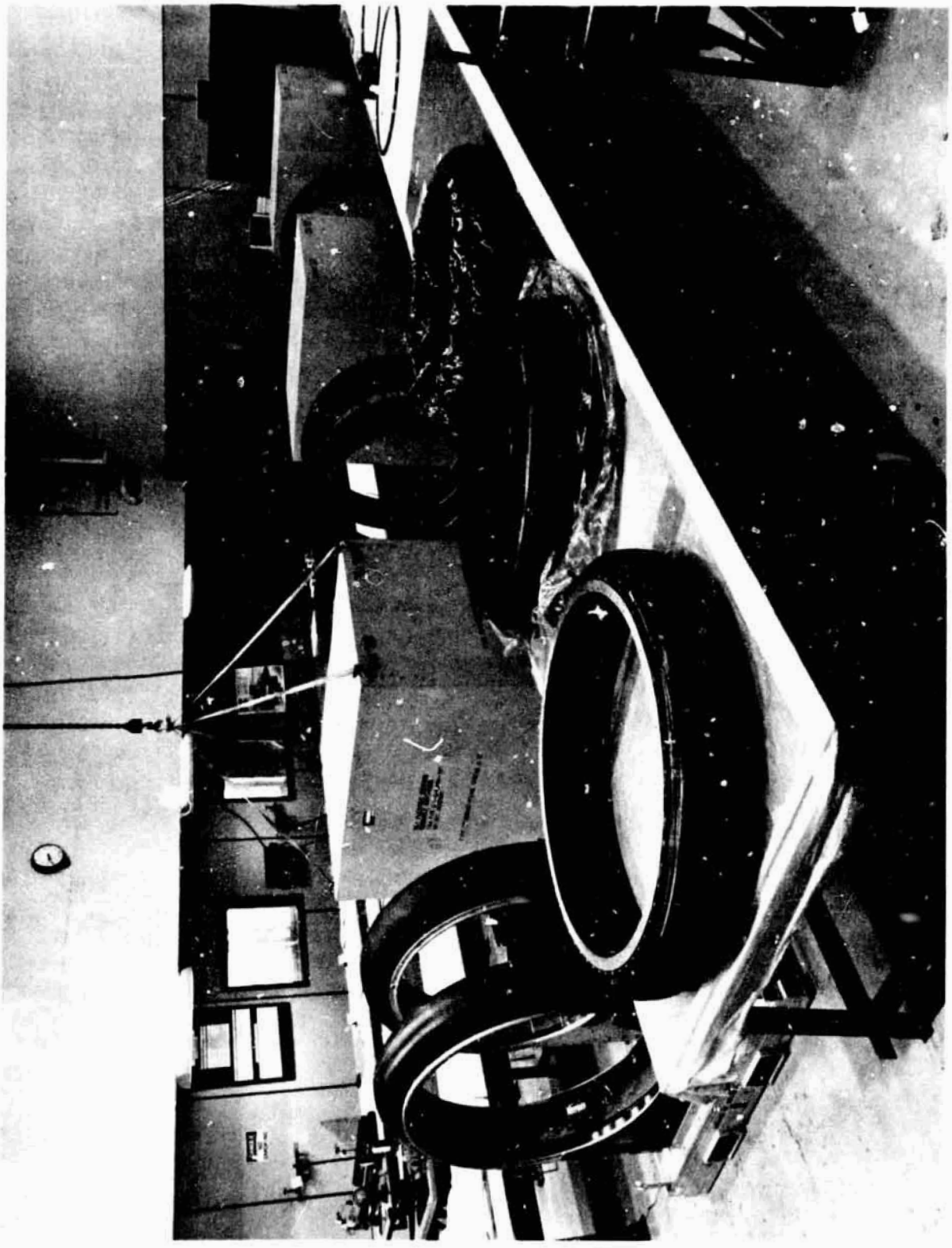

FIGURE A-2. FLEX SECTION QUALIFICATION AND FLIGHT HARDWARE

The bead itself was made from 51 continuous wraps of 0.037" diameter steel wire which tested to an ultimate strength of over 15,000 pounds. This strength is needed to react the stresses in the fabric. The use of a continuous wire bead is not a new concept, buthas been used in the manufacture of automobile and truck tires.

The inner and outer rings provide a means of interfacing the flexible element with the hard sections of the tunnel. The rings also force the beads of the flexible element outward and upward to effect the pressure seal.

The negative pressure rings ensure that the flexible element stops within a desired envelope under pressure-reversal conditions.

The bonding strip provides for an electrical path to ensure that both sides of the flexible element attachment rings are at the same electrical potential.

The debris shield used to protect the flexible element from falling debris is constructed of a stretch-type cloth of Kevlar 29 sewn at each side to preformed and precoated Nomex tapes which are fastened to the inner rings by clamp bars.

The flex section weight was approximately 133 pounds of which the flexible element represented a little over 20 percent.

The flex section design criteria were basically as follows:

-Accommodate

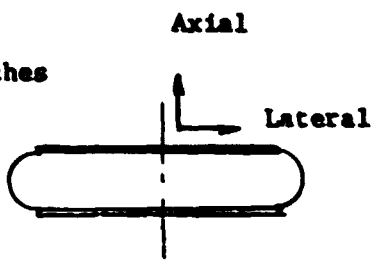

  -Axial deflections of +2.43 inches to -1.81 inches

  -Lateral deflection of 2.69 inches

  -Torsional deflections of 0.67 degrees

  -Pitch deflections of 1.33 degrees

-Operate between -0.5 psig and +15.9 psig

-Withstand 50 x 4 = 200 flight cycles (motions and pressures associated with each orbital flight) (Total of 40,000 cyclic loadings)

-Withstand a 1/2 inch slit under pressure without resulting in a catastrophic failure

-Not burn or off gas in an oxygen enriched atmosphere

-Minimize interface loads

-10 year life

The tunnel flex section is a toroidal section, similar to a tire, composed of two flexible wire hoops or beads joined by two plies of elastomer-coated, undirectional fabric. If the end rings are displaced laterally or rotated relative to each other one ply supports more of the load than the other ply, or all of the load if the displacement is large enough. The ring loadings are determined by defining the displacements of one end of the threads or yarns relative to the other end of the same thread. Only geometric displacements were considered in the analysis. The thread tensions are resolved into components parallel to the system global axis at both ends. These loadings are integrated around the entire circumference to determine the loads acting on the rings.

An analytic model of the flexible element called FLEXSECT was made that can be displaced over the various axial, lateral, torsional and pitch motions while under internal pressures. Outputs from this computer program are cord tension (from which fabric stresses are determined, and distributed reaction loads on the rings (which when integrated give the interface loads and moments). The distributed reaction loads are then used in the standard STRUDL (Structural Design Language) computer program along with the bead pretension load and eccentricities for the part to establish the stresses in the ring. These stresses are then used to calculate margins of safety of the ring.

The interface loads and moments were computed on GAC's FLEXSECT Program and up-dated by the inputs from the full scale test program.

Detailed development tests were conducted on components and sub-systems for the flex section. Viton B-50 elastomer and Nomex cloth were chosen because of the long life and off-gassing/flammability requirements. Material specimens were fabricated and tested to determine the effect of cut fill yarns, cure/post cure, and vacuum bakeoff on strip tensile strength and peel adhesion.

Bead strength tests were made along with extensive investigations of bead incorporation within the flex element to assure structural adequacy.

Fabric strips of the basic flex element material were Rotoflex and tensile tested to determine any degradation due to cyclic loading.

Several full scale flex sections were fabricated and tested to verify that the safe life, leak before burst, and burst pressure requirements were met. In addition, test data on interface loads and moments were also obtained. Figure A-3 shows the flex section mounted in a computer-controlled cyclic test fixture under normal and distorted conditions. The safe-life test

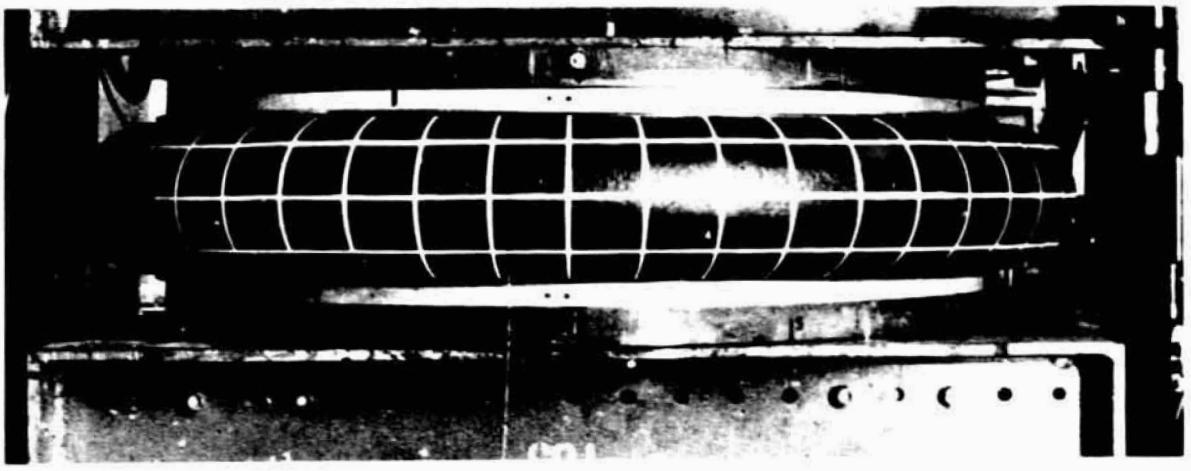

a) Normal Spacing and at 15.9 Psig Pressure

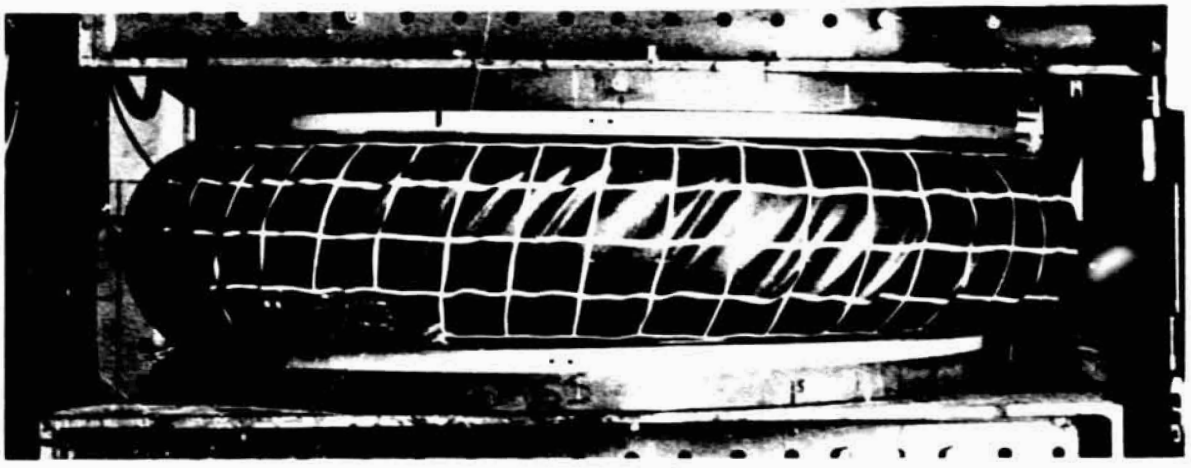

b) In Extended and Displaced Condition at 15.9 Psig Pressure

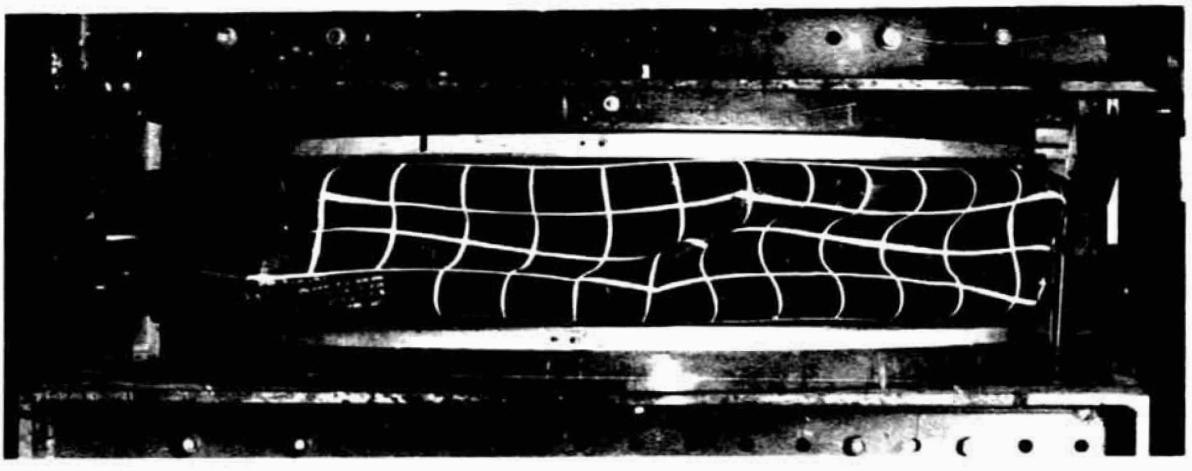

c) At Lateral Displacement and at -0.5 Psig Pressure

FIGURE A-3. FLEX ELEMENT ASSEMBLY IN CYCLIC TEST FIXTURE

demonstrated that the flexible element design could survive fifty (50) operational cycles times a time-life factor of four (4) or two-hundred (200) design life cycles. A visual examination of the flex element was made during and after almost every flight cycle. There was no evidence of wear on the outside of the unit throughout the 200 cycles. The success of the leak-before-burst test demonstrated that the design of the flex element was stable under limit conditions with readily detectable damage. A one-half inch cut in the flex element did not grow beyond the initial cut length even under pressure. The element burst at a pressure three times the minimum required pressure.